

©Copyright 2013

Allan C. Hicks

The utility of catch-per-unit-effort when assessing and managing
long-lived fish stocks

Allan C. Hicks

A dissertation
submitted in partial fulfillment of the
requirements for the degree of

Doctor of Philosophy

University of Washington

2013

Reading Committee:

Ray Hilborn, Chair

André E. Punt

Tim Essington

Program Authorized to Offer Degree:
School of Aquatic and Fishery Sciences

University of Washington

Abstract

The utility of catch-per-unit-effort when assessing and managing long-lived fish stocks

Allan C. Hicks

Chair of the Supervisory Committee:
Professor Ray Hilborn
School of Aquatic and Fishery Sciences

The research in this Ph.D. dissertation focuses on the relationship between fishery-dependent catch-per-unit-effort (CPUE) and abundance and how its use when assessing and managing fisheries may be affected by some of its shortcomings. CPUE data are often used to provide information on the historical and current stock size, but changes in CPUE may not be proportional to abundance. Hyperstability is when CPUE declines slower than abundance and can result in optimistic estimates of abundance and risk of overfishing. Hyperdepletion is when CPUE declines faster than abundance and using these data in an assessment can produce pessimistic estimates of abundance. Assuming a proportional relationship between CPUE and abundance when CPUE actually has a nonlinear relationship with abundance can misinform management and result in overfishing or lost yield. Instead, the nonlinear relationship can be modeled and estimated. Three stand-alone chapters are presented in this dissertation with methods and results from analyses estimating the amount of nonlinearity in the relationship between CPUE and abundance and its implications on fisheries management.

The first chapter investigated the nonlinearity between empirical CPUE data and abundance from orange roughy fisheries in Australia and New Zealand. Data from four orange roughy stocks were integrated using a Bayesian hierarchical state-space model to estimate the hyperparameters of a distribution for a nonlinearity parameter in the relationship between CPUE and abundance. Hyperdepletion was more probable than hyperstability and a

prior distribution for an unknown stock showed a 83% probability of hyperdepletion. This study is unique because it used data from the beginning of a fishery and created a prior distribution that may be used in future assessments.

The second chapter used simulation to look at the ability to estimate nonlinearity in CPUE data using different models, assumptions, and types of data. A deterministic delay-difference model, a deterministic age-structured model, and a state-space delay-difference model were used to estimate the nonlinearity parameter of simulated CPUE data with a hyperstable, proportional, or hyperdepleted relationship to abundance. Estimates of the nonlinearity parameter were mostly unbiased, but highly variable. Using an informative prior distribution resulted in lower variance, but higher bias when the prior was not congruent with the true level of nonlinearity. Overall, the state-space model showed the best performance, and an informative prior distribution was useful as long as it is appropriate, justifiable, and wide enough to support all possible values of the nonlinearity parameter.

The final chapter performed a management strategy evaluation to determine the consequences of managing a fish stock with and without estimating a nonlinearity parameter between CPUE and abundance. An age-structured operating model was used to simulate a true population from which CPUE and survey data were generated, where CPUE data were either hyperstable, proportional, or hyperdepleted. Estimation models with the nonlinearity parameter estimated or fixed at proportionality were used to estimate population trajectories from the simulated data. Two-area age-structured operating models with movement dependent on fishing effort and density-dependence were also investigated. The benefits to estimates of stock status and yield objectives when estimating a nonlinearity parameter were dependent on the true underlying relationship between CPUE and abundance. Hyperstable scenarios were especially risky, and should always be accounted for, or at least acknowledged, in a management strategy. Hyperdepletion scenarios, on the other hand, may seem to be less of a concern due to reduced conservation risk, but the negative consequences of reduced yield, at least in the short term, and a pessimistic view of the stock, and thus the management system, make it worthwhile to at least acknowledge the

potential for hyperdepletion and that not accounting for it is a chosen management strategy. In the long-term, yield was similar whether or not nonlinearity was estimated, but if when estimating nonlinearity, risk to the stock was reduced when CPUE were hyperstable and although risk increased when CPUE showed hyperdepletion, stock status was typically always higher than the hyperstable scenarios.

Nonlinearity in CPUE is common in many fisheries and it was seen that CPUE declined faster than abundance during the initial development of orange roughy fisheries. The presence of hyperdepletion can result in pessimistic views of stock status which may result in lost yield, the closure of fisheries, and conflict amongst user groups. Estimating a nonlinearity parameter in assessments and acknowledging that nonlinearity exists can improve management by bringing catches and stock depletion closer to target levels.

TABLE OF CONTENTS

	Page
List of Tables	iv
List of Figures	viii
Introduction	1
A derivation of CPUE	2
Assumptions for CPUE to be a proportional index of abundance	4
The effect of fish behavior and fishing operations on catchability	5
Analyzing and standardizing catch and effort data	7
Modeling catchability as a function of abundance	8
Evidence of departures from a proportional relationship	12
Motivation	14
Chapter 1: A meta-analysis of nonlinearity in the relationship between catch-per-unit-effort and abundance in orange roughy (<i>Hoplostethus atlanticus</i>) stock assessments	16
1.1 Introduction	16
1.2 Materials and Methods	21
1.2.1 Stocks and data	22
1.2.2 State-space model	23
1.2.3 Hierarchical state-space model	25
1.2.4 Estimation of parameters	26
1.2.5 A prior distribution for β	27
1.3 Results	28
1.3.1 Individual stocks	28
1.3.2 Parameters shared between stocks	29
1.3.3 Prior distribution for the nonlinearity parameter	30
1.4 Discussion	30
1.5 Tables	37

1.6	Figures	42
Chapter 2:	Estimating nonlinearity between CPUE and abundance	50
2.1	Introduction	50
2.2	Materials and Methods	53
2.2.1	Operating model and data	53
2.2.2	Estimation models	54
2.2.3	Scenarios and simulations	55
2.2.4	Analysis	58
2.3	Results	59
2.3.1	Estimates of the nonlinearity parameter	60
2.3.2	Estimates of relative depletion and trend in biomass	63
2.4	Discussion	65
2.5	Tables	70
2.6	Figures	76
Chapter 3:	Managing a long-lived fish stock when there is a nonlinear relationship between CPUE and abundance	85
3.1	Introduction	86
3.2	Materials and methods	89
3.2.1	Operating model and data	89
3.2.2	Assessment model	91
3.2.3	Management strategies and control rules	92
3.2.4	Design	95
3.2.5	Analysis and performance measures	96
3.3	Results	96
3.3.1	Historical model-based control rule	98
3.3.2	Current management strategies	99
3.3.3	Estimates of the nonlinearity parameter	101
3.4	Discussion	102
3.5	Tables	109
3.6	Figures	116
Conclusions	128
Caveats and future work	131

Bibliography 134

Appendix A: Stock-specific data for the meta-analysis (Chapter 1) 145

Appendix B: Stock specific results for the meta-analysis (Chapter 1) 156

Appendix C: Operating and estimation models 165

LIST OF TABLES

Table Number	Page
1.1	Catch-per-unit-effort (CPUE) data for the four stocks of orange roughy from Wayte and Bax (2002) and Ministry of Fisheries (2007). 37
1.2	The type of fishery-independent abundance data and years for which estimates were available for the four stocks of orange roughy. BUC, COR, and TAN refer to <i>F/V Otago Buccaneer</i> , <i>F/V Cordella</i> , and <i>R/V Tangaroa</i> , respectively, and are the vessels that performed trawl surveys. The parameterizations for the catchability coefficients (q) are given along with prior distributions taken from previous stock assessments (Wayte and Bax 2002; Ministry of Fisheries 2007). The priors with normal distributions are parameterized with a mean and standard deviation and U refers to the uniform distribution. 38
1.3	Parameters in the delay-difference state-space model for a single stock. An asterisk preceding the variable indicates that it was fixed or determined from fixed parameters. 39
1.4	Hyperparameters in the hierarchical delay-difference state-space model that are shared across stocks. 39
1.5	Prior distributions assigned to the estimated parameters. See Tables 1.3 and 1.4 for descriptions of the parameters. Biomass is in tonnes and β or ω equal to 1 implies a proportional relationship. 40
1.6	The medians of the posterior distributions for the nonlinearity parameter, β_u , with the 90% HPD interval reported in parentheses. The probability that β_u is greater than one is also given. 40
1.7	Parameters in log space and back-transformed quantiles for empirical and parameterized prior distributions. Empirical refers to the integrated sample from the MCMC. The parameters are the mean, standard deviation (sd), and degrees of freedom (df). See Equation 1.12 for the parameterization of the logistic distribution. The empirical summary of the prior distribution when natural mortality was halved (Half M) is also given. 41
2.1	Parameters used in the operating model. 70
2.2	Levels of the different variables tested. 71
2.3	The median ratio between estimated and true β . Values less than 1 indicate that the estimate was more often less than the true value. 72

2.4	Mean Absolute Logged Ratio (MALR) for the estimated and true β . A value of zero indicates a perfect estimate over all simulations while larger numbers show worse estimation ability.	73
2.5	Medians of the mean depletion error (<i>MDE</i>) for the three estimation models with β fixed at one and the three estimation models with β estimated using different prior assumptions for the level of true nonlinearity. Negative values indicate that the estimated relative depletion trajectory was on average more depleted than the true relative depletion trajectory (see Equation 2.7). Numbers in italics indicate the true scenario which most closely matches the assumption in the estimation model.	74
2.6	Medians of the mean absolute depletion error (<i>MADE</i>) for the three estimation models with β fixed at one under assumptions of different levels of true nonlinearity. Larger values indicate increased estimation error (see Equation 2.8).	75
3.1	Parameters used in the single-area and two-area operating models, and for data generation.	109
3.2	Equilibrium reference points for the single area and two-area operating models.	110
3.3	Simplified historical control rule. Each box corresponds to the current biomass (B_{curr}) and the rows corresponds to the five-year projected biomass (B_{+5}).	110
3.4	Cases used for each control rule. Data generation refers to the nonlinear relationship between CPUE and abundance. Perfect means that perfect information was available when applying the control rule (biomass for model-based control rules and CPUE for CPUE-based control rules). Low catch is 2000 tons and high catch is 4000 tons.	111
3.5	Metrics used to investigate performance of the simulations.	112
3.6	Medians of the minimum depletion, median depletion, average annual catch rounded to the nearest 100 tons (AAC), and the standard deviation of the annual catch rounded to the nearest 100 tons (SDAC) for the first 10 years of management (years 11 to 20 after fishing began) using the historical model-based control rule. The operating model assumptions are shown as rows for each metric, and the assessment assumptions are shown as columns within each time period.	113
3.7	Medians of the minimum depletion, median depletion, average annual catch rounded to the nearest 100 tons (AAC), and the standard deviation of the annual catch rounded to the nearest 100 tons (SDAC) for the first 10 years of management (years 11 to 20 after fishing began) using the current model-based control rule. The operating model assumptions are shown as rows for each metric, and the assessment assumptions are shown as columns within each time period.	114

3.8	Medians of the minimum depletion, median depletion, average annual catch rounded to the nearest 100 tons (AAC), and the standard deviation of the annual catch rounded to the nearest 100 tons (SDAC) for the first 10 years of management (years 11 to 20 after fishing began) using the current CPUE-based control rule. The operating model assumptions are shown as rows for each metric, and the assessment assumptions are shown as columns within each time period.	115
A.1	Catch (mt) and CPUE indices for the Eastern Chatham Rise stock. Year refers to the latter part of the fishing year (i.e, 1979 refers to 1 October 1978 to 30 September 1979). Coefficients of variation (CV) were those used in the 2007 assessment (Ministry of Fisheries 2007) without additional error from unobserved processes added in.	150
A.2	Fishery-independent abundance estimates (mt) for the Eastern Chatham Rise stock. BUC, COR, and TAN refer to trawl surveys done by the vessels <i>F/V Otago Buccaneer</i> , <i>F/V Cordella</i> , and <i>R/V Tangaroa</i> , respectively. Coefficients of variation (CV) are given without additional error from unobserved processes and “Year” refers to the latter part of the fishing year (i.e, 1979 refers to 1 October 1978 to 30 September 1979).	151
A.3	Catch (mt), CPUE indices, and fishery-independent abundance estimates (mt) for the Mid-East Coast stock. Year refers to the latter part of the fishing year (i.e, 1979 refers to 1 October 1978 to 30 September 1979). Coefficients of variation (CV) were those used in assessments reported by Ministry of Fisheries (2007) without additional error from unobserved processes added in.	152
A.4	Catch (mt), CPUE indices, and fishery-independent abundance estimates (mt) for the Northwest Chatham Rise stock. Year refers to the latter part of the fishing year (i.e, 1979 refers to 1 October 1978 to 30 September 1979). Coefficients of variation (CV) were those used in assessments reported by Ministry of Fisheries (2007) without additional error from unobserved processes added in.	153
A.5	Catch (mt), CPUE indices, and fishery-independent abundance estimates (mt) for the Australian Eastern Zone stock. Coefficients of variation (CV) were those used in assessments reported by Wayte and Bax (2002).	154

B.1	The medians of the posterior distributions for the unfished biomass (B_0), last predicted biomass (B_{last}), and depletion (last predicted biomass divided by unfished biomass) from recent assessments (Ministry of Fisheries 2007; Wayte and Bax 2002) and the state-space model with all stocks (SSM results are in bold). The 2.5% and 97.5% quantiles are given in parentheses for comparison because that is what is reported from the stock assessments. For the ECR stock, the assessment results were summed over results from the three sub-areas. B_{last} was the year 2006 from the assessments for ECR and NWCR stocks while the last year was 2005 in the SSM model for these stocks. The last year was 2004 for all models of the MEC stock and 2001 for the AUS stock. Estimates of β are shown for the three CPUE series from the ECR stock and the single CPUE series for each of the other stocks.	160
C.1	Parameters in the operating and estimation models.	170

LIST OF FIGURES

Figure Number	Page
1	Three possible relationships between CPUE and abundance as described by Hilborn and Walters (1992). 6
2	Areas where CPUE is declining faster than abundance (blue long dashes) and declining slower than abundance (red short dashes) in the power function αN^β , with $\alpha=1$ and $\beta=0.4, 1, \text{ or } 2.5$ 11
1.1	Orange roughy stocks in Australian and New Zealand exclusive economic zones (EEZ) used in the meta-analysis. AUS refers to Australia’s Eastern Zone stock while MEC, NWCR, and ECR refer to New Zealand’s Mid-East Coast, Northwest Chatham Rise, and East Chatham Rise stocks of orange roughy, respectively. 42
1.2	The assumed prior distribution for a stock-specific nonlinearity parameter, β_u , given the prior distributions of the hyperparameters. 43
1.3	Posterior distributions for the estimated additional coefficient of variation of each CPUE series (ξ_u) with 90% HPD intervals marked in gray. The posterior distribution for AUS is plotted with a different x-axis than the rest. 44
1.4	Posterior distributions for the nonlinearity parameter in each CPUE series (β) for the four stocks plotted on a log scale. The estimated density of the posterior distribution for the analysis with all four stocks is shown with the median (solid vertical line) and a 90% HPD interval marked in gray. Below the posterior distributions are the 90% HPD interval and median for the nonlinearity parameter with one stock removed. 45
1.5	Posterior distributions for additional error (as a coefficient of variation, CV) for survey data and the CV of the process error (although estimated as variance). The median (solid vertical line) and the 90% HPD interval (gray area) are shown. The prior distribution for the CV of process error, converted from the prior on σ_ε^2 , is shown with a light grey line. Actual samples from the posterior distribution are indicated with small black marks immediately below the nonparametric density estimate of the posterior distribution. 46
1.6	Posterior distributions for the hyperparameters ω and σ_ω with prior distributions drawn as gray lines, the median of the posterior distribution drawn as a solid vertical line, individual samples from the MCMC as small marks below the nonparametric density estimate, and the 90% HPD interval in gray (top plots). A scatterplot of σ_ω vs. ω is shown on the lower plot. 47

1.7	Estimated nonparametric density of a prior distribution for the nonlinearity parameter, β_u , in the relationship between CPUE and abundance with all stocks included (top left). The solid gray line is the prior distribution without any data. The additional panels show the integrated nonparametric density estimates with the indicated stock excluded from the analysis or the sensitivity where natural mortality was halved with all stocks in the analysis (Half M). The shaded area represents the 90% HPD interval and darker shaded areas indicate overlap between the two distributions.	48
1.8	Parametric distributions fitted to the estimated nonparametric density of the prior distribution for the nonlinearity parameter (β) in the relationship between CPUE and abundance for an unknown stock.	49
2.1	The fixed catch (thousands of metric tons) used in the models.	76
2.2	The four prior distributions for β used in the estimation models. The <i>Harley Prior</i> is a normal distribution in real space (left panel). The <i>Hicks Prior</i> and <i>Hicks(1) Prior</i> are logistic distributions in log space and the <i>Uniform Prior</i> is also in log space (right panel).	77
2.3	Simulated trajectories of beginning of the year spawning biomass from the true population with recruitment variability equal to 1.1 and an ending depletion of 0.15 (top panel) or 0.45 (bottom panel). The thick dark line is the deterministic trajectory ($\sigma_R = 0$) and the light colored horizontal line is the simulated final level of depletion. Data were generated from these "true" trajectories.	78
2.4	Ratio of the estimated β parameter to the true β parameter for the simulations. The four priors are shown down the rows while the three true β parameters are shown across columns. Within each box, the eight combinations of <i>Depletion</i> , <i>CPUEcv</i> , and <i>Period</i> are displayed. The mean ratio for each of the three models is shown for each case with a letter indicating the model and bars encompassing the central 75% of the values observed from the simulations. Random values from the prior distribution, divided by the true β are shown in the center of each plot with the median marked by a "P" for comparison.	79
2.5	MALR for different true values of β (lines) and the three models (x-axis within each subplot) from simulations using CPUE and survey data and estimating β with different prior distributions (subplots), integrated over <i>Depletion</i> , <i>CPUEcv</i> , and <i>Period</i> (top row). Also shown are MALR values for simulations using only CPUE data, integrated over <i>Depletion</i> and <i>CPUEcv</i> (bottom row). The results for the true β equal to 0.6 estimated with a uniform prior and only CPUE data in the <i>DDD</i> and <i>AWA</i> models (bottom left plot) are higher than the upper limit of the plot.	80

2.6	Ratio of the estimated β parameter to the true β parameter for the simulations with only CPUE data . The four priors are shown down the rows while the three true β parameters are shown across columns. Within each box, the four combinations of <i>Depletion</i> and <i>CPUEcv</i> are displayed. The mean ratio for each of the three models is shown for each case with a letter indicating the model and bars encompassing the central 75% of the values observed from the simulations. Random values from the prior distribution, divided by the true β are shown in the center of each plot with the median marked by a “P” for comparison.	81
2.7	The mean true depletion trajectory (solid line) with a final depletion of 0.15. Mean estimated depletion trajectories are shown where β was fixed at 1 (dashed line) or estimated with a uniform prior distribution (dotted line) in the three estimation models (rows) with the three levels of true nonlinearity (columns).	82
2.8	The mean true depletion trajectory (solid line) with a final depletion of 0.45. Mean estimated depletion trajectories are shown where β was fixed at 1 (dashed line) or estimated with a uniform prior distribution (dotted line) in the three estimation models (rows) with the three levels of true nonlinearity (columns).	83
2.9	Estimated depletion in year 16 from the operating model (True) and the three models given different levels of nonlinearity (β), depletion (columns), and priors (rows). The median value is shown with a '+' and the 75% probability interval is shown with the vertical line. The horizontal dashed line indicates the median of the true depletion.	84
3.1	Movement rates from the available area to unavailable area and the unavailable area to available area as a function of harvest rate for the effort-dependent two-area model (top row) and as a function of density in the available area for the density-dependent two-area model (bottom row).	116
3.2	The current control rules based on the New Zealand harvest strategy standard (Ministry of Fisheries 2008a). The model-based control rule (a) is dependent on depletion. The CPUE-based control rule (b) is dependent on CPUE. The target is 0.3, the threshold is 0.2865, the soft limit is 0.2 (although it was not used), and the hard limit is 0.1.	117
3.3	Simulated trajectory for the single area model and a constant exploitation rate for the last 10 years. The mean trajectory is shown as the dark dotted line and the light dotted lines represent the 5th and 95th quantiles. The light gray lines are individual simulated trajectories.	118

3.4	Trajectories of depletion for total, available, and unavailable spawning biomass relative to the total unfished equilibrium spawning biomass from deterministic two-area effort-dependent (a) and two-area density-dependent (c) models. Shown on the right (plots b and d) are the differences of the natural log of the available spawning biomass from one year to the next divided by the difference in the natural log of the total spawning biomass for the same years. Values above one indicate that available biomass was changing faster than total biomass (hyperdepletion) while values below one indicate the opposite (hyperstability).	119
3.5	Median depletion trajectories with 5th and 95th quantiles from simulations using different operating model assumptions (rows) using the historical model-based (left), current model-based (middle), and current CPUE-based (right) control rules. The vertical line shows when management using the control rule began, and the horizontal dashed line is 30% B_0 for reference.	120
3.6	The probability of the true depletion for the single-area (left column) and two-area models (middle and right columns) being below the 30% (top) and 10% (bottom) for each year when using the historical model-based control rule. The assessment-based control rules, with and without estimating β , are shown along with perfect knowledge of abundance applied to the control rule.	121
3.7	Median of the median depletion vs. median average annual catch with bars indicating the 25 th and 75 th percent quantiles for different periods of the historical control rule analysis: a–b) first 10 years after management began (years 11–20), d–f) years 21–30, and g–i) years 51–70. The horizontal dashed line is the 30% depletion target and the vertical dashed line is $C_{30\%}$	122
3.8	The probability of the true depletion for the single-area (left column) and two-area models (middle and right columns) being below the 30% (top) and 10% (bottom) for each year when using the current model-based control rule. The assessment-based control rules, with and without estimating β , are shown along with perfect knowledge of abundance applied to the control rule.	123
3.9	Median of the median depletion vs. median average annual catch with bars indicating the 25 th and 75 th percent quantiles for different periods of the current model-based control rule analysis: a–c) first 10 years after management began (years 11–20), d–f) years 21–30, and g–i) years 51–70. The horizontal dashed line is the 30% depletion target and the vertical dashed line is $C_{30\%}$	124
3.10	The probability of the true depletion being below the targets of 30% (top) and 10% (bottom) for each year that fishing occurred in the future analysis when using the CPUE-based control rule with the single-area and two-area operating models (columns). The low catch is 2000 metric tons and is near the MSY catch target and the high catch is 4000 metric tons. Perfect knowledge assumes that CPUE is exactly known and the catch target is 2000 metric tons.	125

3.11	Median of the median depletion vs. median average annual catch with bars indicating the 25 th and 75 th percent quantiles for different periods of the current CPUE-based control rule analysis: a–c) first 10 years after management began (years 11–20), d–f) years 21–30, and g–i) years 51–70. The horizontal dashed line is the 30% depletion target and the vertical dashed line is $C_{30\%}$. The “low catch” target was 2000 metric tons and the “high catch” target was 4000 metric tons. The perfect knowledge scenarios almost exactly overlap the corresponding low catch scenarios.	126
3.12	Estimates of β in each year that had an assessment for the single-area operating model. The “x” points denote estimates from individual simulations. The blue dots are the median of the estimates for that year. The line connects the blue dots in every 5 th year, which are the years with most assessments since that is the default assessment period in the control rule.	127
A.1	Catches (’000 mt) by year of orange roughy from four different stocks: East Chatham Rise (ECR), Mid-East Coast (MEC), Northwest Chatham Rise (NWCR), and Australia’s Eastern Zone (AUS).	155
B.1	Median of the posterior distribution for the spawning biomass trajectory of the East Chatham Rise (ECR) stock with a 90% HPD interval in grey (panels a and b). Fitted CPUE (panel a) and survey indices (panel b) are also plotted with 90% confidence intervals calculated from the CV’s provided with the data (grey lines) and CV’s with the median of the estimated extra variability included (darker extended lines). The same plots are shown in panels c) and d), but with 90% posterior predictive distributions instead of confidence intervals for the data. Posterior distributions for depletion (e) and unfished spawning biomass, B_0 (f) are also shown with the median and the 90% HPD interval. Actual samples from the posterior are indicated immediately below the posterior distributions with small black marks.	161
B.2	Median of the posterior distribution for the spawning biomass trajectory of the Mid-East Coast (MEC) stock with a 90% HPD interval in grey (panels a and b). Fitted CPUE (panel a) and survey indices (panel b) are also plotted with 90% confidence intervals calculated from the CV’s provided with the data (grey lines) and CV’s with the median of the estimated extra variability included (darker extended lines). The same plots are shown in panels c) and d), but with 90% posterior predictive distributions instead of confidence intervals for the data. Posterior distributions for depletion (e) and unfished spawning biomass, B_0 (f) are also shown with the median and the 90% HPD interval. Actual samples from the posterior distribution are indicated with small black marks immediately below the nonparametric density estimate of the posterior distribution.	162

B.3	Median of the posterior distribution for the spawning biomass trajectory of the Northwest Chatham Rise (NWCR) stock with a 90% HPD interval in grey (panels a and b). Fitted CPUE (panel a) and survey indices (panel b) are also plotted with 90% confidence intervals calculated from the CV's provided with the data (grey lines) and CV's with the median of the estimated extra variability included (darker extended lines). The same plots are shown in panels c) and d), but with 90% posterior predictive distributions instead of confidence intervals for the data. Posterior distributions for depletion (e) and unfished spawning biomass, B_0 (f) are also shown with the median and the 90% HPD interval. Actual samples from the posterior distribution are indicated with small black marks immediately below the nonparametric density estimate of the posterior distribution.	163
B.4	Median of the posterior distribution for the spawning biomass trajectory of the Eastern Zone of Australia (AUS) stock with a 90% HPD interval in grey (panels a and b). Fitted CPUE (panel a) and survey indices (panel b) are also plotted with 90% confidence intervals calculated from the CV's provided with the data (grey lines) and CV's with the median of the estimated extra variability included (darker extended lines). The same plots are shown in panels c) and d), but with 90% posterior predictive distributions instead of confidence intervals for the data. Posterior distributions for depletion (e) and unfished spawning biomass, B_0 (f) are also shown with the median and the 90% HPD interval. Actual samples from the posterior distribution are indicated with small black marks immediately below the nonparametric density estimate of the posterior distribution.	164

ACKNOWLEDGMENTS

I express sincere appreciation to the University of Washington and the School of Aquatic and Fishery Sciences. Funding was provided by the New Zealand Seafood Industry Council, the Orange Roughy Management Company (now part of the Deepwater Group), and SAFS. I am also grateful to the Northwest Fishery Science Center for employing me and allowing me the time to complete this dissertation.

I was very fortunate to have a diverse committee composed of extremely knowledgeable individuals. Juan Pampin from the DXARTS department was gracious enough to be my initial GSR, but unfortunately was unable to continue due to sabbatical. Danny Grunbaum from the School of Oceanography quickly filled in and was an asset by providing a different way of looking at my questions. I thank all of my committee members for their patience and mentoring throughout. John Horne pushed my horizon of thought beyond boundaries that I thought were possible. Kevin Stokes secured funding for many years, supported me through difficult assessment meetings in New Zealand, and is a great friend. Tim Essington taught me that not everything is pure mathematics and modeling, and that considering ecological relationships can help one understand the issues. André Punt is absolutely amazing with his knowledge and how quickly he would read my drafts and provide highly constructive comments. And finally, I cannot thank Ray Hilborn enough for his mentoring, patience, understanding, and all of the opportunities he gave me. I am very fortunate to have these people as my committee members and I thank them all.

I could not have completed my degree without the help and support of many friends. I cannot possibly name them all, but I appreciate them all. Those morning swims followed by bacon maple bars and engaging conversations energized me to continue working. My lab-mates were incredibly supportive, especially during my written and oral exams. My friends outside of school were always supportive and kept encouraging me to finish. Special

thanks go to Neala Kendall, Sam Warren, Matt and Carly Baker, Carey McGilliard, Chad Jennings, Eva Dusek, Melissa Haltuch, and especially Juan Valero. I am also very grateful for my long-time friends Ben Allen and Ryan Leong. I have known them since I was in 6th grade and they have always been there to tell me I can do it, whether it was finishing a Ph.D. or paddling out to a big wave.

I cannot thank my family enough for the support, understanding, and patience they have shown throughout the years of my education. My sisters, Joanne and Janine, have always been looking out for me, and my niece, Alyssa, and my nephew, Luke, were amazed when they realized I was going to be a “fish doctor.” Aunt Ev has always been a huge support and the inspiration from my Uncle Bob carried me through many late nights. My mother taught me that I can do anything and in tough times I could hear her say “you know what you want, so get to work and do it.” The family I married into during my Ph.D. education made me feel like I have always been a part of that family and showed an amazing amount of support and understanding.

I was fortunate to have met my wife while I was finishing my education. She was always understanding of the late nights, the frustration, and the doubts, and she was always there for me to tell that I can do this. I am extremely grateful for her support and her love.

This dissertation is dedicated to my father. He is a huge inspiration and has shown an extraordinary level of care for me all of my life. It was 20 years ago that I told my father I would finish a Ph.D. at the University of Washington, and he never once doubted that I would reach that goal. Thank you Dad for your support.

DEDICATION

to

my father

INTRODUCTION

The effective management of a fishery requires tracking abundance in some way such that the total fishing mortality can be adjusted to optimize yield and avoid low stock levels. Management tools include restricting effort through capacity limitations and seasonal/area closures, imposing gear restrictions, and setting quotas on the harvest. To ensure a sustainable fishery, these management tools require reliable assessments of stock status using informative data that are representative of changes in abundance. Not only is successful management more likely when scientists use the best available information to assess a stock, but policy-makers, stakeholders, and the general community are better informed about the condition of the stock as well as that of the fishery (Maunder *et al.* 2006).

Catch-rate data are commonly used as an index of abundance when assessing a stock, and can be derived from fishery-dependent or fishery-independent (survey) data. Collecting these data from statistically-designed research surveys is preferred, but for many stocks, sufficient fishery-independent data are not available to adequately track trends in abundance. Therefore, scientists often rely upon fishery-dependent data, in the form of commercial catch and effort records, even though these data may violate some statistical assumptions or may not be as informative as survey data (Maunder *et al.* 2006; Winters and Wheeler 1985).

Commercial catch and effort data are commonly compiled into a relative index of abundance called catch-per-unit-effort (CPUE) and assumed to be proportional to abundance.

$$\frac{C_y}{f_y} = U_y = qN_y \quad (1)$$

where C and f refer to catch and effort, U is CPUE, q is a catchability coefficient, and N is the average abundance, in numbers of fish or more commonly biomass, over one fishing season (y), which is typically a year. For most fisheries, catch is relatively easy to measure, but a proper measure of effort can be difficult to obtain (Rothschild 1977). The standardization of CPUE can solve many of these difficulties (Maunder and Punt 2004), but assuming a proportional relationship between CPUE and abundance is risky (Hilborn

and Walters 1992).

Fishery scientists have emphasized the use of fishery catch and effort data to provide indices of abundance for over a century (Smith 1994). For example, Garstang (1900) reported catch rate data for many species of fish caught in the English trawl fishery to support his hypothesis that the bottom fisheries are exhaustible, and Schaefer (1954) used catch-per-unit-effort to estimate stock size. Currently, CPUE is one of the most common pieces of management-useful information from a fishery and is still of interest to scientists, as indicated by Maunder *et al.* (2006) who discuss methods to overcome some of the common problems with catch and effort data.

A derivation of CPUE

Baranov (1918) mathematically explained the concept of mortality as the decrease over time (t) in numbers of a cohort of a fish population (N) due to natural mortality (M) and fishing mortality (F) using the differential equation

$$\frac{dN}{dt} = -FN - MN \quad (2)$$

The solution to Equation 2 is

$$N_t = N_0 e^{-(F+M)t} = N_0 e^{-Zt}, \quad (3)$$

where Z is the total instantaneous mortality. The average size of the cohort over one season of fishing (time interval $[0,1]$ and subscripted with y) is then

$$\begin{aligned} \overline{N}_t &= \int_0^1 N_0 e^{-Zt} dt / (1 - 0) \\ \overline{N}_t &= \frac{N_0 (1 - e^{-Z})}{Z} \end{aligned} \quad (4)$$

The relationship of catch over time is similar to the relationship of abundance over time, but is a function of only fishing mortality (F).

$$\frac{dC}{dt} = -FN \quad (5)$$

The instantaneous fishing mortality rate is a measure of fishing effort that is not easily interpreted. Therefore, a more meaningful metric for effort, such as boat days or number

of trawls, is often assumed as proportional to the fishing mortality rate,

$$F = qf_t, \quad (6)$$

where q is the catchability coefficient (Holt *et al.* 1959), and nominal effort (f) occurs over one fishing season. Paloheimo and Dickie (1964) defined the catchability coefficient as the product of the gear efficiency (c) and the area swept by a standard unit of gear (a), divided by the total area occupied by the stock (A).

$$q = \frac{ca}{A} \quad (7)$$

Substituting the nominal effort relationship for F into Equation 5 and rearranging gives

$$dC = qf_t N dt,$$

and integrating over one season leads to

$$\begin{aligned} \int_0^{C_y} dC &= \int_0^1 qf_t N_0 e^{-Zt} dt \\ C_y &= \frac{qf_y}{Z} N_0 (1 - e^{-Z}) \end{aligned} \quad (8)$$

Equation 8 is the Baranov catch equation discussed by Baranov (1918), Ricker (1940), and Delury (1947), among others and can be further simplified by substituting in Equation 4

$$C_y = qf_y \overline{N}_y \quad (9)$$

Dividing by f_t gives Equation 1, which is a proportional relationship between CPUE and abundance.

Furthermore, defining density (D) as the abundance of fish per area,

$$D_y = \frac{\overline{N}_y}{A},$$

and using Equation 7, Paloheimo and Dickie (1964) showed that the density of the stock is also proportional to CPUE.

$$U_y = q' D_y,$$

where q' is the fraction of the overall density reduced by the application of one unit of gear.

$$q' = ca$$

Assumptions for CPUE to be a proportional index of abundance

The following assumptions that led to the derivation of CPUE above are important when judging its utility as a proportional index of stock abundance.

1. There is no recruitment to the population during the time period of interest (one year),
2. natural mortality, M , does not vary with time,
3. nominal effort is measured in terms of one standard unit,
4. fishing mortality is linearly related to nominal effort (Equation 6), and
5. catchability (q) is constant over time and space (i.e., within and between seasons).

Assumption 1 can be satisfied if recruitment into the population occurs mainly at one time of year either before or after the fishery occurs, and 2) although natural mortality is likely to vary over time, it is commonly assumed to be constant. Ricker (1940, 1944) discussed cases where recruitment is present during the fishing season, and Quinn and Deriso (1999) present more complex descriptions of recruitment and natural mortality. The three assumptions related to fishing mortality and effort (3–5) are critical when assuming that catch-per-unit-effort (CPUE) is linearly related to abundance, thus is the focus below.

As noted earlier, nominal effort is a more meaningful measure than instantaneous fishing mortality and introducing a more common measurement of effort can be useful in additional analyses, especially those related to economics (Rothschild 1977). However, an appropriate measure, such as boat days, hauls, or searching time, must be defined and standardized. Hours trawled or number of trawls are typical measures in bottom trawl fisheries and searching time is usually a better measure for purse-seine fisheries (Punsly 1987) or fisheries that incur a lot of searching and handling time (Cooke 1985b).

A crucial assumption is that catchability remains constant within a season and between seasons. Many factors that may cause changes in catchability are discussed below, but first,

for a proportional relationship between fishing mortality and fishing effort (Equation 6) to be satisfied, the area occupied by the stock must remain constant, the units of gear must operate independently, and fishing must occur in a random manner, at least with respect to the distribution of fish (Beverton and Holt 1957). In the derivation of the catch equation, Baranov (1918) assumed a population of immobile fish distributed uniformly over the area A , and the units of effort were independent and not overlapping. Ricker (1944) satisfied the assumption of random fishing by thinking of a mobile population that would quickly repopulate the area fished. However, fishing is not random (Hilborn and Walters 1992) and the relationship between fishing mortality and fishing effort is not likely to be linear (Rothschild 1977).

The effect of fish behavior and fishing operations on catchability

The behavior of a fish population and how the fishery responds to that fish population frequently results in catchability changing over time (Hilborn and Walters 1992; Maunder *et al.* 2006). Change in catchability is often related to abundance, and three general relationships between CPUE and abundance have been described by Hilborn and Walters (1992): proportional, hyperstability, and hyperdepletion. Proportional is the commonly-assumed linear relationship between CPUE and abundance. Hyperstability occurs when CPUE declines at a slower rate than abundance, making it difficult to detect initial declines in abundance. Hyperdepletion is when CPUE declines more rapidly than abundance, which may result in a pessimistic view of the stock when using CPUE as an index of abundance. Figure 1 shows these three relationships between CPUE and abundance.

Many authors have examined reasons why catchability may not be proportional to abundance. First, the total area occupied by a stock often shrinks with declines in total abundance, resulting in an inverse relationship between stock abundance and catchability (Crecco and Overholtz 1990; Rose and Leggett 1991; Winters and Wheeler 1985). In addition, Paloheimo and Dickie (1964) noted that heterogenous schooling behavior may result in CPUE reflecting changes in fish distributions rather than fish abundance. For example, catchability may remain stable for aggregating species as the overall abundance decreases (Hanchet *et al.* 2005; Paloheimo and Dickie 1964). Fish behavior, how fish distribute themselves,

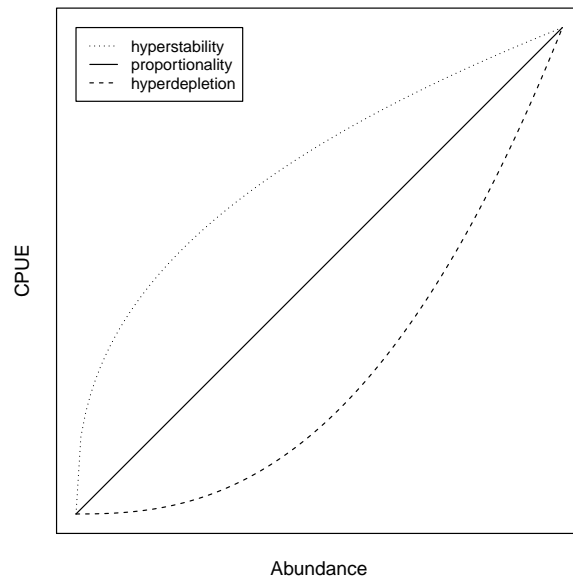


Figure 1: Three possible relationships between CPUE and abundance as described by Hilborn and Walters (1992).

has resulted in hyperstability being observed in many fisheries (Crecco and Overholtz 1990; MacCall 1976; Rose and Kulka 1999), but a prevalence of low densities of fish with few high densities is likely to result in hyperdepletion (Hilborn and Walters 1992). Hyperdepletion may also occur when catch and effort data are not analyzed in a proper spatial manner (Walters 2003).

The behavior of fishermen can also be the cause of a nonlinear relationship between CPUE and abundance. Fishing is not a random process and fishermen often compete or cooperate when searching for concentrations of fish (Hilborn and Walters 1992). Competition among units of gear, known as interference, results in asymptotic fishing mortality with increasing effort, causing a breakdown in the proportional relationship between CPUE and abundance (Gillis and Peterman 1998; Hilborn and Walters 1992; Rothschild 1977). Conversely, cooperation, or information sharing, between fishermen results in a faster increase in fishing mortality as more units of gear are added (Branch *et al.* 2006; Hilborn and Walters 1992; Rothschild 1977). Additionally, changes in catchability can be a result of changes in the fleet's spatial extent and the degree of the fleet's spatial patchiness, as

observed in cod (Salthaug and Aanes 2003; Swain and Sinclair 1994), tuna (Maunder *et al.* 2006; Punsly 1987), and whale (Cooke 1985b) fisheries.

Knowledge, technology, and gear also play an important role in the relationship between CPUE and abundance. The efficiency of a fleet is likely to change over time due to increases in technology and knowledge (Maunder *et al.* 2006) and from boats and skippers joining or dropping out of the fishery (Hilborn and Walters 1992). Gear may also have limitations such as reductions in catchability as the gear becomes full or experiences similar catch rates at high abundances, called saturation (Rothschild 1977). These examples result in a violation of the proportional assumption between fishing mortality and nominal effort seen in Equation 6.

Analyzing and standardizing catch and effort data

The effects of many of the factors leading to a change in catchability can be removed by using an appropriate measure of effort (Cooke 1985b; Hilborn and Walters 1992), through proper spatial analysis of the catch and effort data (Hilborn and Walters 1992; Walters 2003), and by standardizing the catch-per-unit-effort (Maunder and Punt 2004). An appropriate measure of effort is one that is related to the abundance. For example, if handling time is significant or fishing vessels search for aggregations of animals, then searching time should be used (Hilborn and Walters 1992). However, Cooke and Beddington (1984) and Cooke (1985b) explain that variable catchability can result in lost searching time when catchability is good and catches must be handled more often than when conditions are bad, thus CPUE will decline at a slower rate than abundance.

Given that fishing is not random and that fish are not distributed uniformly, catch and effort data can be stratified into smaller spatial cells which are more likely to show random fishing behavior (Beverton and Holt 1957; Hilborn and Walters 1992). This is unlikely, even in somewhat small spatial areas (Hilborn and Walters 1992). When catch and effort data are spatially stratified, unfished strata must not be ignored and assumptions will have to be made regarding the unobserved catch rate in these cells (Walters 2003).

Beverton and Holt (1957) suggested choosing a standard vessel and determining the relative fishing power of all other vessels, but there are other important variables not specif-

ically related to a fishing vessel, such as depth and location. Currently, statistical methods such as generalized linear models are commonly used to standardize catch and effort data, and can incorporate qualitative and quantitative variables including vessel characteristics, time of year, area, and depth (Maunder and Punt, 2004). However, standardizing the catch and effort data does not ensure that catchability will remain constant over time and other factors that cannot be accounted for may invalidate the assumed proportional relationship shown in Equation 1.

Modeling catchability as a function of abundance

Fishery-independent data are not available for all stocks, and discarding the catch and effort data may not be a solution when the stock size must be estimated. An integrated assessment is one way to use all available information to assess a stock, and can provide insight on inconsistencies among different data sources, although it may be difficult to reconcile those differences (Maunder *et al.* 2006). A more complex model than strict proportionality between CPUE and abundance can be used in a stock assessment to reconcile inconsistencies in the CPUE data, and to reduce bias in the estimates of stock size and status. Various methods have been used to model changes in catchability, including assuming density-dependent catchability (Harley *et al.* 2001) and time-varying equations where catchability is random with or without autocorrelation (National Research Council 1998; Wilberg *et al.* 2010).

A power function is often used to model the relationship between CPUE and abundance by assuming that catchability (q) is a nonlinear function of abundance (N) (e.g., Bannerot and Austin 1983; Hanchet *et al.* 2005; Harley *et al.* 2001).

$$q = \alpha N^{\beta'}$$

The relationship between CPUE and abundance can be derived by substituting this model for nonlinear catchability into Equation 1.

$$U = \alpha N^{\beta'} N$$

$$U = \alpha N^{\beta'+1}$$

Simplifying notation, the relationship can be defined as

$$U = \alpha N^\beta \quad (10)$$

where α and β are parameters. A hyperstable relationship occurs when $\beta < 1$ and $\beta > 1$ indicates hyperdepletion. A proportional relationship occurs when $\beta = 1$.

In a few cases, the relationship between CPUE and abundance has been modeled with equations allowing more flexibility. Peterman and Steer (1981) used the Michaelis-Menten equation to allow for gear saturation. Richards and Schnute (1986) also modeled catchability as density-dependent, but with an even more general and flexible model. Rindorf and Andersen (2008) extended the power function in Equation 10 to include the possibility of biomass remaining in refugia and being unavailable to the fishery.

Regardless of the functional form used to model the relationship between CPUE and abundance, it is important to understand the relationship at different levels of abundance. First, CPUE is defined to be zero when abundance is zero. Second, for the case of this argument, assume that CPUE is one when the abundance is equal to the equilibrium unfished abundance. If CPUE declines slower than abundance at high abundance, then it must decline faster than abundance at low abundances for the relationship to equal zero when abundance is zero (and vice versa if CPUE declines faster at high abundances). This, of course, assumes that the relationship between CPUE and abundance is a smooth function and, for example, doesn't suddenly drop to zero with an infinite slope at some low biomass or CPUE doesn't become zero before the abundance is equal to zero.

This can be investigated further using the power function presented in Equation 10. We scale the CPUE (U) such that it has a value of 1 at the unfished equilibrium abundance, noted as K .

$$1 = \alpha K^\beta \quad (11)$$

Then, solving for alpha,

$$\alpha' = K^{-\beta} \quad (12)$$

provides us with the proper scalar. This allows us to make a direct comparison between CPUE and abundance because the slope for the proportional relationship ($U = \alpha N$) is $1/K$.

The derivative of the relationship between CPUE and abundance with the slope defined in Equation 12 is

$$\frac{dU}{dN} = K^{-\beta} \beta N^{(\beta-1)} \quad (13)$$

And, solving for the abundance (N) where the slope is equal to $1/K$.

$$\begin{aligned} \frac{1}{K} &= K^{-\beta} \beta N^{(\beta-1)} \\ N &= \left(K^\beta / K \beta \right)^{1/(\beta-1)} \end{aligned} \quad (14)$$

Furthermore, if abundance is rescaled such that $K = 1$ ($N' = N/K$), then

$$N' = \left(\frac{1}{\beta} \right)^{1/(\beta-1)} \quad (15)$$

As seen in Figure 2, using the hypothetical example described above, the abundance at which the slope equals α is less when $\beta < 1$ than when $\beta > 1$. As β approaches 1, the abundance at which the slope equals 1 approaches 0.37. Therefore, over the range of abundance between zero and K , CPUE is more commonly decreasing slower than abundance.

Even though the slope of the relationship between CPUE and abundance changes over the range of abundance, estimates of β remain constant with subsets of data, as long as the true abundance is known. For example, if CPUE data showed hyperdepletion, but were available only for the range of abundances between 0.1 and 0.3 where CPUE is declining more slowly than abundance, the estimate of β would not, in fact, be less than one (indicating hyperstability), but would be the same as if you had the CPUE data over the entire range of abundance. This can be shown in two ways. First, the second derivative of the power function indicates the curvature of the line,

$$\frac{d^2U}{dN^2} = K^{-\beta} (\beta - 1) \beta N^{(\beta-2)} \quad (16)$$

And given that N is always positive, the second derivative shows that the relationship is concave up when $\beta > 1$ and concave down when $\beta < 1$, as expected. Therefore, even though the slope of the relationship between CPUE and abundance changes in relation to the true abundance, the concavity remains the same, which is determined by β . A

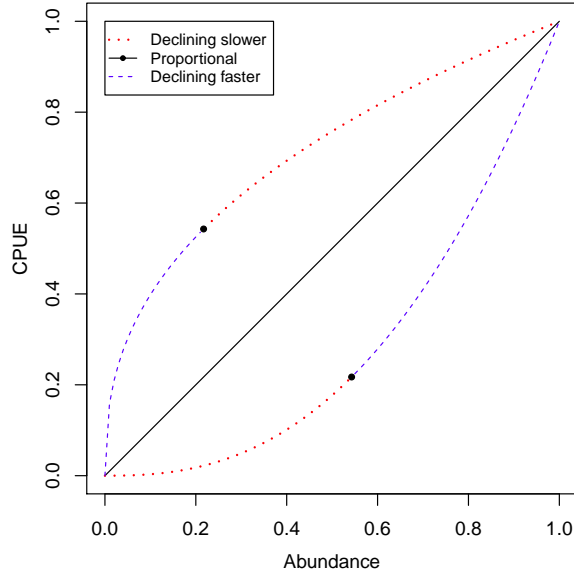


Figure 2: Areas where CPUE is declining faster than abundance (blue long dashes) and declining slower than abundance (red short dashes) in the power function αN^β , with $\alpha=1$ and $\beta=0.4, 1, \text{ or } 2.5$.

second demonstration can be seen by taking the natural log of CPUE. This makes a linear relationship between the natural log of CPUE and the natural log of abundance, where β is the slope.

$$\ln(U) = \ln(\alpha) + \beta \ln(N) \quad (17)$$

Because this is a linear relationship, β remains constant throughout the range of abundances, and α is adjusted as K changes, as in Equation 12. This result is important because even if K is estimated with error, the estimate of β will not change, given that all other factors are constant.

The implication of this thought experiment is that the absolute change in CPUE (the difference between two values) is dependent on absolute abundance (i.e., where the CPUE was observed relative to unfished abundance). However, the proportional change in CPUE is independent of what absolute abundance is, but is a function of the proportional change in abundance.

$$\frac{U_{y+1}}{U_y} = \left(\frac{N_{y+1}}{N_y} \right)^\beta \quad (18)$$

For example, if $\beta = 2$ and the abundance (relative to 1) declines from 1.0 to 0.9, the CPUE declines from 1.0 to 0.81. However, if abundance declines by half from 0.2 to 0.1, the CPUE declines from 0.01 to 0.0025, an absolute value of 0.0075, but a ratio of 0.25. Additionally, if abundance declines by half from 1.0 to 0.5, the CPUE declines from 1.0 to 0.25, which is an absolute value of 0.75, but the same ratio of 0.25. In other words, the ratio of the differences in log space equals β , which is the slope of Equation 17.

This thought experiment applies only when the true relationship between CPUE and abundance is density-dependent and described by the power function in Equation 18. This is likely a simplistic assumption useful for describing specific time periods of CPUE, and not the entire time that fishing has occurred. It is likely that there are other factors contributing to a non-proportional relationship, which, depending on the state of the population, may change the relationship between CPUE and abundance (e.g., the stock is heavily fished and decreasing as opposed to lightly fished and possibly increasing). If CPUE is nonlinearly related to abundance because fish are disturbed by fishing and migrate away from the fishing areas, it may not be practical to assume the same level of nonlinearity when the stock is lightly exploited and fish are migrating back to the fishing area.

Evidence of departures from a proportional relationship between CPUE and abundance

Regardless of all the warnings, fish population abundance is often estimated using catch and effort data while assuming that CPUE is proportional to abundance (Harley *et al.* 2001; National Research Council 1998). This can lead to misinforming scientists, managers, the fishing industry, and the general public about the status of fisheries (Maunder *et al.* 2006). For example, Myers and Worm (2003) concluded that the biomass of tuna, billfishes, and swordfish has severely declined based on the observation that catch-rates quickly fell when first exploited. But, Polacheck (2006) and Hampton *et al.* (2005) explained that catch rates of tuna are most likely not a proportional index of abundance in the early years of the fishery, and Walters (2003) suggested that calculating CPUE over a wide area may artificially introduce hyperdepletion. An example of hyperstability causing misleading advice occurred in the northern cod fisheries. Rose and Kulka (1999) noted that northern cod (*Gadus*

morhua) were assessed in the 1980's under the assumption that CPUE was linearly related to abundance, but found that although CPUE was locally related to abundance, it was not regionally because of hyperaggregation.

Many studies on the relationship between CPUE and abundance have found empirical evidence of CPUE declining slower than abundance. Hyperstability has been observed in pelagic fisheries for herring (*Clupea harengus*) and sardine (*Sardinops sagax*) (MacCall 1976; Ulltang 1980; Winters and Wheeler 1985) and groundfish fisheries for cod (*Gadus morhua*) and haddock (*Melanogrammus aeglefinus*) (Crecco and Overholtz 1990; Rose and Leggett 1991; Swain and Sinclair 1994). Additionally, Chinook salmon (*Oncorhynchus tshawytscha*) (Peterman and Steer 1981), American shad (*Alosa sapidissima*) (Crecco and Savoy 1985), and yellowtail snapper (*Ocyurus chrysurus*) (Bannerot and Austin 1983) fisheries have seen an inverse relationship between catchability and abundance. Harley *et al.* (2001) compiled CPUE and independent abundance data collected by the International Council for the Exploration of the Sea (ICES) and performed a meta-analysis to test the hypothesis that CPUE is proportional to abundance. They found evidence supporting hyperstability for all of the stocks included, although one stock was weakly supported. Finally, recreational fisheries targeting spawning aggregations of barred sand bass (*Paralabrax nebulifer*) and kelp bass (*Paralabrax clathratus*) have also shown stable or slowly declining CPUE (Erisman *et al.* 2011).

Hyperdepletion is also believed to occur in the CPUE data from some fisheries (Hilborn and Walters 1992; Walters 2003). The meta-analysis performed by Harley *et al.* (2001) showed support for hyperdepletion in hake (*Merluccius merluccius*) fisheries. Ahrens and Walters (2005) reported that even after correctly analyzing spatial longline catch and effort data for tuna and billfish species, hyperdepletion was still present. Sosa-Lopez and Manzo-Monroy (2002) came to a similar conclusion after analyzing yellowfin tuna (*Thunnus albacares*) catch and effort data. Furthermore, Fonteneau and Richard (2003) reported that trends in CPUE are likely to be overly pessimistic for bycatch species such as billfishes. Surprisingly, Davies and Jonsen (2011) found evidence of hyperdepletion in the fishery-independent survey index of cusk (*Brosme brosme*), although parameter estimates were uncertain.

Despite this evidence that CPUE is not always proportional to abundance, some data indicate that CPUE is a good indicator of abundance. Dunn *et al.* (2000) concluded that proportionality is a reasonable assumption for many New Zealand stocks, although the variability in their results was high. Hanchet *et al.* (2005) found that CPUE tracked the abundance of an aggregating species, southern blue whiting (*Micromesistius australis*).

Motivation

As can be seen, fish and fisheries behave in different ways and the relationship between CPUE and abundance not only depends on behavior, but also on how the catch and effort data are analyzed. Therefore, determining how CPUE relates to abundance should be done on a case by case basis to determine the possibility of using CPUE for the assessment and management of a specific species or type of fishery. Simulation techniques and management strategy evaluation (Butterworth *et al.* 1997; Sainsbury 2000) may also be used to determine how CPUE can best be used.

Fishery-independent catch-rate data are more likely to be proportional to abundance than fishery-dependent CPUE because surveys are typically well designed and appropriate for the stock being surveyed, and it may seem appropriate to simply omit the questionable fishery-dependent CPUE. However, there is a benefit to using CPUE data in an assessment. CPUE data are often available for more years than survey data and can provide insight into historical time periods. Fishers are most familiar with catch-rates and often appreciate their use in assessments. Survey data may not be proportional to abundance (Davies and Jonsen 2011) and simply omitting CPUE would imply that the survey data are the representative dataset. Finally, it is useful to use CPUE and survey data in an assessment to further understand the relationship between CPUE and abundance, which can then be applied to the assessment and management of stocks that have only CPUE data or are using a CPUE-based control rule.

The research in this Ph.D. dissertation focuses on the relationship between CPUE and abundance and how its use when assessing and managing fisheries may be affected by some of its shortcomings. Three stand-alone chapters are presented with methods and results from analyses estimating the amount of nonlinearity in the relationship between CPUE and

abundance and its implications on fisheries management. The first chapter looks at the nonlinearity of empirical CPUE data from orange roughy fisheries in Australia and New Zealand. The second chapter investigates the ability to estimate nonlinearity in CPUE data using different models, assumptions, and types of data. The final chapter performs a management strategy evaluation to determine the consequences of managing a fish stock with and without estimating nonlinearity. Finally, the results presented in this dissertation are summarized and discussed.

Chapter 1

A META-ANALYSIS OF NONLINEARITY IN THE RELATIONSHIP BETWEEN CATCH-PER-UNIT-EFFORT AND ABUNDANCE IN ORANGE ROUGHY (*HOPLOSTETHUS ATLANTICUS*) STOCK ASSESSMENTS***Abstract***

Catch-rate data are commonly used as an index of abundance when assessing a stock, and can be derived from fishery-dependent or fishery-independent data. Commercial catch and effort data are commonly standardized into a relative index of abundance called catch-per-unit-effort (CPUE) and are often assumed to be proportional to abundance. However, there are many reasons for a departure from a proportional relationship. This study used fishery CPUE data from four orange roughy fisheries in a hierarchical state-space model to estimate the hyperparameters of a distribution for a nonlinearity parameter in the relationship between CPUE and abundance. A prior distribution for the nonlinear parameter was developed and showed that hyperdepletion (CPUE declines faster than abundance) was more probable than hyperstability (CPUE declines slower than abundance). Although hyperdepletion was unexpected for an aggregating species, explanations include depletion of localized aggregations, natural variation in the size of spawning aggregations, and disruption due to fishing. This prior distribution may be used to improve assessments of orange roughy and other similar species where fishery-dependent catch-rates are an important source of information.

1.1 Introduction

The effective management of a fishery requires tracking the abundance of target species in some way such that the total fishing mortality can be adjusted to optimize yield and avoid low stock levels. Management tools include restricting effort through capacity limitations and seasonal/area closures, imposing gear restrictions, and setting quotas on the harvest.

To ensure a sustainable fishery, these management tools require reliable assessments of stock status using informative data that are representative of changes in abundance. Not only is successful management more likely when scientists use the best available information to assess a stock, but policy-makers, stakeholders, and the general community are better informed about the condition of the stock as well as of the fishery (Maunder *et al.* 2006).

Catch-rate data are commonly used as an index of abundance when assessing a stock, and can be derived from fishery-dependent or fishery-independent (survey) data. Collecting these data from statistically designed research surveys is preferred, but for many stocks sufficient fishery-independent data are not available to adequately track trends in abundance. Therefore, scientists often rely upon fishery-dependent data, in the form of commercial catch and effort records, even though these data may violate some statistical assumptions or may not be as informative as survey data (Winters and Wheeler 1985; Maunder *et al.* 2006).

Commercial catch and effort data are commonly standardized using statistical approaches into a relative index of abundance called catch-per-unit-effort, or CPUE (Maunder and Punt 2004), and is usually assumed to be proportional to abundance.

$$\frac{C}{E} = U = qB, \quad (1.1)$$

where C and E refer to catch and effort, U is CPUE, q is a catchability coefficient, and B is the average abundance, in numbers of fish or biomass, over one fishing season. Standardizing catch and effort data may reduce the nonlinearity (Ye and Dennis 2009), but it does not guarantee a linear relationship between CPUE and abundance. For most large fisheries in developed countries, catch is relatively easy to measure, but a proper measure of effort can be difficult to obtain (Rothschild 1977) which often results in a nonlinear relationship between CPUE and abundance (Cooke 1985a; Hilborn and Walters 1992; Gillis and Peterman 1998; Walters 2003). Understanding the true relationship between CPUE and abundance is important to reduce bias when assessing a fish stock (Hilborn and Walters 1992).

The behavior of a fish population and how the fishery responds to that fish population frequently change catchability over time resulting in a nonproportional relationship between CPUE and abundance (Hilborn and Walters 1992; Maunder *et al.* 2006). Changes in catchability are often related to the abundance of the population and three general relationships

between CPUE and abundance have been described by Hilborn and Walters (1992): proportional, hyperstability, and hyperdepletion. Proportional is the commonly assumed linear relationship between CPUE and abundance. Hyperstability occurs when CPUE declines at a slower rate than abundance making it difficult to detect initial declines in abundance. Hyperdepletion is when CPUE declines more rapidly than abundance, which may result in a pessimistic view of the stock when using CPUE as an index of abundance.

Many authors have studied the relationship between CPUE and abundance and what may cause a departure from a proportional relationship (for a review see Wilberg *et al.* 2010). Factors due to fish behavior include heterogenous aggregations, schooling, stock area, the distribution of fish, and differing susceptibility to harvest between members within a population (Paloheimo and Dickie 1964; Winters and Wheeler 1985; Hilborn and Walters 1992; Swain and Sinclair 1994; Rose and Kulka 1999). Fishing behavior is rarely random and many authors have studied how catchability relates to factors such as handling time, searching time, gear saturation, and cooperation among fishers (Cooke and Beddington 1984; Hilborn and Walters 1992; Gillis and Peterman 1998; Salthaug and Aanes 2003; Branch *et al.* 2006). Improper methods used to analyze catch and effort data may also result in a hyperdepleted CPUE series (Walters 2003; Kleiber and Maunder 2008).

Despite these known difficulties, CPUE is commonly assumed to proportionally index the abundance of fish stocks. For example, Myers and Worm (2003) used Japanese longline catch-rates to conclude that the biomass of tuna, billfishes, and swordfish has declined greatly based on rapid declines in catch-rates when first exploited. The conclusions of Myers and Worm (2003) was disputed by Polacheck (2006) and Hampton *et al.* (2005) who explained that the catch rates of tuna are most likely not proportional to abundance in the early years of the fishery, and Walters (2003) who suggested that calculating the CPUE over a wide area may have artificially introduced hyperdepletion. Rose and Kulka (1999) noted that northern cod were assessed in the 1980s under the assumption that CPUE was linearly related to abundance, but concluded that CPUE was locally related to abundance and not regionally due to hyperaggregation. Harley *et al.* (2001) compiled CPUE and independent abundance data from the International Council for the Exploration of the Sea (ICES) and performed a meta-analysis to test the hypothesis that CPUE is proportional

to abundance. They found evidence supporting hyperstability, but hyperdepletion could not be ruled out and was most evident in hake fisheries. In contrast, Dunn *et al.* (2000) performed an empirical analysis of CPUE from mostly New Zealand stocks and concluded that a proportional relationship between CPUE and abundance may actually be a reasonable assumption, although the variability in their results was very high.

Fishery-independent data are not available for all stocks and discarding the catch and effort data may not be a solution when the stock size must be estimated. Simultaneously analyzing all sources of data for stocks with fishery-independent and fishery-dependent data, as in an integrated assessment (Maunder 2003), can provide insight into inconsistencies between survey and CPUE data (Maunder *et al.* 2006). Furthermore, using a model with a relationship between CPUE and abundance that is more complex than strict proportionality may reconcile inconsistencies between the CPUE and survey data, and reduce bias in the estimates of stock size and status. These more complex models can then be applied to assessments of similar stocks which do not have fishery-independent data.

Various methods have been used to model changes in catchability including density-dependent catchability (Harley *et al.* 2001) and time-dependent equations where catchability is random with or without autocorrelation (National Research Council 1998; Wilberg and Bence 2006). In particular, a power function has often been used to model the relationship between CPUE and abundance by assuming that catchability (q) is a nonlinear function of abundance (B) (e.g. Bannerot and Austin 1983; Harley *et al.* 2001; Hanchet *et al.* 2005).

$$q = \alpha B^{\beta'}$$

The relationship between CPUE and abundance can be derived by substituting this model for nonlinear catchability into Equation 1.1 and simplifying notation.

$$U = \alpha B^{\beta} \tag{1.2}$$

where α and β are parameters, and β is defined as $(\beta' + 1)$. A hyperstable relationship occurs when $\beta < 1$, while $\beta > 1$ indicates hyperdepletion. A proportional relationship occurs when $\beta = 1$.

Data are available to study the relationship between CPUE and abundance for many fisheries (Harley *et al.* 2001; Hanchet *et al.* 2005), but orange roughy (*Hoplostethus atlanticus*) fisheries offer a unique opportunity to study this relationship for a number of reasons. First, some orange roughy stocks have fishery-independent data that can be utilized to examine the relationship between CPUE and abundance, which may also be helpful in determining how CPUE alone can be useful when assessing these stocks. Second, catch and effort data are available from when the fisheries began, offering a unique opportunity to look at the behavior of CPUE in a developing fishery instead of the relationship between CPUE and abundance after the stock has been fished for many years.

Nearly all orange roughy assessments have at one time used CPUE as a proportional index of abundance even though many scientists questioned whether CPUE is useful when managing stocks of orange roughy (e.g. Clark 1996) because catch rates typically decline quickly during the first few years of the fishery (Ministry of Fisheries 2007). Even though CPUE was not initially used as an abundance index in New Zealand because the fishery mainly occurred on aggregations and the catch rate may have remained high due to the availability of the fish in the aggregation, or the catch rate may decline faster than the abundance due to disturbance dissipating the aggregation, Francis and Clark (2005) argue that CPUE is a useful indicator of biomass for this species. Standardized CPUE is an important source of data for this high profile species because it not only offers potential information about changes in abundance, but for many stocks it is often the only information available.

This study combines CPUE and fishery-independent survey data from 4 stocks of orange roughy from New Zealand and Australia in a meta-analysis to investigate the relationship between CPUE and abundance. A hierarchical state-space model is used to estimate the hyperdistribution of the nonlinearity parameter (β) from Equation 1.2. This distribution is then summarized to provide a prior distribution for a nonlinearity parameter that may be used in future stock assessments.

1.2 *Materials and Methods*

The difficulty with analyzing the relationship between CPUE and abundance is that reliable fishery-independent estimates of abundance are needed to compare to the estimates of CPUE. Dunn *et al.* (2000) found that with fewer than nine paired observations a large reduction in biomass was necessary to accurately estimate a departure from linearity, thus limiting the number of stocks for which an analysis could be done. Rindorf and Andersen (2008) alleviated this problem by using biomass estimates from stock assessments that were not fitted to CPUE data. However, model-based estimates may not be an appropriate choice for this type of analysis for a number of reasons including that it would be treating correlated model outputs as independent data (Harley *et al.* 2001).

When paired observations are available, a power function can be used (Equation 1.2) to model the relationship between CPUE and abundance. Both variables are subject to measurement error, thus measurement error models must be used to provide unbiased estimates of the parameters (Fuller 1987). Dunn *et al.* (2000) and Harley *et al.* (2001) compared fishery-independent abundance indices to CPUE using a structural measurement error model, assuming that the abundance estimates are random variables from a common distribution. A functional model, on the other hand, assumes that the independent variables are fixed and the true values must be estimated (Fuller 1987). This allows for temporal changes to be modeled, but the estimates of the true independent variables are not statistically consistent (Thompson and Carter 2007) and are not integrated out of the likelihood (de Valpine and Hilborn 2005).

Alternatively (and more appropriately), when paired observations are not readily available, a state-space model can be used to estimate a biomass trajectory which is fitted to fishery-independent indices of abundances and fishery-dependent CPUE data (Schnute 1994). This approach was taken here because the availability of a sufficient number of independent paired observations of biomass and CPUE is uncommon for a single orange roughy stock. A discussion of the hierarchical state-space model used for this analysis follows a brief description of the data available for this meta-analysis.

1.2.1 Stocks and data

Data from Australian and New Zealand stocks of orange roughy that have been assessed and reported by Wayte and Bax (2002) and Ministry of Fisheries (2007) were considered for this analysis. The definition of a stock occasionally equates to a management area, but in many cases a stock is a subset of a management area or may be comprised of multiple management areas. There are four main stocks of orange roughy in the Australian exclusive economic zone (EEZ) and nine in the New Zealand EEZ that were considered for this study, but not all stocks were included in the final analysis due to lack of fishery-independent data. The most recent assessments of the stocks included in this analysis presented models that did not use CPUE as a data source to ensure there is agreement that the fishery-independent data is an appropriate index of the stock abundance.

Overall, three stocks in the New Zealand EEZ and one stock in the Australian EEZ fit the criteria for this study. New Zealand stocks were the Mid-East Coast (MEC), East Chatham Rise (ECR), and Northwest Chatham Rise (NWCR), and the single Australian stock was the Eastern Zone stock (AUS) (Figure 1.1). The MEC stock is comprised of management areas 2A South, 2B, and 3A, while the NWCR and ECR stocks are smaller areas within the ORH 3B management area of New Zealand. The Eastern Zone in Australia, east of Tasmania, is managed as a stock on its own. These four fisheries have supported large catches exceeding 7,000 tonnes in some years.

The East Chatham Rise stock has three separate CPUE series reflecting different fishery types and locations while the remaining stocks have only one CPUE series (see Table 1.1). More than one fishery-independent abundance series from three different types (including trawl, egg, and acoustic surveys) are also available for each stock. Table 1.2 shows the types and years of survey estimates for each stock, as well as the prior assumed for the catchability coefficient, q , of each series. More information about each stock, including the available data, is provided in supplemental material.

1.2.2 State-space model

State-space models (Harvey 1990), a special case of hidden-process models (Newman *et al.* 2006), are used to model two time series in parallel, each with error. One time series uses state equations to model the true, but unobserved, underlying process with error conditioned on the previous state. This process error may include both demographic and environmental variability. The second time series consists of observation equations with error that relate the observed data to the true states. This observation error consists of sampling variation around observations such as CPUE. State-space models have occasionally been used to analyze fisheries data (Sullivan 1992; Schnute 1994; Newman 1998; Meyer and Millar 1999b; Millar and Meyer 2000; de Valpine and Hilborn 2005) and we extend the analysis of Meyer and Millar (1999a) by using multiple sources of information in a hierarchical state-space model for orange roughy populations. Details of the state-space model are given in Appendix C.

A delay-difference model was chosen because it is a compromise between production models and age-structured models, and uses many of the parameters that are assumed known in orange roughy age-structured assessment models. Accepting the assumptions that fishery selectivity, survey selectivity, and the maturity ogive are equal and knife-edged at age k , we were able to use the weight-at-length, length-at-age, natural mortality, and age of 50% recruitment from the individual stock assessments to parameterize the delay-difference model. Additionally, because orange roughy populations have been fished for about 30 years, which is approximately their age of recruitment, we assumed that recruitment, on average, was constant (R_0). This leaves the states (biomass time series and B_0) and the process error (σ_ε^2) unknown in the state equations.

The observation equations relate CPUE and survey biomass estimates to the predicted biomass.

$$\ln(U_{u,i}) = \ln(\alpha_u^*) + \beta_u \left(\ln(B_i^{mid}) - \overline{\ln(B_{all\ i}^{mid})} \right) + \nu_{u,i} - \frac{\sigma_{\nu_{u,i}}^2}{2} \quad 1 < i \leq T \quad (1.3)$$

$$\ln(Z_{z,j}) = \ln(q_z) + \ln(B_j^{mid}) + \tau_{z,j} - \frac{\sigma_{\tau_{z,j}}^2}{2} \quad 1 \leq j \leq T, \quad (1.4)$$

where B^{mid} is the mid-year biomass, calculated as the average of the start of the year biomass

(Equation C.19) and the end of the year biomass (Equation C.19 without the recruitment, R_0 , added in) and $\overline{\ln(B_{all\ i}^{mid})}$ is the mean of the logged mid-year biomasses that have a corresponding CPUE value. The notation $U_{u,i}$ represents the CPUE for series u in year i and $Z_{z,j}$ represents the survey biomass for survey series z in year j . For the four stocks, there were six CPUE series ($u = 1..6$), each with estimated α_u and β_u parameters (see Table 1.1). Initial investigations suggested that centering the CPUE equation would improve the performance of the Markov chain Monte Carlo (MCMC) procedure when estimating β_u , and the parameter α_u can be calculated as $\alpha_u^* - \beta_u \overline{\ln(B_{all\ i}^{mid})}$, where α_u^* was directly estimated. There were also 14 survey series, of the type trawl, acoustic, or egg, assumed to be proportional to the estimated biomass with a catchability coefficient, q_z (see Table 1.2). The catchability coefficients were estimated for the trawl and acoustic surveys, while q_z for egg surveys was assumed to equal one. Many of the survey catchability coefficients were estimated with a prior distribution when available from recent stock assessments (Table 1.2).

The errors for each CPUE series, $\nu_{u,i}$, and each survey series, $\tau_{z,j}$, were assumed normal

$$\nu_{u,i} \sim N\left(0, \sigma_{\nu_{u,i}}^2\right) \quad (1.5)$$

$$\tau_{z,j} \sim N\left(0, \sigma_{\tau_{z,j}}^2\right). \quad (1.6)$$

An estimate of variability for each CPUE or survey value was available from the analyses of catch-rate data, but only estimated within year variability. Stock assessments in New Zealand often add an additional amount of error to the variability estimated from the data to account for between year variability in the series (Francis *et al.* 2003; Ministry of Fisheries 2007). Therefore, our approach was to use the observation-specific variability determined from the analysis of the CPUE or survey data and estimate an additional error parameter, ξ , for each CPUE series or each survey type (i.e., trawl, acoustic, or egg), where multiple series within a survey type would have the same additional error.

$$\sigma_{\nu_{u,i}}^2 = \ln(\text{CV}_{u,i}^2 + \xi_u^2 + 1) \quad (1.7)$$

$$\sigma_{\tau_{z,j}}^2 = \ln(\text{CV}_{z,j}^2 + \xi_y^2 + 1) \quad (1.8)$$

where y indicates the survey type (trawl, acoustic, or egg) and CV is a coefficient of variation. This means that ξ was also parameterized as a coefficient of variation, and because it

was estimated with a lower bound of zero, the CV's supplied with the data (within year variability) were taken as the minimum error for each observation. A single additional observation error was estimated for each survey type across stocks because it is believed that surveys of a similar type behave in similar ways, while CPUE series between stocks may show differences in between year variability.

Overall, the estimated parameters were biomass for each year from the state equations, two parameters for each CPUE series, one parameter for each trawl or acoustic survey series, and process error. Also, an additional observation error parameter for each CPUE series and one additional observation error parameter for each of three survey types were estimated. Descriptions of the parameters are given in Table 1.3.

1.2.3 Hierarchical state-space model

A Bayesian hierarchical model combines information from similar sources to estimate parameters related to all of those sources through a hyperdistribution. The state-space model above was combined into a hierarchical model using multiple stocks of orange roughy with a hyperdistribution for the nonlinearity parameter, β . Following the notation of Newman (2000), the hierarchical state-space model can be written as,

$$\begin{aligned}
 \text{hyperdistribution: } & h(\beta_n | \omega, \sigma_\omega^2) & n = 1, \dots, N, \\
 \text{state process: } & g(B_{n,t_n} | B_{n,t_n-1}, B_{n,t_n-2}, \Theta_n) & t_n = 2, \dots, T_n, \\
 \text{survey observations: } & f_1(Z_{n,j_n} | B_{n,j_n}, \Theta_n) & 1 \leq j_n \leq T_n, \\
 \text{CPUE relationship: } & f_2(U_{n,i_n} | B_{n,i_n}, \Theta_n) & 1 < i_n \leq T_n,
 \end{aligned}$$

where ω and σ_ω^2 are hyperparameters and n indexes the stock. We also use $\mathbf{B}^{N,T}$ to refer to a vector of the states for all stocks and years, \mathbf{Z}^N and \mathbf{U}^N to represent the survey and CPUE data for all stocks, respectively, and Θ^N to notate the parameters for all stocks including the hyperparameters, but excluding the states. Descriptions of parameters are given in Tables 1.3 and 1.4.

The posterior distribution for the parameters and hyperparameters given the data is proportional to the joint posterior distribution of all parameters and data (Meyer and Millar

1999a). Assuming that the priors for the parameters are independent and using the above notation where the superscripts N and T notate all stocks and time periods, respectively, the posterior distribution for the states and the parameters is,

$$\pi(\Theta^N, \mathbf{B}^{N,T} | \mathbf{Z}^N, \mathbf{U}^N) = \frac{P(\mathbf{Z}^N, \mathbf{U}^N | \mathbf{B}^{N,T}, \Theta^N) P(\mathbf{B}^{N,T} | \Theta^N) P(\Theta^N)}{P(\mathbf{Z}^N, \mathbf{U}^N)} \quad (1.9)$$

The posterior distribution for the parameters given the data can be obtained by integrating equation (1.9) over the state variables (de Valpine and Hilborn 2005),

$$\pi(\Theta^{N,T} | \mathbf{Z}^N, \mathbf{U}^N) = \int \pi(\Theta^{N,T}, \mathbf{B}^{N,T} | \mathbf{Z}^N, \mathbf{U}^N) d\mathbf{B}^{N,T} \quad (1.10)$$

and is available from Monte Carlo samples of the posterior distribution (Equation 1.9).

1.2.4 Estimation of parameters

The software WinBUGS (Lunn *et al.* 2000) was used to perform the MCMC procedure necessary for the integration of the posterior distribution for the hierarchical state-space model (Equation 1.9). Initial investigations of MCMC convergence showed slow mixing of the nonlinearity parameters. Therefore, 21 million MCMC iterations were conducted with an appropriate burn-in and thinning determined from autocorrelation plots, trace plots of the MCMC samples, and statistical tests available in the software package R (R Development Core Team 2010) to create a sample of the parameters and state variables from the posterior distribution. The posterior distribution is summarized by a median value and a 90% highest posterior density (HPD) interval, which is the shortest interval in a unimodal distribution which contains 90% of the data (Carlin and Louis 2000).

Prior distributions for parameters other than survey catchabilities were generally non-informative, although some were given reasonable bounds (Table 1.5). The prior for the process error (σ_ε^2) was inverse gamma with parameters specified such that the 5%, 50%, and 95% quantiles for the CV of B_t ($CV_{B_t} = \sqrt{e^{\sigma_\varepsilon^2} - 1}$) were approximately 0.8%, 2%, and 11%, respectively. Simulations of an unfished population of orange roughy with recruitment variability equal to 1.1, as is assumed in New Zealand stock assessments of orange roughy (Ministry of Fisheries 2007), resulted in a CV near 3% for B_t . The log of the hyperparameter ω was assigned a wide normal prior such that *omega* would have a median of 1 and a

CV of 2. The prior used for the hypervariance parameter, σ_ω , was a half-Cauchy, and is appropriate when using less than 5 hierarchical groups (Gelman 2006), although we included six CPUE series. The probability distribution of the stock-specific nonlinearity parameters, β_u , depends on the hyperparameters, and the prior for β_u is given in Figure 1.2.

1.2.5 A prior distribution for β

The main interest of this study was the marginal distribution of β for an unknown stock, which can be used as a prior when estimating β for that unknown stock. Minte-Vera *et al.* (2005) showed this distribution as,

$$p(\beta_{N+1} | \mathbf{Z}^N, \mathbf{U}^N) \propto \int_{\omega} \int_{\sigma_{\omega}^2} \int_{\Theta^N} p(\beta_{N+1} | \omega, \sigma_{\omega}^2) p(\Theta^N, \omega, \sigma_{\omega}^2 | \mathbf{Z}^N, \mathbf{U}^N) d\Theta d\sigma_{\omega}^2 d\omega \quad (1.11)$$

This integration was accomplished by randomly generating 1,000 realizations from $\text{LN}(\omega_l, \sigma_{\omega,l}^2)$ for all l where l is a sample from the final thinned MCMC chain. Additionally, Gaussian, logistic, and t parameterized distributions were fitted to these integrated samples using maximum likelihood to make the prior distribution more practical for future analyses. The logistic parameterization was

$$P(\beta) = \frac{e^{-(x-\mu)/b}}{b [e^{-(x-\mu)/b}]^2} \quad (1.12)$$

$$\text{Variance} = \pi^2 b^2 / 3$$

where μ is a location parameter and b is a scale parameter.

Some additional analyses were done to provide priors for the stocks used in this analysis and to explore the sensitivity of the results to the fixed natural mortality parameter. Minte-Vera *et al.* (2005) warn of the double use of data when developing priors and suggest repeating the meta-analysis without the data set for which the prior will be used. Therefore, this meta-analysis was repeated four times, removing one stock at a time to provide a prior for β that may be used in an assessment of the removed stock. Sensitivity to the fixed natural mortality was also explored by halving the assumed natural mortality for each stock. A New Zealand assessment of orange roughy in the Spawning Box subarea did this

same sensitivity to determine the effect of reducing the productivity of the stock (Ministry of Fisheries 2007).

1.3 Results

The first 600,000 samples of the Markov Chain Monte Carlo chain were discarded and then the chain was thinned to every seventeen-thousandth sample, resulting in 1,200 samples to describe the posterior distribution. All parameters passed a test of convergence (Geweke 1992) and showed insignificant amounts of autocorrelation within the thinned chain. Due to the length of the chain, multiple chains were not simulated.

Stock specific posterior distributions of the additional CPUE errors and nonlinearity parameters are discussed below and followed by a discussion of parameters which span multiple stocks, such as process error and the hyperparameters for β . Additional stock-specific details, such as biomass and depletion estimates, are given in the supplemental materials.

1.3.1 Individual stocks

Posterior distributions for the additional error of each CPUE series showed that in terms of a coefficient of variation these values were likely to be less than 0.3 (Figure 1.3). The single CPUE series for the Mid-East Coast stock had small variances assigned to the yearly estimates, thus the estimated additional error did not favor low values as with other series. The Australian Eastern Zone CPUE series, however, showed a considerable amount of interannual variability and the estimated additional error was larger than the additional error for the other CPUE series (a median of 0.89 and a 90% HPD interval between 0.47 and 1.58).

The estimated posterior distributions for the nonlinearity parameter (β_u) for the six CPUE series of the four stocks are shown in Figure 1.4. The median β_u was greater than one for all CPUE series and the 90% HPD interval (converted from the posterior distribution of $\ln(\beta_u)$) was entirely greater than one for the Eastern Flats and East Hills CPUE series. The median for the Spawning Box CPUE series was closest to one and the probability that β was greater than one for this series was 0.78 (Table 1.6). Figure 1.4 also shows the median

and 95% probability regions of the posterior distributions for the nonlinearity parameter when one stock was removed from the analysis. Removing the MEC or AUS stock shifted the posterior distribution slightly to the right, while removing the ECR or NWCR stock shifted the distribution slightly to the left when compared to the analysis using all four stocks. The nonlinearity parameter for each CPUE series was not highly correlated with the additional CPUE error for the corresponding series (the maximum absolute Pearson's correlation coefficient was 0.19).

1.3.2 Parameters shared between stocks

Parameters that were not unique to an individual stock were the additional errors for the three survey types (trawl, egg, and acoustic), the variance of the process error, and the hyperparameters for the nonlinearity parameter relating CPUE to abundance. The additional CV for trawl surveys ranged from near zero to almost entirely less than one with a median of 0.16 and a 90% HPD interval between 0.0 and 0.35 (Figure 1.5). The additional CV for acoustic surveys spanned a wider range, and the additional CV for egg surveys was typically large with the posterior spanning the entire range of the uniform prior (0–2). This large additional error for egg surveys could be a result of catchability fixed at one and the stocks with an egg survey having only one estimate for the entire time series.

The estimated posterior distribution for the CV of the process error is shown in Figure 1.5. The CV is well informed with a median of 0.030, and a 90% HPD interval between 0.012 and 0.049. The estimated nonlinearity parameter showed negative correlation with the estimated process error (Pearson's correlation coefficient for each CPUE series ranged from -0.23 to -0.52). Larger values of the nonlinearity parameter were more common when the process error was small and as the process error increased the estimate of β_u approached a value of one.

The posterior distributions of the hyperparameters, ω and σ_ω , are shown in Figure 1.6. The hyperparameter ω was shifted a considerable amount to the right of the prior distribution (a lognormal distribution with a median of one). The median of the posterior for ω was 1.6 with a 90% HPD interval between 0.82 and 2.42. The median of the posterior for

σ_ω was 0.42, which corresponds to a CV of 0.43, and there was a fair amount of density near zero in the posterior distribution. The 90% HPD interval for σ_ω was between 0.01 and 0.82, respectively, corresponding to CV's of 0.01 and 0.97. The hyperparameters did not show high correlation in the MCMC sampling, although at high and low values of ω , the variability, σ_ω , was typically higher (Figure 1.6).

1.3.3 *Prior distribution for the nonlinearity parameter*

A prior distribution for the nonlinearity parameter, β , was developed by integrating over the possible hyperdistributions predicted from the MCMC sampling of the joint posterior distribution (Figure 1.7). This integrated distribution had a median of 1.56, and a 90% HPD interval (converted from log space) between 0.61 and 4.34. The probability that β is greater than one was 0.83.

Removing a single stock and repeating the analysis with only three stocks did not greatly change the shape of the estimated distribution for a prior (Figure 1.7). The prior without the ECR stock was wider than any other case, but removing the ECR stock resulted in a substantial loss of data as it contained three of the six CPUE series.

The fits of parametric distributions to the log of the integrated prior distribution from the MCMC sample are shown in Figure 1.8. The estimated mean and standard deviation for each back-transformed distribution as well as some quantiles from are shown in Table 1.7. A normal distribution with a mean and standard deviation calculated directly from the log of the integrated samples was much wider than the prior. The t -distribution produced the best fit because it was able to better represent the tails of the prior distribution.

The sensitivity where natural mortality was halved, but fixed for each stock, widened and shifted the distribution of beta to the left so that the median was closer to 1 (Figure 1.7). However, the median remained above 1 (Table 1.7) and the probability of hyperdepletion in this integrated prior was 0.72.

1.4 *Discussion*

The estimated distribution of the nonlinearity parameter for an unknown orange roughy stock, which can be used as a prior distribution in the analysis of other stocks, had 83%

of its mass above one, indicating that hyperdepletion is more likely than hyperstability for CPUE data from orange roughy fisheries. However, this distribution was wide and incorporated much uncertainty. The hierarchical state-space model was uncertain because process error and observation error were both estimated, and few stocks were available for the meta-analysis. Each of the stocks analyzed here has been assessed elsewhere as a single stock and the results from this hierarchical analysis differed mostly with regard to the amount of uncertainty in the estimates of biomass. The purpose of this analysis, however, was not to provide management advice for each individual stock, but to develop a prior distribution for the nonlinearity parameter in the relationship between CPUE and abundance, for which appropriate levels of uncertainty were included.

Although different types of uncertainty were included in this analysis, many assumptions were still made that could bias the results. For example, natural mortality was fixed and a sensitivity of halving natural mortality shifted the estimated distribution for the nonlinearity parameter to the left. Other assumptions included knife-edged maturity, commercial selectivity, and survey selectivity that were equal to each other, but different among stocks. Acoustic and egg survey estimates are typically given as estimates of spawning biomass, but estimated trawl survey selectivity ogives from age-structured orange roughy assessment models are typically shifted to the left of the maturity ogive, and estimated commercial selectivity curves have been occasionally estimated to the right of the maturity ogive (see Orange Roughy Introduction in Ministry of Fisheries (2007), page 472). Estimating catchability for the survey indices may alleviate some of the bias associated with these assumptions, but the effects on the estimated prior are uncertain. Determining bias associated with fixing commercial selectivity and maturity to be the same is even more difficult because it is uncertain if the two actually are significantly different (see Francis 2006) or if assumptions in past age-structured assessments (such as a linear relationship between CPUE and abundance) were the cause of an estimated difference. In comparison, the fixed age-length and weight-length relationships for each stock likely have less effect than the assumptions regarding selectivity and maturity. Further investigating these effects and their interactions would require a model that is more flexible than the delay-difference model used here.

Fishery surveys are often used in orange roughy assessments and were used in this analysis with the assumption that the index is proportional to biomass. Surveys are designed to randomly sample a large area over which a stock is expected to occupy, and are theoretically not likely to suffer from the same difficulties as CPUE. However, surveys for orange roughy may be subject to some of the same problems as catch-rate data and may show a nonlinear relationship with abundance. For example, trawl surveys use similar gear and techniques as the commercial fishery and may be designed to concentrate in areas commonly fished (such as the Spawning Box). If hyperdepletion was also present in the survey indices used in this analysis, the detection of nonlinearity in the CPUE relationship with abundance could be masked and assessment models relying on CPUE and survey data could possibly be biased.

Previous research suggests that hyperstability is more commonly expected in the relationship between CPUE and abundance (Wilberg *et al.* 2010), and it may seem counter-intuitive that hyperdepletion would be apparent in this study. Contraction in the range of historical orange roughy aggregations (Clark 1995) as well as fishers targeting spawning aggregations, not searching at random, often cooperating, and trying to avoid saturation of the trawl gear all suggest that catch-rates should remain high. These traditional explanations of hyperstability, however, do not seem to hold when describing catch-rates in orange roughy fisheries. Hyperdepletion can result when inappropriately accounting for spatial expansion of fisheries in the analysis of catch-rate data (Polacheck 2006; Walters 2003), although orange roughy fisheries have not shown spatial expansion as extensive as tuna fisheries. More plausible explanations of hyperdepletion in the catch-rates of orange roughy are the depletion of known high density areas and fish behavior in response to fishing. These explanations of hyperdepletion are discussed next.

The depletion of high-density areas may result in a population that is fished less often, but maintains a low-density, yet high overall population size with lower and more stable catch-rates (Hilborn and Walters 1992). The largest orange roughy fisheries typically began in areas with dense aggregations and catch-rate analysis is often constrained to those main fishing areas. For example, the Spawning Box has been one of the main fishing areas on the Chatham Rise since the start of the fishery, and new areas, such as the East Hills and Andes Hills, were found when management greatly reduced catch levels in the Spawning

Box. Ritchie Hill is the main fishing area off of the Mid-East Coast of New Zealand, and St. Helen's and St. Patrick's hills are the main fishing areas for the Eastern Zone of Australia orange roughy fishery from which CPUE is determined. Additionally, the Challenger Plateau fishery off of the West Coast of New Zealand initially focused on a few locations with large aggregations which showed quick declines in catch rates. The fishery then moved southeast of those areas, maintaining low catch rates before the fishery was effectively closed (Ministry of Fisheries 2010, page 578). The greater orange roughy fishery in New Zealand has expanded into new areas, and catch rates have quickly declined in various hot spots, but the assessments of the major stocks typically use CPUE data from traditional fishing areas, as were also used in this analysis.

The presence of hyperdepletion in the CPUE data may also be related to fish behavior. One explanation is that natural variation in spawning may result in the fluctuation of the size of spawning aggregations and in the number of fish migrating. Orange roughy are believed to migrate long distances to form spawning aggregations (Francis and Clark 1998), but not all mature orange roughy will spawn in a given year (Bell *et al.* 1992; Koslow *et al.* 1995a; Zeldis *et al.* 1997). Estimates of the proportion of non-spawning mature orange roughy have been as high as 50% on the east coast of Tasmania, but fewer non-spawning fish (29%) were found after the stock was fished down (Koslow *et al.* 1995a). Bell *et al.* (1992) suggest that food limitations may influence the development of viable oocytes, and Bull and Shine (1979) explain that migration may have an energy cost such that infrequent spawning and migration can actually result in greater overall fecundity. Whatever the process may be, there is variability in the proportion of adult orange roughy spawning each year and the disappearance and reappearance of some spawning aggregations may be due to their ephemeral nature on a time scale much longer than the fishery has operated.

Additionally, rapid declines in catch rates may occur if orange roughy are less likely to return to fished areas due to environmental disturbance or disruption from fishing activity. Orange roughy have a pronounced lateral line (Paulin 1979) and anecdotal evidence suggests that orange roughy react to fishing activity in both the short and long term. Koslow *et al.* (1995b) reported orange roughy reacting to a camera being lowered to depth and also noted that a layer of orange roughy dispersed when an iron bar dropped over the side of a ship

descended to within 60 meters of the school. During an acoustic survey, a school of fish on a small underwater hill was observed to disappear over a short period while a single vessel was fishing nearby and at the same time (Doonan *et al.* 2003). Trawl surveys for orange roughy on the Chatham Rise were discontinued due to changes in fish distribution, abundance, and availability thought to be a result of fishing pressure disrupting the stability and formation of aggregations (Clark 1996). And, more recently, a combined trawl and acoustic survey off of the west coast of New Zealand (Challenger Plateau) estimated an unexpectedly large biomass of fish within a few years after fishing was halted, and reported the reappearance of orange roughy aggregations that have not been observed in this area since the early years of the fishery (Ministry of Fisheries 2010, page 578).

The Challenger Plateau stock of orange roughy is an interesting case study which highlights the nonlinearity between catch rates and abundance and its effect on management. Unstandardized and standardized CPUE in this area quickly declined in the first eight years of the fishery, and then declined at a slower rate, nearly remaining stable, from 1990 onward when vessels began fishing longer tows away from the spawning grounds (Field and Francis 2001). In the late 1980's the total allowable catch (TAC) was increased as part of a management program to determine how the stock responded to increased effort and was followed by a large reduction in the TAC in 1989 (Clark and Tracey 1994). Using CPUE as the only data, a stock assessment of this area in the year 2000 concluded that the spawning biomass was at 3% of its original unfished size (Field and Francis 2001) and the TAC was subsequently reduced to one tonne, effectively closing the fishery. After five years of no fishing (2001–2005), a combined trawl and acoustic survey noted a larger than expected biomass of orange roughy (nearly 20 000 tonnes), but also noted that spawning aggregations were not present in the main historical fishing areas. In 2009, a continuation of this combined trawl and acoustic survey estimated an even larger biomass (52 000 tonnes) that, when adjusted to account for spawning biomass only, was approximately 32 000 tonnes, or 35% of unfished spawning biomass (Ministry of Fisheries 2010). Given the assumptions of slow growth and low productivity for orange roughy, it would be impossible for the stock to increase from 3% to 35% of unfished biomass in nine years, and the only alternate explanations are either immigration into the area or a change in fish behavior regarding how they aggregate after

the fishery was stopped.

The Challenger Plateau example shows the difficulty of attempting to maximize sustainable or economic yield of orange roughy stocks when determining stock size from CPUE. Stock status and sustainable yields for many of the orange roughy stocks in Australia and New Zealand have been determined using catch-rates from fishing vessels and in a few cases from survey vessels. Many of these stocks have been declared overfished (Lack *et al.* 2003a) under the assumption that catch-rates are directly proportional to abundance. Ignoring the possibility of hyperdepletion in these assessments may actually lead to risk-averse and possibly more conservative management than intended.

If catch-rates of orange roughy from fishery-independent and fishery-dependent data are prone to hyperdepletion, and traditional stock assessment methods are less accurate and likely to be conservative, alternative management methods may outperform a biased assessment in terms of managing towards maximum sustainable yield or maximum economic yield. Management strategy evaluation could help determine alternative management methods which will perform better when hyperdepletion or hyperstability are present. For example, differences between the current management regime and the management outcomes when attempting to account for nonlinearity in assessments of particular stocks could be investigated. Furthermore, managing based on alternative indicators, such as CPUE, could reduce risk, stabilize catches, and result in a sustainable fishery which maximizes long-term catches or profits (Butterworth *et al.* 1997; Holland *et al.* 2005).

CPUE is an inexpensive data source that can be collected from every fishery, and understanding the relationship between CPUE and abundance results in a better understanding of the effects of fishing on a stock of fish, and can lead to the better management of fish stocks. There is a continued interest in utilizing CPUE from orange roughy fisheries because they are often the only data available, or are the only data spanning a large portion of time since fishing on a specific stock began. Research surveys are expensive and time-consuming, and if the relationship between abundance and CPUE is understood it can be used as an alternative or additional management tool. These results indicate that CPUE is likely to decline faster than abundance in the early part of a fishery for orange roughy, which may lead to a pessimistic view of the stock status as well as the fishery after a number of years

of fishing. Hyperdepletion was unexpected for an aggregating species, and these results can not only be used to more accurately determine the historical biomass trend, but may also be applicable to other species of fish, such as oreos (family Oreosomatidae), which are commonly associated with orange roughy in catches and also form feeding and spawning aggregations near seamounts. Possibilities of bias in an assessment could be mentioned due to the nonlinear relationship between CPUE and abundance, or a nonlinear parameter making catchability density-dependent could be incorporated to estimate the biomass trajectory with less bias but possibly more uncertainty. This study provides a range of possible values for a nonlinearity parameter in the relationship between CPUE and abundance and also provides a prior distribution which may be used in a Bayesian analysis of the catch-rates for orange roughy or similar species.

1.5 Tables

Table 1.1: Catch-per-unit-effort (CPUE) data for the four stocks of orange roughy from Wayte and Bax (2002) and Ministry of Fisheries (2007).

Stock	CPUE	Years
East Chatham Rise	Spawning Box	1981–88, 1990–1992
	Eastern Flats	1983–88
	East Hills	1991–2005
Mid–East Coast	MEC	1988, 1990–97
Northwest Chatham Rise	NWCR	1981–2005
East Australia	AUS	1989–1999

Table 1.2: The type of fishery-independent abundance data and years for which estimates were available for the four stocks of orange roughy. BUC, COR, and TAN refer to *F/V Otago Buccaneer*, *F/V Cordella*, and *R/V Tangaroa*, respectively, and are the vessels that performed trawl surveys. The parameterizations for the catchability coefficients (q) are given along with prior distributions taken from previous stock assessments (Wayte and Bax 2002; Ministry of Fisheries 2007). The priors with normal distributions are parameterized with a mean and standard deviation and U refers to the uniform distribution.

Stock	Index	Years	Parameterization	Prior
East Chatham Rise (ECR)	BUC trawl	1984–87	$\ln\left(\frac{q_{BUC}}{q_{COR}}\right)$	$N(0.405, 0.15)$
	COR trawl	1988–90	$\ln\left(\frac{q_{COR}}{q_{TAN}}\right)$	$N(0.220, 0.12)$
	TAN trawl	1992, 94	$\ln(q_{TAN})$	$U(-6, 6)$
	Acoustic	1998, 2004	$\ln(q_{A_{ECR}})$	$N(-0.11, 0.50)$
Mid–East Coast (MEC)	Trawl survey	1992–94	$\ln(q_{T_{MEC}})$	$U(-6, 6)$
	Egg survey	1993	$\ln(q_{E_{MEC}})$	$= 0$
	Acoustic survey	2001	$\ln(q_{A1_{MEC}})$	$N(-0.26, 0.53)$
	Acoustic survey	2003	$\ln\left(\frac{q_{A3}}{q_{A1}}\right)$	$N(-0.62, 0.23)$
Northwest Chatham Rise (NWCR)	Egg survey	1996	$\ln(q_{E_{NWCR}})$	$= 0$
	Acoustic survey	1999	$\ln\left(\frac{q_{A9}}{q_{A5}}\right)$	$N(0.00, 0.23)$
	Acoustic survey	2002	$\ln\left(\frac{q_{A2}}{q_{A5}}\right)$	$N(-0.05, 0.03)$
	Acoustic survey	2005	$\ln(q_{A5_{NWCR}})$	$N(-0.05, 0.56)$
East Australia (AUS)	Egg survey	1992	$\ln(q_{E_{AUS}})$	$= 0$
	Acoustic survey	1990–93, 96, 99	$\ln(q_{A_{AUS}})$	$U(-6, 6)$

Table 1.3: Parameters in the delay-difference state-space model for a single stock. An asterisk preceding the variable indicates that it was fixed or determined from fixed parameters.

Parameter	Description
<i>Survey parameters</i>	
* $Z_{z,j}$	Survey index for series z and year j
q_z	Survey catchability for series z
$\tau_{z,j}$	Error for survey series z in year j
$\sigma_{\tau_{z,j}}^2$	Total variability of survey series z in year j
* $CV_{z,j}$	Coefficient of variation calculated from data of survey series z for year j
ξ_y	Additional coefficient of variation for data of survey type y (trawl, egg, or acoustic)
<i>CPUE parameters</i>	
* $U_{u,i}$	CPUE for series u and year i
α_u	Multiplier in relationship between CPUE and abundance for CPUE series u
β_u	Power parameter in relationship between CPUE and abundance for CPUE series u
$\nu_{u,i}$	Error for CPUE series u in year i
$\sigma_{\nu_{u,i}}^2$	Total variability of CPUE series u in year i
* $CV_{u,i}$	Coefficient of variation calculated from data of CPUE series u for year i
ξ_u	Additional coefficient of variation for data of CPUE series u

Table 1.4: Hyperparameters in the hierarchical delay-difference state-space model that are shared across stocks.

Parameter	Description
σ_ε^2	Process error variance (same as in Table 1.3 but shared across stocks)
ω	Mean of the hyperprior for β_u
σ_ω	Standard deviation of the hyperprior for β_u

Table 1.5: Prior distributions assigned to the estimated parameters. See Tables 1.3 and 1.4 for descriptions of the parameters. Biomass is in tonnes and β or ω equal to 1 implies a proportional relationship.

Parameter	Number of parameters	Prior Distribution	5% & 95% quantiles
<i>Population parameters</i>			
$B_{0,n}$	N	U(30, 6000)	(329, 5702)
$B_{t,n}$ ($t = 1 \dots T_n$)	$\sum_{n=1}^N T_n$	see Equation C.19	
<i>Survey parameters</i>			
See Table 1.2 for the description of 11 estimated catchability parameters			
ξ_y	3	U(0, 2)	(0.1, 1.9)
<i>CPUE parameters</i>			
$\ln(\alpha_u)$	6	U(-20, 20)	(-18, 18)
$\ln(\beta_u)$	6	N($\ln(\omega)$, σ_ω)	Figure 1.2 [†]
ξ_u	6	U(0, 2)	(0.1, 1.9)
<i>Hyperparameters</i>			
σ_ε^2	1	IG(0.7, 0.00015)	($6e^{-5}$, $1.2e^{-2}$)*
$\ln(\omega)$	1	N(0, 1.27)	(-2.09, 2.09)
σ_ω	1	half-Cauchy	(0.08, 12.7)

[†]A function of the hyperparameters ω and σ_ω

*When parameterized as the CV of a lognormal distribution, the quantiles would be (0.008, 0.11)

Table 1.6: The medians of the posterior distributions for the nonlinearity parameter, β_u , with the 90% HPD interval reported in parentheses. The probability that β_u is greater than one is also given.

CPUE series	$\hat{\beta}$	P($\beta > 1$)
ECR Spawning Box	1.2 (0.77–2.07)	0.78
ECR Eastern Flats	2.0 (1.16–3.57)	0.98
ECR East Hills	2.3 (1.21–5.41)	0.99
MEC	1.4 (0.80–2.25)	0.85
NWCR	1.5 (0.82–2.47)	0.88
AUS	1.4 (0.70–3.01)	0.82

Table 1.7: Parameters in log space and back-transformed quantiles for empirical and parameterized prior distributions. Empirical refers to the integrated sample from the MCMC. The parameters are the mean, standard deviation (sd), and degrees of freedom (df). See Equation 1.12 for the parameterization of the logistic distribution. The empirical summary of the prior distribution when natural mortality was halved (Half M) is also given.

Distribution	Parameters			Quantiles (back-transformed)						
	mean	sd	df	2.5%	5%	25%	50%	75%	95%	97.5%
Empirical	0.465	0.632	–	0.45	0.61	1.15	1.56	2.19	4.37	5.94
Normal	0.465	0.632	–	0.46	0.56	1.04	1.59	2.44	4.51	5.50
Logistic	0.459	0.592	–	0.48	0.61	1.11	1.58	2.27	4.14	5.24
t	0.456	0.449	4	0.45	0.61	1.13	1.58	2.20	4.11	5.48
<i>Half M</i>										
Empirical	0.300	0.661	–	0.36	0.49	0.95	1.33	1.92	3.87	5.23

1.6 Figures

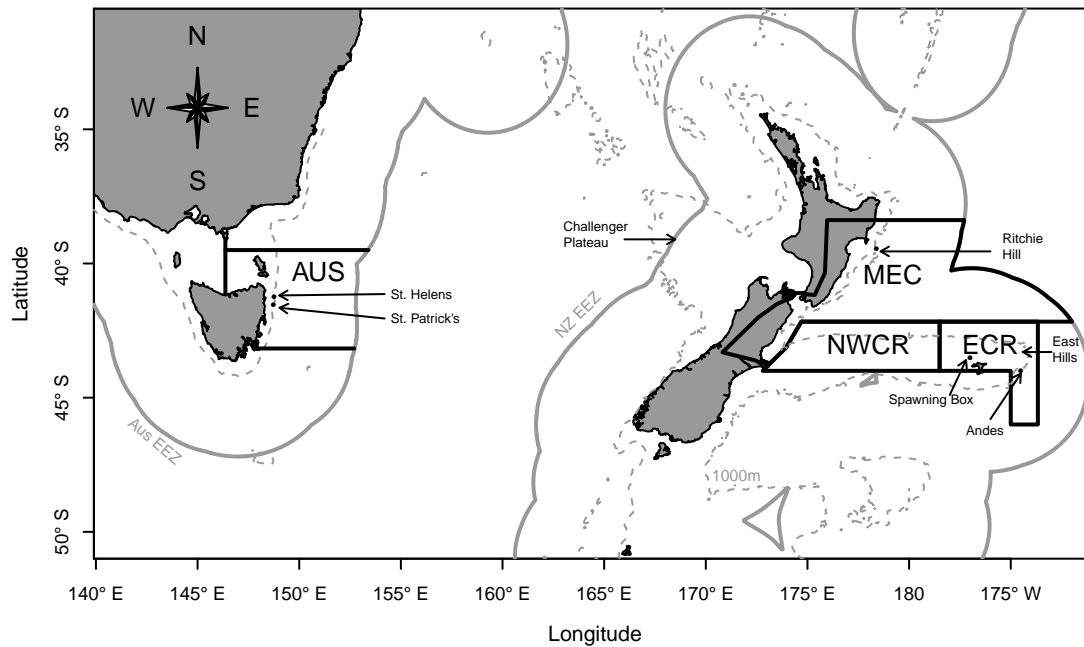


Figure 1.1: Orange roughy stocks in Australian and New Zealand exclusive economic zones (EEZ) used in the meta-analysis. AUS refers to Australia's Eastern Zone stock while MEC, NWCR, and ECR refer to New Zealand's Mid-East Coast, Northwest Chatham Rise, and East Chatham Rise stocks of orange roughy, respectively.

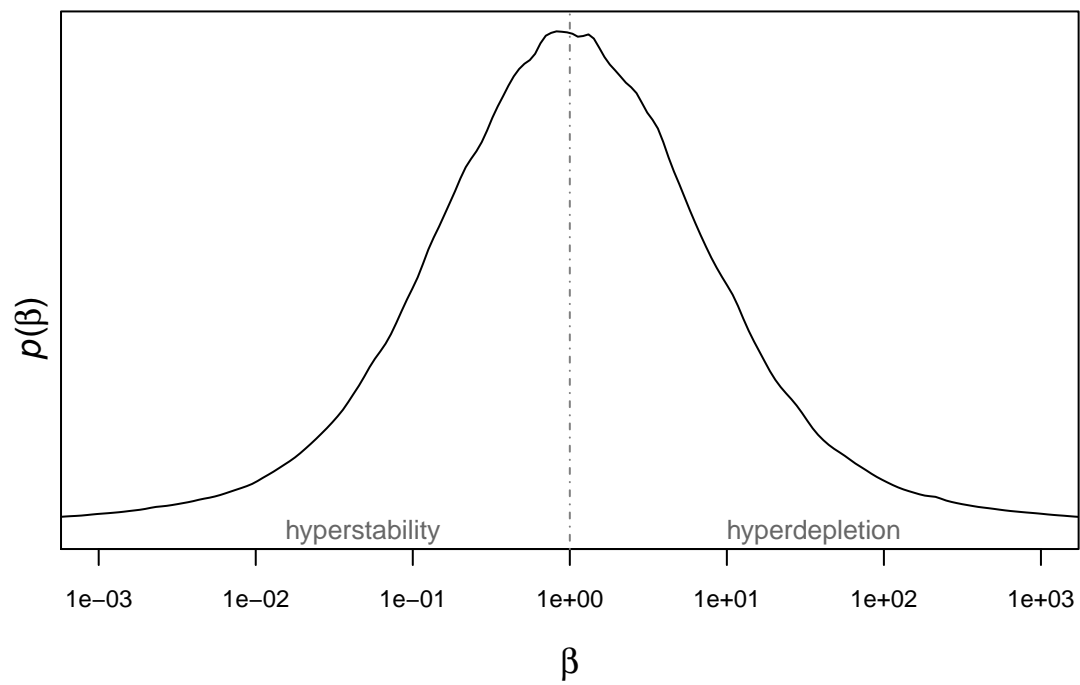


Figure 1.2: The assumed prior distribution for a stock-specific nonlinearity parameter, β_u , given the prior distributions of the hyperparameters.

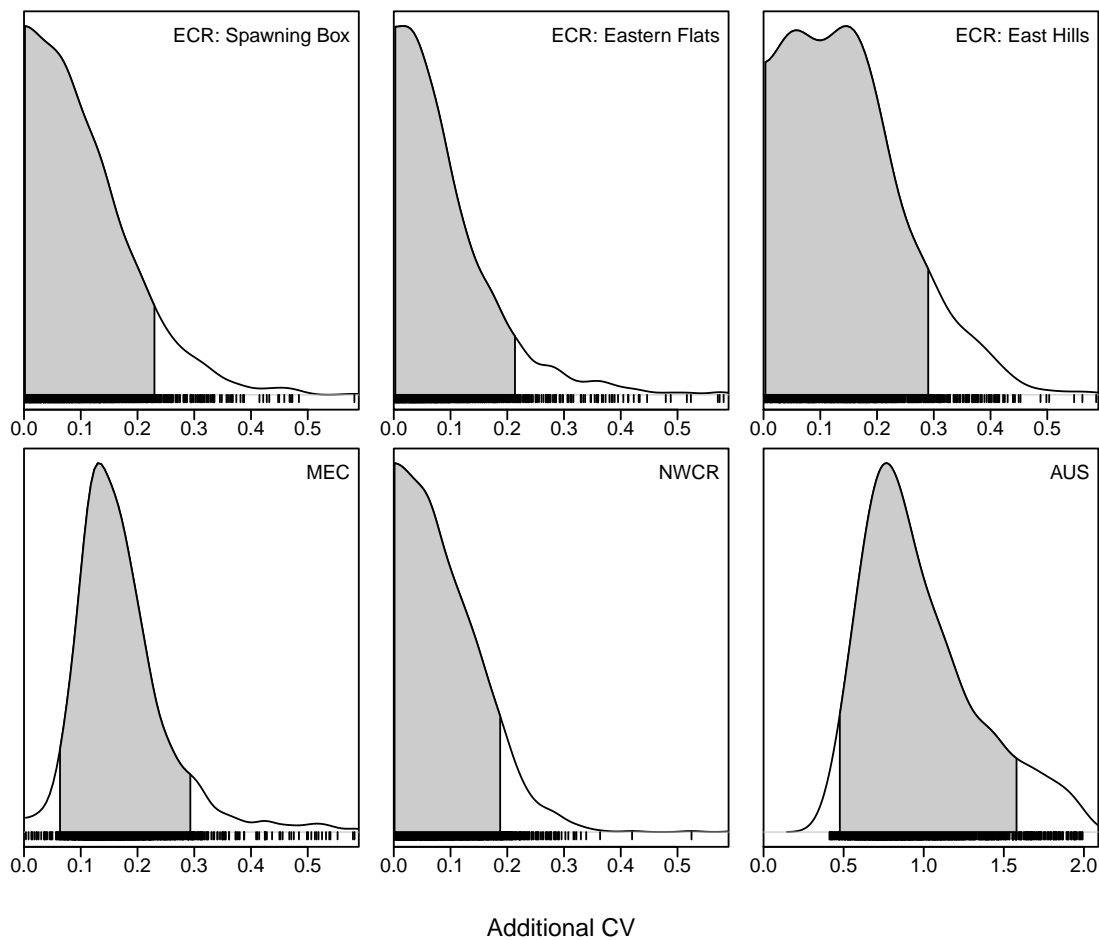


Figure 1.3: Posterior distributions for the estimated additional coefficient of variation of each CPUE series (ξ_u) with 90% HPD intervals marked in gray. The posterior distribution for AUS is plotted with a different x-axis than the rest.

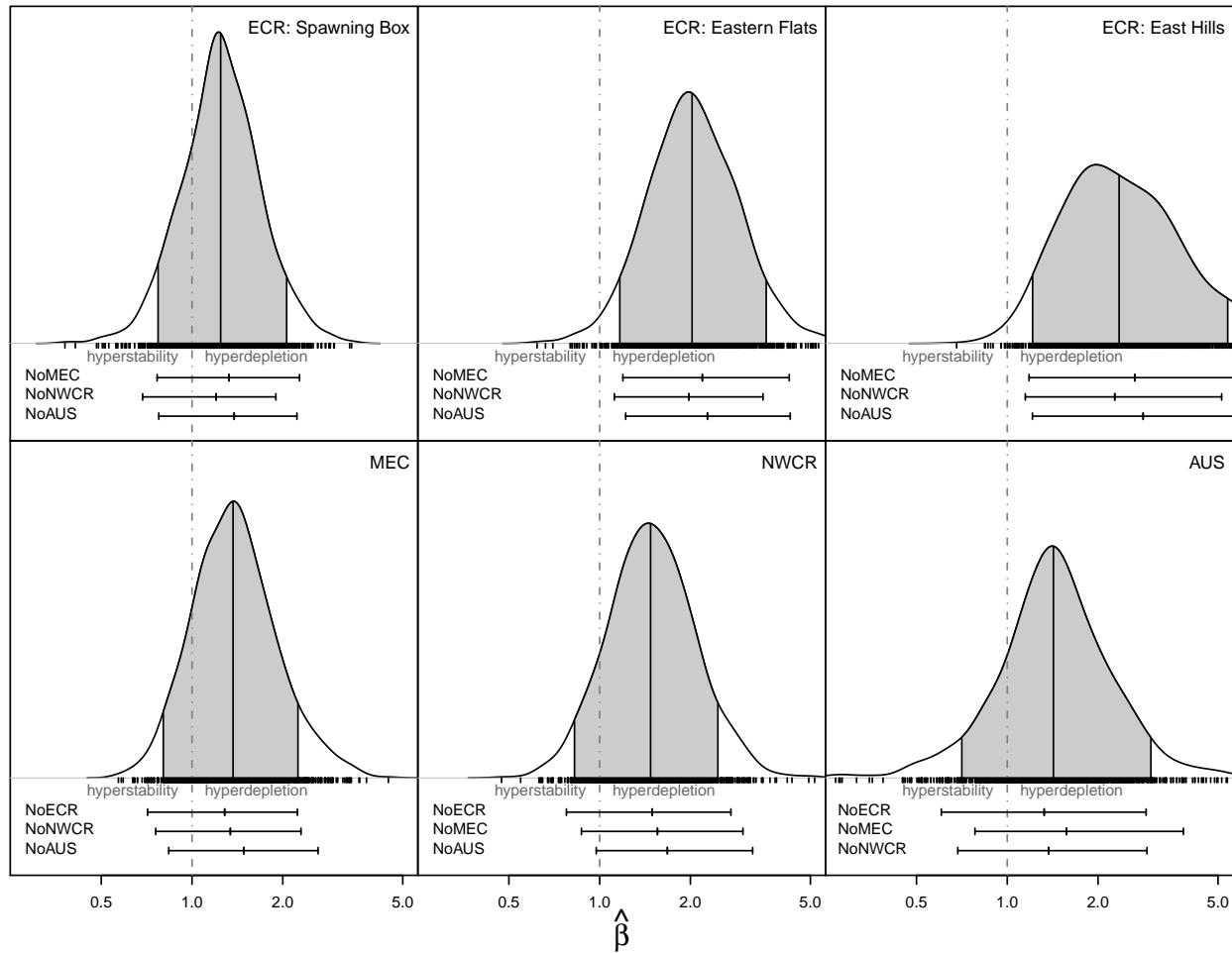


Figure 1.4: Posterior distributions for the nonlinearity parameter in each CPUE series (β) for the four stocks plotted on a log scale. The estimated density of the posterior distribution for the analysis with all four stocks is shown with the median (solid vertical line) and a 90% HPD interval marked in gray. Below the posterior distributions are the 90% HPD interval and median for the nonlinearity parameter with one stock removed.

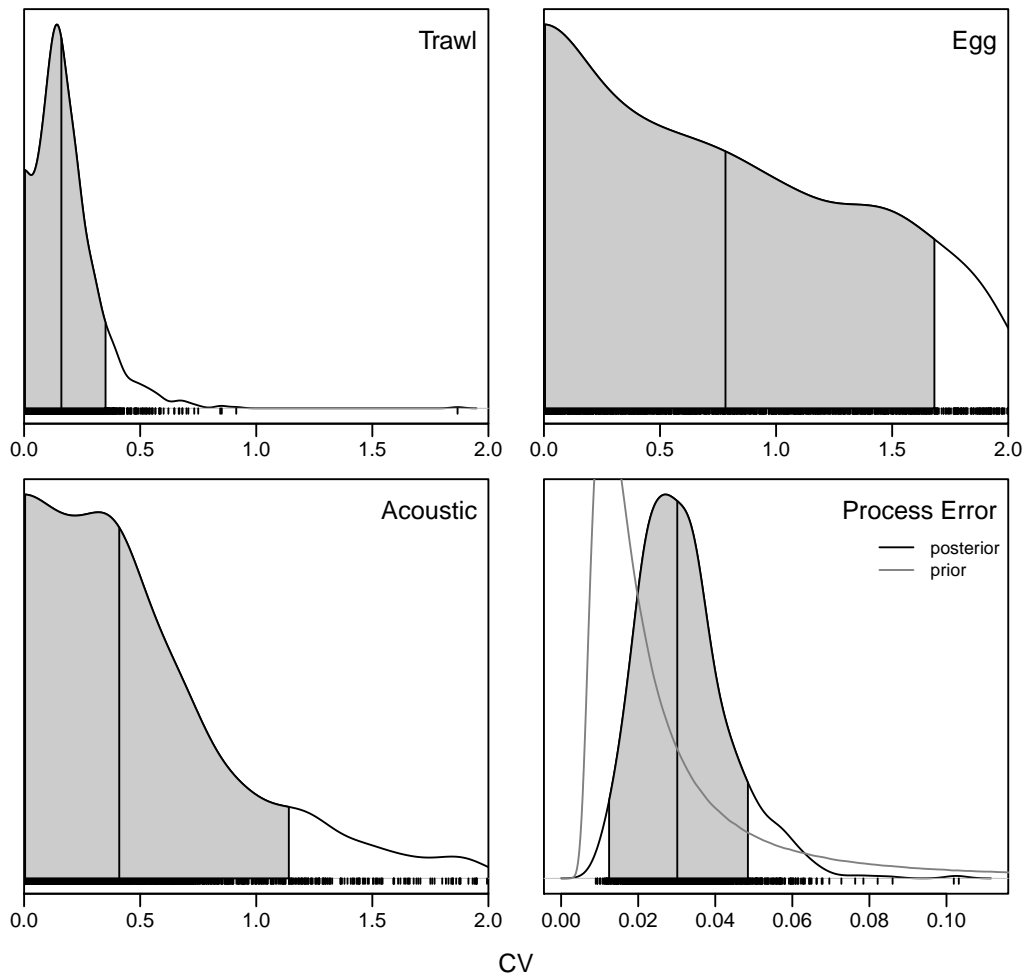


Figure 1.5: Posterior distributions for additional error (as a coefficient of variation, CV) for survey data and the CV of the process error (although estimated as variance). The median (solid vertical line) and the 90% HPD interval (gray area) are shown. The prior distribution for the CV of process error, converted from the prior on σ_{ε}^2 , is shown with a light grey line. Actual samples from the posterior distribution are indicated with small black marks immediately below the nonparametric density estimate of the posterior distribution.

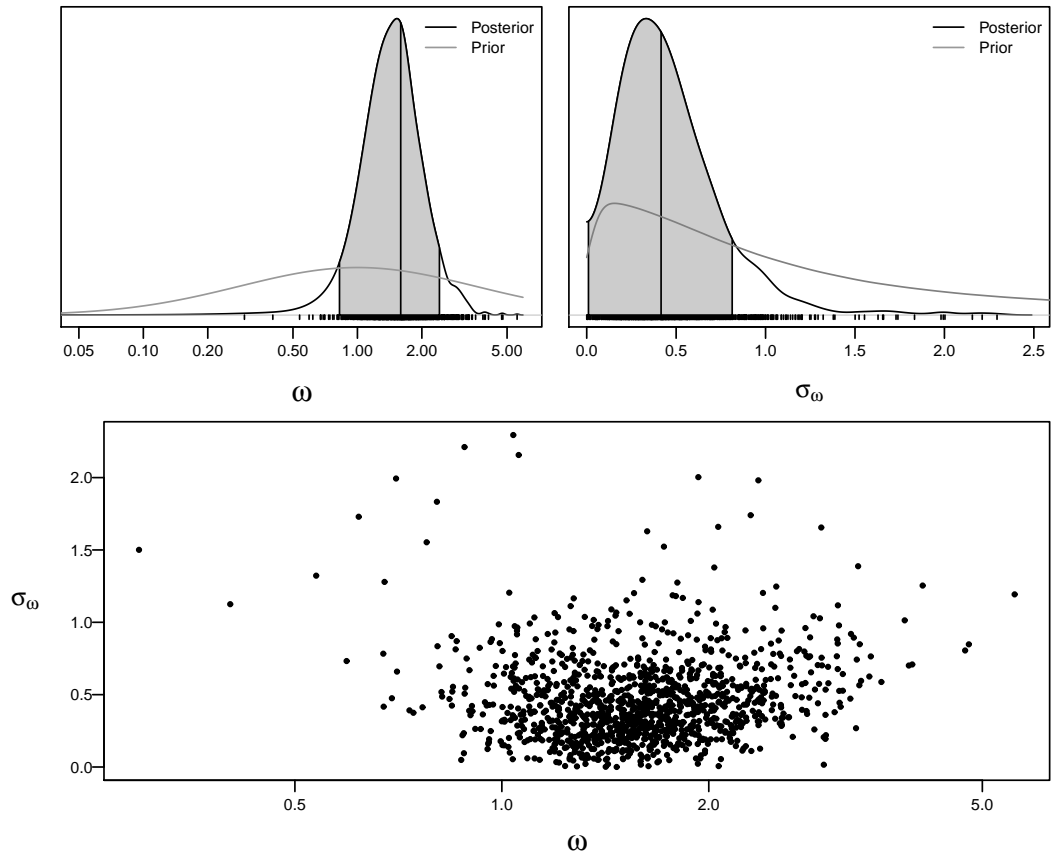


Figure 1.6: Posterior distributions for the hyperparameters ω and σ_ω with prior distributions drawn as gray lines, the median of the posterior distribution drawn as a solid vertical line, individual samples from the MCMC as small marks below the nonparametric density estimate, and the 90% HPD interval in gray (top plots). A scatterplot of σ_ω vs. ω is shown on the lower plot.

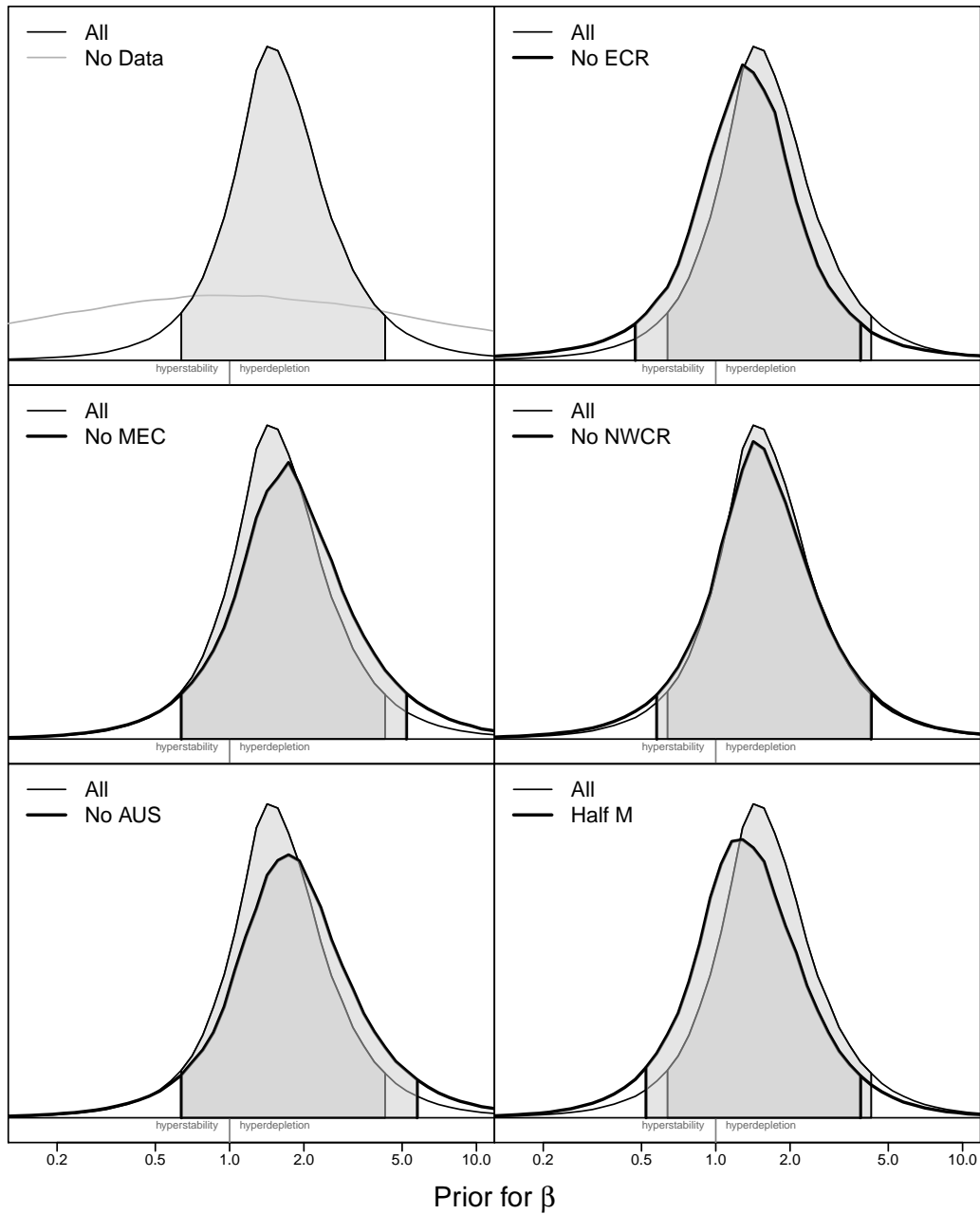


Figure 1.7: Estimated nonparametric density of a prior distribution for the nonlinearity parameter, β_u , in the relationship between CPUE and abundance with all stocks included (top left). The solid gray line is the prior distribution without any data. The additional panels show the integrated nonparametric density estimates with the indicated stock excluded from the analysis or the sensitivity where natural mortality was halved with all stocks in the analysis (Half M). The shaded area represents the 90% HPD interval and darker shaded areas indicate overlap between the two distributions.

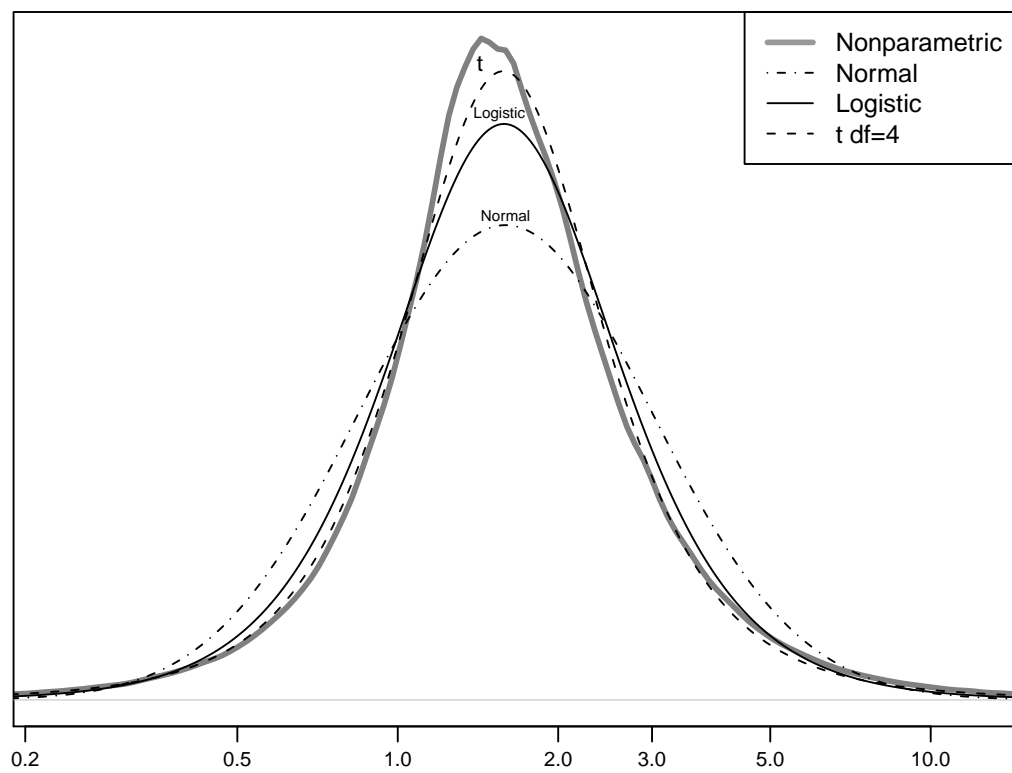


Figure 1.8: Parametric distributions fitted to the estimated nonparametric density of the prior distribution for the nonlinearity parameter (β) in the relationship between CPUE and abundance for an unknown stock.

Chapter 2

ESTIMATING NONLINEARITY BETWEEN CPUE AND ABUNDANCE***Abstract***

Catch-rate data are commonly used to determine fish stock status by assuming that catch-rates are proportional to abundance, but fishery-dependent catch-per-unit-effort (CPUE) may not always be proportional to abundance. During fishery development, CPUE may decline more rapidly or more slowly than abundance, giving a false impression of the rate of change in abundance. This study investigated the ability to estimate the direction and magnitude of nonlinearity in the relationship between CPUE and abundance using simulated survey and CPUE data input into delay-difference, age-structured, and state-space models. Estimates of nonlinearity were mostly unbiased but highly variable, ranging from one-half to double the true value. Introducing an informative prior distribution resulted in lower variance, but higher bias when the prior was not congruent with the true level of nonlinearity. Deterministic models showed a slight improvement in the estimation of nonlinearity when CPUE data were more variable and did not estimate the initial trend in abundance as well as the state-space model. Overall, the state-space model showed the best performance, with mean absolute log ratios of the estimated to true nonlinearity parameter at least half that observed in the other models, and an informative prior distribution was useful as long as it is appropriate, justifiable, and wide enough to support all possible values of the nonlinearity parameter.

2.1 Introduction

Accurate determination of fish stock status is important to effectively manage a fishery to achieve management objectives. Catch-rate data are commonly used as an index of abundance to estimate stock status by assuming that catch-rates proportionally index abundance.

Although fishery-independent survey data are preferred indices of abundance because they come from scientifically designed sampling regimes, they are not always available. Alternatively, fishery-dependent catch and effort data are available for most fisheries and can be standardized to create an index of abundance called catch-per-unit-effort (CPUE) (Maunder and Punt 2004).

While survey indices of abundance are more likely to be proportional to abundance, fishery CPUE is often not proportional to abundance due to factors associated with fishing behavior, fish behavior, and improper analysis (Wilberg *et al.* 2010). Not accounting for such a nonlinear relationship in a fish stock assessment may result in biases that compromise the effective management of that stock (Wilberg *et al.* 2010). However, attempting to account for an unknown relationship between CPUE and abundance is likely to result in additional uncertainty about the stock status.

These tradeoffs between bias and variance are important to consider when deciding on the complexity of any model (Burnham and Anderson 2002). Admitting uncertainty through a complex model can greatly benefit management (Hilborn and Peterman 1996), but there may not be sufficient information to adequately estimate the parameters of interest (Adkison 2009). Additional information about the likely relationship between CPUE and abundance, such as a prior distribution in a Bayesian analysis (Gelman *et al.* 1995), may be useful to the analysis by reducing uncertainty. However, a misspecified prior distribution may introduce unnecessary bias (Chen *et al.* 2000).

Even though there may be potential for a nonlinear relationship between CPUE and abundance, this does not mean that CPUE has no value or is completely uninformative. Fishery-dependent catch and effort data take little extra effort and cost to record, collect, and analyze because most fisheries already record catches, and many fisheries have implemented requirements for fishermen to record catches at sea. Additionally, catch and effort data are often of interest to the fishing industry as these are the data they are most familiar with and often feel are indicative of the biomass trends. Including CPUE in an assessment and estimating the nonlinear relationship with abundance can help fishers and scientists understand their observations better. Understanding this relationship can then improve the assessment of similar stocks and fisheries with little or no fishery-independent data. CPUE

are often the only data available to inform status for many fisheries, and simply discarding those data is not an option for many fisheries.

The nonlinear relationship between CPUE and abundance can be modeled within an assessment in a number of ways (Wilberg *et al.* 2010), but is typically done by assuming that catchability q is not constant, and may be density-dependent, time-varying, or autocorrelated. If only density effects are considered, then a useful framework is:

$$q_y = \alpha B_y^{(\beta-1)} \quad (2.1)$$

where B is the average abundance (numbers or biomass) during year t , α and β are parameters, and q is the density-dependent catchability coefficient. This power function for catchability can be substituted in the proportional relationship between CPUE (U) and abundance,

$$U_y = qB_y \quad (2.2)$$

to develop a more complex model where CPUE is density-dependent,

$$U_y = \alpha B_y^\beta \quad (2.3)$$

Hilborn and Walters (1992) refer to $\beta > 1$ as hyperdepletion, meaning CPUE declines more rapidly than abundance, and $\beta < 1$ as hyperstability, because CPUE declines more slowly than abundance.

Equation 2.3 has been used extensively to model the relationship between CPUE and abundance (e.g., Bannerot and Austin 1983; Harley *et al.* 2001) and its estimation properties deserve further investigation. This study uses simulation to quantify the estimation bias and variability of the nonlinearity parameter, β under different scenarios of hyperstability, proportionality, and hyperdepletion. A deterministic delay-difference model, a deterministic age-structured model, and a state-space delay-difference model were used with different assumptions about the amount of variability on fishery-dependent indices, the rate at which survey abundance estimates are available, and prior distributions on the nonlinearity parameter proposed by Harley *et al.* (2001) and proposed in Chapter 1. Although the estimation of β is the focus of this study, the effects of estimating a nonlinear relationship between

CPUE and abundance on the estimates of stock biomass and status determination were also explored.

2.2 *Materials and Methods*

An operating model was used to generate data from an assumed “true” population, and the ability of three alternative models to estimate the nonlinearity parameter (β) was tested. These models and their assumptions are discussed below.

2.2.1 *Operating model and data*

The operating model was an age-structured model with stochastic recruitment, written in the R statistical software (R Development Core Team 2010). The “true” population was loosely based on the East Chatham Rise stock of orange roughy (see Ministry of Fisheries (2010) for a more detailed description) because orange roughy CPUE has shown hyper-depletion (Chapter 1) and there is concern about estimating a nonlinearity parameter in orange roughy stock assessments (see the orange roughy introduction in Ministry of Fisheries (2010)). Many life-history parameters other than recruitment variability were assigned a single value and kept fixed throughout the simulations (Table 2.1). Some important assumptions were: selectivity and maturity ogives were equal, and abruptly changed from zero to one at age 29 (knife-edged), natural mortality (M) was fixed at 0.045 yr⁻¹, growth was fixed and variability of length-at-age (σ_L) was negligible. The fishery was simulated for 30 years and catches were constant across simulations, fixed at values to mimic a fishing-down phase similar to that seen in New Zealand orange roughy fisheries (Ministry of Fisheries 2010) with large catches for 15 years, followed by a 50% reduction in catches for 10 years, and finishing with another 50% reduction for 5 years (Figure 2.1). The population was initialized at an unfished state, but due to stochastic recruitment, the biomass in year 1 was not necessarily the equilibrium unfished biomass (B_0). Beginning of the year biomass was simulated for 31 years to one of two specific levels of depletion (15% and 45% of unfished biomass) by solving for the unfished biomass that resulted in the specified level of depletion given randomly generated lognormal recruitment deviates, the fixed parameters, the catch series, and the condition that the exploitation rate never exceeded 0.67. When the given

set of recruitment deviations could not satisfy the specific level of depletion, new recruitment deviates were randomly generated until 100 trajectories ending at the desired level of depletion were available.

Data were generated for a single CPUE series and a single survey series (Table 2.1). A lognormal distribution was used to draw a single CPUE value for year y with a mean equal to $\alpha V_{(i,y)}^\beta$ and an assigned coefficient of variation (CV), where $V_{(i,y)}$ is the mid-year biomass vulnerable to the fishery from simulation i in year y (see Equation C.8), β is the nonlinearity parameter, and α is a scalar and nuisance parameter. Survey observations were simulated starting in year 5 using a similar method with a mean equal to $qV_{(i,y)}$ where the catchability coefficient (q) is also a scalar and nuisance parameter. The CV for the CPUE series ($CPUEcv$) was part of the experimental design (see below).

2.2.2 Estimation models

The three estimation models were a deterministic delay-difference model (DDD) written in ADMB (Fournier *et al.* 2011), a deterministic age-structured model called Awatea (AWA) that was adapted from code for the stock assessment program called Coleraine (Hilborn *et al.* 2003), and a state-space delay-difference model (SSM) implemented in WinBUGS (Lunn *et al.* 2000). The DDD and SSM models are the same as those described by Chapter 1, and assumed constant recruitment for all years modeled (the spawner-recruit relationship will have very little effect in a model of a population that matures at age 29 and is fished for 30 years). The SSM model estimated process error whereas the DDD model did not. The AWA model was the most similar to the operating model because it incorporates full age-structure, although some differences were present, such as deterministic recruitment. Details of the three models are given in Appendix C.

These three models were chosen because they have been used to analyze and assess orange roughy data. The AWA model has been used to assess stocks of orange roughy (Ministry of Fisheries 2010) and is similar to many of the age-structured models used to assess many different stocks of fish. The SSM was used in Chapter 1 to quantify the amount of nonlinearity in the relationship between orange roughy abundance and CPUE. The DDD

model is examined here as a comparison to the *SSM*.

Four prior distributions were used for the nonlinearity parameter (Figure 2). The priors are

1. A uniform distribution on $\ln(\beta)$ with bounds between -10 and 10 (*Uniform Prior*),
2. a logistic distribution on $\ln(\beta)$ with mean=0.4591 and variance=0.3266 (*Hicks Prior*),
3. a logistic distribution on $\ln(\beta)$ with mean=0.0 and variance=0.3266 (*Hicks(1) Prior*),
and
4. a normal distribution on β with mean=0.73 and variance=0.1 (*Harley Prior*).

The logistic prior distribution (*Hicks Prior*), which provides more support for hyperdepletion than hyperstability, is from Chapter 1 and incorporates between stock uncertainty in β as well as estimation uncertainty. The prior distribution for hyperstability (*Harley Prior*), taken from Harley *et al.* (2001), was different from the others in that it was a normal distribution for β in real space. The estimation models estimated β directly instead of $\ln(\beta)$ when using the *Harley Prior*. Being a normal distribution in real space there was the possibility that β could take on negative values, although the probability was small (about 1% of this distribution was less than zero).

Priors for other parameters were uniform with bounds outside the expected range of estimates. The natural log of unfished biomass or unfished recruitment was estimated with a uniform prior. For the *SSM*, the process error variance, σ_e^2 , was estimated using an inverse gamma prior which, when translated to a CV, had 2.5%, 50%, and 97.5% quantiles of 2.0%, 3.4%, and 7.0%, respectively. This distribution was developed such that it was centered around the expected CV of biomass from test simulations without fishing. Appendix C provides additional information on the models.

2.2.3 Scenarios and simulations

The design of the scenarios included three estimation models (*DDD*, *AWA*, and *SSM*), two levels of depletion (*Depletion*), three values for the nonlinearity parameter (β), two CV's for

the simulated CPUE data ($CPUE_{cv}$), two values for the rate at which survey estimates are obtained ($Period$), and four priors on the nonlinearity parameter (Table 2.2). Depletion is defined as the current biomass divided by the unfished equilibrium biomass and were pre-defined as 0.15 and 0.45, where 0.15 indicates a stock at lower levels of biomass relative to unfished equilibrium conditions when compared to 0.45. The values of the nonlinearity parameter included a linear relationship (1.0), hyperdepletion (1.6, approximately the mean from Chapter 1), and hyperstability (0.6, which is the approximate symmetric counterpart to 1.6 in log space). Values of 0.1 and 0.3 were chosen for $CPUE_{cv}$ because these values mostly span the range of estimated CV's seen for New Zealand stocks of orange roughy (Ministry of Fisheries 2010), and Francis *et al.* (2003) suggest that the default CV for CPUE series should be between 0.15 and 0.2. All of the factors and their values are listed in (Table 2.2).

There are 288 combinations of factors, 96 for each estimation model, which are referred to as cases. One-hundred data sets ($i = 1, \dots, 100$) were generated for each combination of $Depletion$, β , $CPUE_{cv}$, and survey $Period$. The same data were used across models and priors, which allowed for direct comparison between the models and priors without confounding of results due to variability in the generated data. Each of these 100 simulations estimated four parameters for each model, which included two parameters for CPUE catchability (β and α^* , see Appendix A for a definition of α^*), survey catchability (q), and either the natural log of unfished equilibrium biomass (DDD and SSM) or unfished equilibrium recruitment (AWA). Parameters other than estimated parameters and recruitment deviates were fixed at the values used in the operating model. Markov Chain Monte Carlo (MCMC) was performed for all models to produce an estimated Bayesian posterior distribution. Based on initial simulations, and in the interest of time, 100,500 iterations were conducted with a burn-in of 500 and thinned every 100th value, resulting in 1000 samples from the posterior distribution. Due to the large number of simulations, convergence could not be analyzed for each model, but the burn-in, thinning, and sample size were chosen using test runs on each model. The criteria used were no significant autocorrelation in samples of B_0 , current biomass, and β , stable medians for each of these parameters, and non-significant Z-scores from the Geweke convergence diagnostic (Geweke 1992) for these

parameters.

In most cases, the MCMC estimation completed with little difficulty. For the SSM, precautions were taken in the code to avoid negative stock sizes and errors due to evaluating the log of negative numbers. However, due to random chance, errors infrequently occurred within WinBUGS and the MCMC would stop. These issues were often resolved by starting the chain from new initial values. In very few simulations a new data set from the same trajectory was generated to complete the 100 desired simulations. The highest number of failures for a single case was 13 out of 100 simulations and failures were most prevalent when depletion was at 0.15 and the CV for the CPUE was at 0.1. This pattern was seen for each of the four priors, thus the cause of the high occurrence of errors cannot be attributed solely to a prior type. The AWA and DDD models were coded in ADMB and once the MCMC started, it had no difficulty finishing. However, for ADMB to start an MCMC, an invertible Hessian must be estimated through maximum likelihood estimation to provide a starting point for the covariance matrix in the MCMC algorithm. In a small number of simulations, the Hessian was not invertible, but new starting values solved that issue and new datasets were never generated for these models.

To eliminate spurious model estimates, when the estimate of β was greater than five times or less than one-fifth of the true value, two additional starting points were used and the best estimate was kept, which may have still been an extreme outlier. In some cases, the estimation failed due to various reasons, such as the inability to estimate a Hessian, which is needed to start the MCMC algorithm in ADMB, or errors in WinBUGS, even though the code was written to avoid these. These errors were often reconciled by starting the model at different starting values or a different random number seed, but in very few cases WinBUGS was unable to complete the full MCMC, and a new dataset was simulated. This ensured that 100 converged estimates were available for each combination of factors.

After analyzing the balanced design described above, some specific cases were defined to investigate other properties of the results. These additional cases included not estimating the nonlinearity parameter and simulating the true population with different levels of recruitment variability.

2.2.4 Analysis

The results focus on the bias and precision of estimates of the nonlinearity parameter (β), where an estimate is defined as the median of the posterior distribution. Statistics were expressed in terms of ratios and the natural log because the β parameter is expected to be greater than zero (it is unlikely that CPUE increases when abundance decreases, although the Harley Prior allows negative estimates), hyperdepletion occurs when $\beta > 1$, and hyperstability occurs in the contracted range $0 < \beta < 1$. The ratio of estimated β to the true β , called the estimation ratio, was used to measure bias and variability in the estimates.

$$R_{i,j} = \frac{\hat{\beta}_{i,j}}{\beta_{i,j}} \quad (2.4)$$

where i indicates the simulation and j indicates the case. Performance among cases was compared using the mean absolute logged ratio

$$MALR_j = \frac{\sum_i |\ln(R_{i,j})|}{nSims} \quad (2.5)$$

where $nSims$ is the total number of simulations. Larger values of $MALR$ indicate worse performance. Absolute values were chosen instead of squared values to reduce the effect of extreme estimates and to help the interpretability of the metric. This metric was also integrated over some factors to provide a performance statistic for a smaller combination of factors. For example, the combination of each model and true β was analyzed by combining all simulations with various values of *Depletion*, *CPUEcv*, and *Period*.

Deterministic models are constrained to the assumptions of the population dynamics and cannot mimic the departure from unfished equilibrium biomass at the start of the time series or the sudden changes in abundance observed in highly variable populations. Often in these models, when catches are suddenly reduced, the model can only predict an increase in abundance towards equilibrium due to assumed production, and the estimate of depletion in the final year may often be biased. Given the difficulty of separating the effects of estimating nonlinearity in the relationship between CPUE and abundance and these confounding biases we chose to use relative depletion defined as the biomass in the year of interest divided by the biomass at the start of the time series (B_1 instead of B_0).

With all of the depletion trajectories starting at one, we were able to directly compare the trend and shape of the predicted biomass trajectory to understand the trade-offs in the estimated trajectory with regard to estimating β without the additional uncertainty of B_0 estimates. Actual error (estimate minus true value) was used instead of the logged ratio to provide an easily interpretable measure of performance for relative depletion.

$$DE_{i,j,t} = \frac{\hat{B}_{t,i,j}}{\hat{B}_{1,i,j}} - \frac{B_{t,i,j}}{B_{1,i,j}} \quad t \in [1, \dots, T] \quad (2.6)$$

Again, j refers to the case, which may be integrated over some factors, i indicates the specific simulation, and t refers to the year of interest.

The entire times series of depletion was used to investigate the overall error instead of specific biases that may be present at a certain time period due to the catch history. To characterize bias in the depletion trajectory, the mean depletion error (MDE) was calculated for each simulation over the entire time series.

$$MDE_{i,j} = 100 \times \frac{\sum_{t=1}^T DE_{i,j,t}}{T} \quad (2.7)$$

To characterize bias and variability, the mean absolute depletion error (MADE) was calculated over the entire time series.

$$MADE_{i,j} = 100 \times \frac{\sum_{t=1}^T |DE_{i,j,t}|}{T} \quad (2.8)$$

These metrics were multiplied by 100 to express them as percent depletion error.

The biases in estimates of depletion were also investigated specifically for year 16. Year 16 was chosen because the period from year 1 to year 16 is when the trajectory is declining the fastest, and year 16 was when catches were first reduced.

2.3 Results

Given recruitment variability, the catch scenario, and a fixed final depletion, the simulated population trajectories did not follow a common trend, but can be characterized as fishing down then either stabilizing or slightly increasing (Figure 2.3). The recruitment deviations were occasionally large, resulting in considerable jumps in biomass. It was more difficult to find a series of recruitment deviations that satisfied the criteria for a depletion of 0.15 than

a depletion of 0.45. Randomly simulated recruitment deviate trajectories failed 12% of the time when depletion was 0.45 and 47% of the time when depletion was 0.15.

2.3.1 Estimates of the nonlinearity parameter

There was difficulty in estimating β for some combinations of factors, mostly resulting in small values (< 0.2 times the true value) even though the convergence criteria were acceptable. This was often a result of the MCMC chain sticking to a local minimum. Providing new starting values usually resulted in more reasonable estimates. However, there were some cases where the parameter estimates remained far from the true values after many restarts. Figure 2.4 shows the estimation ratios for each case. Small estimation ratios were most prevalent with the less depleted and less precise CPUE simulations, occurring across all models. The *DDD* model typically showed the widest range in estimates, but all models showed the worst estimates with true depletion equal to 0.45. These small estimation ratios were even more prevalent in the presence of hyperstability ($\beta = 0.6$). The introduction of prior distributions reduced the number of large or small estimation ratios.

The estimates of β differed most from the true value when the stock was less depleted and a uniform prior was used (Figure 2.4). In the less depleted scenario, median estimation ratios were more variable than the more depleted cases (Figure 2.4). The worst estimates, which were negatively biased, occurred when the CPUE data were more uncertain and the stock was less depleted. For the cases with a highly depleted stock, the median estimation ratios were slightly below one for the *DDD* and *AWA* models, and slightly above or near one for the *SSM* (Table 2.3), but estimates of β were rarely outside the range of 0.75 or 1.5 times the true value (Figure 2.4). *MALR* increased in the less depleted scenarios with an increase in *CPUEcv* and survey *Period*, but an interesting result for the deterministic models (*DDD* and *AWA*) and the more depleted scenarios was that the *MALR* improved when the variability on the CPUE was higher (0.3) and β was 1 or 1.6 (Table 2.4). For all cases using the uniform prior, 10.4% of the 7,200 simulations estimated β to be less than one-half of the true value and 5.4% were greater than twice the true value.

The *Hicks Prior* showed less variability in the estimation ratios when compared to the

uniform prior, but more bias. This bias increased with smaller true values of β , less depletion in the stock, and less precision in the CPUE (Figure 2.4 and Table 2.3). The less depleted and high *CPUE_{cv}* case did not show the extremely negatively biased results seen with the uniform prior, but were positively biased (Figure 2.4). When the true β parameter was 0.6 (much less than the prior suggested) and depletion was 0.15, the estimates of the β parameter were only slightly higher than the estimates using a uniform prior, hence the data were informing the estimate of β , but the *Hicks Prior* was also influential, especially when there was less information about the trend in CPUE (less depleted and higher CV on CPUE). The *MALR* was similar or smaller than the *MALR* when using a uniform prior, with the biggest differences occurring when the stock was less depleted (Table 2.4). An increase in *MALR* occurred when survey *Period* increased. An increase in the CPUE uncertainty resulted in small increases to *MALR* when the CPUE were hyperstable, but *MALR* decreased for the *DDD* and *AWA* models when the CPUE data were proportional or showed hyperdepletion. The ratio between the estimated and true β was less than 0.5 in 1.0% of all simulations, and greater than 2 in 5.9% of the simulations.

The *Hicks(1) Prior*, with a median at one (proportionality), produced similar results as seen with the *Hicks Prior* except that the biases were reduced for true β values of 0.6 and 1.0, and increased with a true β of 1.6 (Table 2.3 and Figure 2.4). As expected, when the true β was 1.6, the estimates of β were more negatively biased. When compared to estimates using a uniform prior, the *MALR* always improved when depletion was 0.45 and almost always showed improvement, although slightly, when depletion was 0.15 (Table 2.4). The increase in survey *Period* typically resulted in a small increase in *MALR*, and an increase in *CPUE_{cv}* resulted in a decrease in *MALR* for the proportional and hyperdepletion cases using the *DDD* and *AWA* models. The ratio between the estimated and true β was less than 0.5 in 1.5% of all simulations, and greater than 2 in 1.8% of the simulations.

The *Harley Prior* was influential on the estimates of β , especially when the true β was 1.6, as can be seen in the low variability and the high bias in the estimation ratio (Figure 2.4). As with other priors, when compared to the *Uniform Prior* case, the *MALR* was lower in the more depleted scenarios, although the *MALR* was greater for a few cases when the true β was 1.0 or 1.6 (Table 2.4). When *Depletion* was 0.45, using the *Harley Prior*

resulted in a lower *MALR*, except for a small number of cases when the true β was 1.6 (Table 2.4). More precise CPUE often resulted in worse estimates of β for the *DDD* and *AWA* models, regardless of the level of depletion, and the *SSM* model typically showed smaller *MALR*'s and less bias than the deterministic models, but not always. The ratio between the estimated and true β was less than 0.5 in 5.0% of all simulations, and greater than 2 in none of the simulations.

The *MALR* integrated over *Depletion*, *CPUEcv*, and survey *Period* factors with both CPUE and survey data are shown in the upper panels of Figure 2.5 to compare the three models in the presence of hyperstability, proportionality, and hyperdepletion. Overall, the *DDD* model had the highest *MALR*, followed, by the *AWA* model, and then the *SSM* model. With the *Uniform Prior*, the *MALR* was approximately 1.5 to 2 times higher when the true β was 0.6 compared to when the true β was 1.6. When an informative prior on β was included, the models typically performed best for the true value of β that the prior was most congruent with, although for the *Hicks Prior*, true β 's of 1 and 1.6 performed similarly. Using an informative prior distribution, even when the central tendency of the prior did not support the true amount of nonlinearity, led to better estimates of β than when using a uniform prior, except when β was 1.6 and the *Harley prior* was used by the *DDD* and *SSM* models.

As expected, when omitting survey data and estimating the model parameters with only CPUE data, the estimates of β were more variable, but the *MALR* showed similar patterns to when survey data were included (Figure 2.5, lower panels). All models showed very poor performance with a uniform prior, especially in a situation with less depletion (Figure 2.6). Variability in the estimates of β was reduced when using an informative prior, but bias was introduced when the true β did not match the prior (Figure 2.6, lower three rows). More uncertainty in the CPUE data also reduced the variability in the estimates of β and the informative priors were more influential. Overall, the *SSM* model outperformed the *DDD* and *AWA* models except when the *Harley Prior* was assigned to a true β of 1.6 (Figure 2.5, lower right panel).

2.3.2 Estimates of relative depletion and trend in biomass

The mean true relative depletion declined rapidly then leveled off with little increase through year 30 for both the high and low depletion scenarios (Figures 2.7 and 2.8). The mean estimated trajectory increased slightly at the end of the time series for all of the models, but the state-space model better captured the trend over the last few years. When the true β was not equal to one, estimating β resulted in a more similar mean relative depletion trajectory to the true mean relative depletion trajectory. When the true β was equal to 1, the mean relative depletion trajectories when estimating β and when fixing β at one were similar to each other as well as the true trajectory of mean depletion, except for *DDD* in the less depleted case. Estimating β in this case better captured the beginning trend in the time series.

The mean bias over the entire trajectory with β fixed at one in the estimation model showed the least bias when the true β was one, and *SSM* showed the most bias and underestimated the depletion by about 0.03, on average, when the true population was highly depleted (Table 2.5). As expected, all models with β fixed at one were negatively biased when CPUE data showed hyperdepletion and were positively biased when CPUE data were hyperstable. The deterministic models overestimated the initial decline and subsequently overestimated an increase at the end of the time series, resulting in an averaging of over- and under-estimates of depletion throughout the entire time series (Figures 2.7 and 2.8).

When estimating β with the deterministic models and the *Uniform Prior*, the median *MDE* was always negative when the stock was highly depleted, and was almost always positive when the stock was less depleted (the case of β equals 1.6, *Depletion* equals 0.45, and *CPUEcv* equals 0.1 resulted in a negative median MDE, Table 2.5). The median MDE was always positive for the *SSM* model regardless of the depletion level, and estimating β with a uniform prior in the *SSM* model resulted in a reduction in bias (*MDE* closer to zero) when the true β was not equal to one and the *CPUEcv* was equal to 0.1 (Table 2.5). The percent change in the absolute value of *MDE* was greater than 44% for all scenarios when the true β was not equal to one, except that the *SSM* model with $\beta = 1.6$, *Depletion*=0.15, and *CPUEcv*=0.3, and the *DDD* with $\beta = 0.6$, *Depletion*=0.15, and *CPUEcv*=0.3 resulted

in higher *MDE* values when estimating β with a *Uniform Prior*.

Introducing an informative prior on the β parameter produced mixed results. For the *DDD* and *AWA* models in the more depleted scenario, the *Hicks Prior* and the *Hicks(1) Prior* resulted in similar or slightly reduced *MDE* values when compared to the *Uniform Prior* case, regardless if the prior was congruent with the true β or not (Table 2.5). The *Harley Prior*, however, reduced the *MDE* only in the hyperstable case. When the stock was less depleted, using the *Hicks Prior* and the *Hicks(1) Prior* in the *DDD* and *AWA* models improved the *MDE* only when they were congruent with the true amount of nonlinearity, except that the *Harley Prior* always worsened the *MDE*. The *MDE* for the *SSM* model improved slightly with the *Hicks Prior* and *Hicks(1) Prior* in the hyperdepleted case. When using the *Harley Prior*, opposite trends were seen, where the *MDE* was worse in the hyperstable case, when compared to the *Uniform Prior*. Overall, the deterministic models (*DDD* and *AWA*) showed the most improvement when using an informative prior, although were still subject to more bias when the prior was not similar to the true level of nonlinearity.

The medians of the *MADE* values for the three models and three true levels of β are shown in Table 2.6 for the case when β was fixed at one in the estimation models. The *MADE* was similar among the models and ranged from 4.9% to 15.9% when CPUE was not proportional to abundance, and ranged from 4.3% to 8.8% when CPUE was proportional to abundance. Estimating β with the *Uniform Prior* resulted in lower median *MADE* for almost all of the non-proportional cases (the difference ranging from 0.9%, indicating a worse fit, to -10.3%) with larger reductions occurring in almost all of the more depleted scenarios when the true relationship between CPUE and abundance was hyperstable and CPUE data were less variable. The median *MADE* increased or remained the same for the proportional cases (the difference ranging from 0% to 2.8%) and the largest increases occurred in the less depleted scenario for all three estimation models. Estimating β with an informative prior resulted in similar median *MADE* for the more depleted scenario when compared to estimating β with the *Uniform Prior*. For the less depleted scenario, the median *MADE* showed improvement, compared to the *Uniform Prior*, when using an informative prior with a median similar to the true level of nonlinearity. Additionally, estimating β with the *DDD* and *AWA* models often resulted in a decrease in *MADE* with higher *CPUE_{cv}*, but an

increase was observed when using the *SSM* models.

The estimates of depletion in year 16 from the operating model (true values) were centered on 0.24 and 0.46 when the final depletion was 0.15 and 0.45, respectively. The depletion in year 16 was negatively biased in the *DDD* and *AWA* models for the more depleted scenarios (Figure 2.9), indicating that the decline was estimated to be faster than the true rate of decline. The *SSM* model estimates of trend were slightly less biased, more variable and showed an opposite bias when compared to the *DDD* and *AWA* models. With a less depleted stock, the depletion in year 16 was similar across models and bias was introduced via the prior distribution. The depletion was more consistent across different true values of β when β was estimated using the *Uniform Prior* distribution. For all prior distributions, the estimates of depletion in year 16 were more variable when *Depletion* was 0.45.

2.4 Discussion

The reliable estimation of a nonlinearity parameter for the relationship between CPUE and abundance is influenced by many factors. In this study we showed that models perform differently, priors may improve estimation error but may also lead to bias, fishery-independent surveys improve estimates, and there is more information about the nonlinearity in CPUE when a stock is more depleted. Estimates of the nonlinearity parameter (β) showed considerable improvement when additional data were available, such as survey data or informative prior information. An unintuitive result was that additional uncertainty in the CPUE data improved estimates of β . Increasing the variability on the CPUE data lessened the influence of those data, allowing the model to put more weight on the prior distribution (if it was informative) and the survey data, which was proportional to abundance. This result was most prevalent in the proportional and hyperdepletion scenarios and was not as stark with the *SSM* model because some process error was modeled. Further investigation into the cause of this result could not be done with this set of simulations, but it would be worthwhile to investigate the contribution of data weighting, prior distributions, the starting year of the survey series, and biases from the estimation models.

Francis (2011) suggested that if survey and fishery abundance data appear to be contradictory, then separate assessments should be done using only subsets of the abundance

data, unless a data set is obviously unrepresentative. As noted by Francis (2011), it may be difficult to portray an accurate level of uncertainty when presenting multiple assessments, and furthermore, detecting unrepresentative data is not straightforward. Our simulations took an additional approach to conducting two separate assessments, and introduced a slightly more complicated model to explain the differences between two abundance indices. We showed that estimating a nonlinearity parameter resulted in improved estimates of depletion and trend in abundance. In addition, estimating this parameter allows for a better representation of the uncertainty that would otherwise be difficult to portray with two separate assessments. The key is to understand the processes that may require a particular data set to be modeled differently. That understanding can also help create useful prior distributions for certain parameters.

Stock assessments commonly assume that the nonlinear parameter is one (proportional to abundance), which is similar to putting an extreme prior on the nonlinearity parameter with all probability on the value of 1.0. If CPUE is not proportional to abundance, a stock assessment may provide biased estimates of depletion, which is especially problematic when reference points are used by managers. Loosening this assumption with a reasonable prior, preferably developed from a meta-analysis, will at least give a better portrayal of the uncertainty in the estimates from the model, especially when CPUE is a major source of information. Additional information, such as informative surveys, or a stock with a lot of contrast in biomass levels will begin to override the influence of the prior distribution and could possibly lead to the state where removing the CPUE index is the best option given the understanding of nonlinearity between CPUE and abundance and being able to determine if it provides useful information about abundance.

Supplying information on the amount of nonlinearity in the relationship between CPUE and abundance to the estimation model in the form of an informative prior distribution resulted in fewer extreme values and more precise estimates of β , but resulted in some bias. In other words, there is a trade-off between bias and variance in the estimate of β , and the bias depends on how accurate the prior distribution is relative to the true level of nonlinearity. When estimating the nonlinearity parameter with a uniform prior, the variability was quite large and estimates were sometimes completely wrong or convergence failed. Therefore, an

informative prior distribution appears to be very useful when estimating nonlinearity in the CPUE, especially when limited data are available, but it must be appropriate, justifiable, and wide enough to support all possible values of β .

Specification of prior distributions can be controversial because of the influence they may have on the results (Punt and Hilborn 1997). With less informative CPUE data, the prior becomes more informative. The *Hicks Prior* used here was developed from a meta-analysis of only four stocks and six CPUE series, but that meta-analysis attempted to incorporate as much uncertainty as possible and was focused on the development of a prior distribution, thus has a wide variance (see Chapter 1). This prior did result in bias, but there was enough variability in the prior to allow the data to have some influence. The *Harley Prior* was also developed from a meta-analysis, which included many sets of data from fisheries for different species using various gear types (Harley *et al.* 2001). This prior was less supportive of hyperdepletion ($P_{Harley}(\beta > 1) = 0.20$) than the *Hicks Prior* was supportive of hyperstability ($P_{Hicks}(\beta < 1) = 0.31$), and the *Harley* prior operated directly on β rather than the natural log of β , although little probability was associated with values less than zero. These two priors were developed from different fisheries and therefore have different uses. The *Harley Prior* was developed using data collected from fisheries which operated for many years before data were collected and are now managed by the International Council for the Exploration of the Sea (ICES). The *Hicks Prior* used data from the early phases of orange roughy fisheries that were first exploited in the late 1970's. Not only is it important to ensure that the prior distribution has a wide enough distribution to allow for every possible value of the parameter, but making sure the prior is representative of the population it is being used for will reduce unnecessary bias.

Other than recruitment variability, the three estimation models fixed many parameters to the true value in the population. In reality, additional bias will likely occur due to misspecification, and Francis (2012) points out that assuming the same parameter values in the operating and estimation models is a weakness in simulation studies because there will always be misspecification, at least in fish stock assessment models. It is unknown how the estimates of β would change when other parameters are incorrect or estimated, but it is likely that estimates of β will likely be more uncertain and biased as this parameter

attempts to correct for other misspecifications.

In these simulations, the three models were unable to completely mimic the entire true trend in abundance, thus the estimates of depletion and biomass for many years were biased. Accurately estimating the trend in depletion is important in assessments because it gives an indication of the historical status of the stock. Depending on the underlying level of nonlinearity (hyperstability or hyperdepletion), the trend can be overestimated or underestimated which can lead to biases that are detrimental to the adequate management of a stock. For example, with hyperstability, the initial decline will likely be underestimated and the stock will appear to be in better shape than it actually was. Conversely, hyperdepletion will likely result in a pessimistic view of stock status. When the initial trend is estimated with bias, the remainder of the biomass trajectory is also subject to biases, as well as the estimated parameters because they are also attempting to balance the biases.

Additionally, when an analysis is focused on estimating the relationship between abundance and CPUE, any bias in the estimates of trend introduced through model misspecification will likely translate into biases in the nonlinearity parameter. The *SSM* model showed the least amount of bias in the initial trend in depletion and is a good candidate for estimating the nonlinearity parameter. However, this model showed bias in the estimates of depletion and may not be the best model for management purposes, although none of the three models here were able to estimate depletion without bias. It does show, however, that even though one may not prefer to use this formulation of a state-space model for management, it is a useful model when investigating the relationship between CPUE and abundance, such as in a meta-analysis. Results from these studies could be used to develop an informative prior for use in stock assessment models that are more focused on the estimation of status.

This study was not focused on the consequences of estimating β on management and conservation. A management strategy evaluation could be used to model a fishery management system including the assessment cycle and the management decisions (McAllister *et al.* 1999, e.g.), and would be useful to investigate the short-term and long-term trade-offs of estimating β in terms of conservation risk, average catch, and catch variability. It appears that estimating β may better define the initial trend in abundance and reduce the

risk of over-harvesting in a hyperstable situation or reduce the risk of under-utilization in the hyperdepleted case. However, this study does not provide any evidence of long-term consequences.

The model with process and observation error showed better ability to estimate the nonlinearity parameter than deterministic (observation error only) models and the addition of prior information helped reduce the variability, but at the expense of bias. Estimating recruitment deviations in an age-structured model may also provide more precise estimates of β , but with only CPUE and survey data, there is likely little information to adequately inform those deviations. It would be worthwhile to investigate this further using the proper bias-correction for the recruitment deviations (Methot and Taylor 2011), especially since age-structured models similar to *Awatea* are commonly used to assess fish stocks around the world.

The estimates of a nonlinearity parameter for the relationship between CPUE and abundance are subject to high variability when a stock has not been fished to low levels and there is not adequate ancillary data to assist in determining the trend in abundance. With CPUE data providing the only information in an assessment, the estimates of β degraded, but an informative prior distribution improved the estimates. The process error model was able to estimate β with more precision because it could better characterize the initial trend in abundance, but it wasn't clear that the estimation models were particularly good at estimating depletion in an absolute sense, especially when other parameters were misspecified. However, these models, especially the state-space model, are useful for investigating and understanding the relationship between CPUE and abundance.

2.5 Tables

Table 2.1: Parameters used in the operating model.

Parameter	Value
Natural mortality (M)	0.045
Recruitment variability (σ_R)	1.1
Steepness (h)	0.75
Knife-edge selectivity	29
Knife-edge maturity	29
<i>Growth</i>	
t_0	-0.491
k	0.059
L_{inf}	37.78
<i>Length-weight</i>	
Intercept (a)	0.08
Exponent (b)	2.75
<i>CPUE</i>	
Years	1981–1992
α	$(1 \times 10^5)^\beta$
β	See Table 2
CV	See Table 2.2
<i>Survey</i>	
Years	5-30*
q	0.25
CV	0.25

*The spacing between surveys was either 1 year or 3 years (Table 2.2)

Table 2.2: Levels of the different variables tested.

Variable	Description	Abbreviation
Model	Deterministic delay-difference	<i>DDD</i>
	Deterministic age-structured (<i>Awatea</i>)	<i>AWA</i>
	Delay-difference state-space model	<i>SSM</i>
Depletion	15%	<i>Depletion0.15</i>
	45%	<i>Depletion0.45</i>
Population	0.6	<i>Beta0.6</i>
nonlinearity	1.0	<i>Beta1.0</i>
parameter (β)	1.6	<i>Beta1.6</i>
Coefficient of variability on CPUE	0.1	<i>CPUEcv0.1</i>
	0.3	<i>CPUEcv0.3</i>
Survey period	Every 1 year	<i>Period1</i>
	Every 3 years	<i>Period3</i>
Prior on estimated nonlinearity parameter (β)	$\ln(\beta) \sim \text{Uniform}(-10, 10)$	<i>Uniform Prior</i>
	$\ln(\beta) \sim \text{Logistic}(\mu = 0.4591, \sigma^2 = 0.3266)$	<i>Hicks Prior</i>
	$\ln(\beta) \sim \text{Logistic}(\mu = 0.0, \sigma^2 = 0.3266)$	<i>Hicks1 Prior</i>
	$\beta \sim \text{Normal}(\mu = 0.73, \sigma^2 = 0.1)$	<i>Harley Prior</i>

Table 2.3: The median ratio between estimated and true β . Values less than 1 indicate that the estimate was more often less than the true value.

Model	True β	0.15		Depletion		0.45				
		0.1	0.3	CPUEcv	Period	0.1	0.3	1	3	
<i>Uniform Prior</i>										
DDD	0.6	0.86	0.88	0.87	0.88	1.02	1.26	0.42	0.40	
DDD	1	0.83	0.83	0.91	0.90	1.03	1.17	0.97	1.01	
DDD	1.6	0.80	0.71	0.91	0.92	0.88	0.77	1.02	1.06	
AWA	0.6	0.89	0.92	0.88	0.87	1.00	1.12	0.39	0.35	
AWA	1	0.85	0.88	0.93	0.93	1.01	1.19	0.94	0.88	
AWA	1.6	0.85	0.83	0.94	0.93	0.93	1.06	1.03	1.02	
SSM	0.6	1.02	1.02	0.95	0.98	0.99	0.93	0.42	0.34	
SSM	1	1.02	1.04	1.00	0.98	0.97	0.99	0.91	0.75	
SSM	1.6	1.01	1.09	1.05	1.07	0.98	1.01	0.97	0.92	
<i>Hicks Prior</i>										
DDD	0.6	0.90	0.91	0.97	1.08	1.34	1.88	1.52	2.05	
DDD	1	0.83	0.86	0.95	0.99	1.17	1.32	1.26	1.35	
DDD	1.6	0.80	0.80	0.92	0.92	0.90	0.93	1.02	1.01	
AWA	0.6	0.91	0.95	0.99	1.08	1.27	1.66	1.50	1.80	
AWA	1	0.87	0.89	0.96	1.00	1.15	1.28	1.16	1.28	
AWA	1.6	0.85	0.83	0.94	0.94	0.93	0.97	1.02	0.99	
SSM	0.6	1.07	1.10	1.10	1.16	1.18	1.26	1.34	1.46	
SSM	1	1.03	1.06	1.06	1.07	1.10	1.13	1.16	1.11	
SSM	1.6	1.02	1.08	1.04	1.04	0.97	0.99	0.97	0.95	
<i>Hicks1 Prior</i>										
DDD	0.6	0.89	0.93	0.95	1.01	1.22	1.40	1.30	1.47	
DDD	1	0.83	0.85	0.92	0.92	1.01	1.03	1.02	1.03	
DDD	1.6	0.80	0.78	0.90	0.88	0.84	0.80	0.90	0.83	
AWA	0.6	0.90	0.95	0.95	1.01	1.13	1.36	1.25	1.33	
AWA	1	0.86	0.88	0.93	0.93	1.01	1.05	1.00	1.00	
AWA	1.6	0.84	0.83	0.92	0.90	0.86	0.82	0.91	0.84	
SSM	0.6	1.05	1.06	1.06	1.10	1.08	1.10	1.17	1.21	
SSM	1	1.02	1.02	1.02	1.00	0.96	1.00	0.97	0.91	
SSM	1.6	0.99	1.01	1.01	0.99	0.92	0.89	0.87	0.81	
<i>Harley Prior</i>										
DDD	0.6	0.89	0.89	0.94	0.98	1.14	1.19	1.15	1.18	
DDD	1	0.81	0.67	0.91	0.89	0.84	0.77	0.87	0.83	
DDD	1.6	0.62	0.55	0.84	0.80	0.64	0.57	0.72	0.66	
AWA	0.6	0.90	0.95	0.95	0.99	1.09	1.22	1.11	1.16	
AWA	1	0.85	0.87	0.91	0.90	0.93	0.92	0.89	0.84	
AWA	1.6	0.82	0.80	0.85	0.81	0.75	0.69	0.72	0.68	
SSM	0.6	1.04	1.05	1.04	1.07	1.07	1.06	1.07	1.07	
SSM	1	0.99	0.99	0.98	0.95	0.91	0.89	0.86	0.81	
SSM	1.6	0.92	0.87	0.90	0.86	0.77	0.71	0.71	0.67	

Table 2.4: Mean Absolute Logged Ratio (MALR) for the estimated and true β . A value of zero indicates a perfect estimate over all simulations while larger numbers show worse estimation ability.

Model	True β	0.15				Depletion CPUEcv Period	0.45			
		0.1		0.3			0.1		0.3	
		1	3	1	3	1	3	1	3	
<i>Uniform Prior</i>										
DDD	0.6	0.20	0.25	0.29	0.31		0.63	0.83	1.65	1.66
DDD	1	0.23	0.33	0.18	0.22		0.61	0.80	0.77	0.84
DDD	1.6	0.31	0.47	0.20	0.20		0.58	0.77	0.59	0.82
AWA	0.6	0.18	0.21	0.29	0.29		0.56	0.68	1.71	1.72
AWA	1	0.22	0.32	0.17	0.20		0.48	0.59	0.74	0.81
AWA	1.6	0.31	0.43	0.16	0.19		0.52	0.74	0.54	0.75
SSM	0.6	0.11	0.17	0.23	0.27		0.41	0.52	1.63	1.75
SSM	1	0.10	0.18	0.13	0.18		0.27	0.36	0.61	0.82
SSM	1.6	0.10	0.17	0.12	0.14		0.22	0.37	0.40	0.59
<i>Hicks Prior</i>										
DDD	0.6	0.18	0.26	0.18	0.26		0.44	0.59	0.50	0.62
DDD	1	0.23	0.30	0.15	0.18		0.31	0.44	0.30	0.34
DDD	1.6	0.32	0.41	0.19	0.18		0.36	0.41	0.21	0.21
AWA	0.6	0.17	0.22	0.17	0.22		0.36	0.50	0.44	0.54
AWA	1	0.21	0.29	0.15	0.17		0.29	0.37	0.27	0.31
AWA	1.6	0.30	0.39	0.15	0.17		0.34	0.41	0.20	0.22
SSM	0.6	0.13	0.20	0.19	0.23		0.25	0.30	0.37	0.41
SSM	1	0.11	0.16	0.12	0.16		0.19	0.24	0.21	0.21
SSM	1.6	0.09	0.15	0.11	0.12		0.17	0.24	0.17	0.19
<i>Hicks1 Prior</i>										
DDD	0.6	0.19	0.22	0.17	0.21		0.32	0.36	0.33	0.36
DDD	1	0.23	0.30	0.16	0.17		0.25	0.33	0.22	0.20
DDD	1.6	0.32	0.44	0.20	0.20		0.37	0.44	0.24	0.29
AWA	0.6	0.16	0.20	0.17	0.18		0.26	0.32	0.28	0.32
AWA	1	0.21	0.28	0.15	0.16		0.24	0.29	0.21	0.21
AWA	1.6	0.30	0.39	0.16	0.18		0.36	0.44	0.24	0.29
SSM	0.6	0.11	0.16	0.16	0.19		0.19	0.22	0.24	0.26
SSM	1	0.10	0.15	0.11	0.14		0.18	0.21	0.17	0.20
SSM	1.6	0.08	0.14	0.11	0.12		0.18	0.27	0.22	0.28
<i>Harley Prior</i>										
DDD	0.6	0.17	0.24	0.17	0.17		0.21	0.25	0.20	0.22
DDD	1	0.26	0.46	0.15	0.16		0.36	0.46	0.18	0.21
DDD	1.6	0.55	0.61	0.20	0.25		0.63	0.71	0.37	0.46
AWA	0.6	0.16	0.19	0.17	0.17		0.22	0.24	0.20	0.20
AWA	1	0.20	0.25	0.15	0.15		0.18	0.21	0.18	0.21
AWA	1.6	0.27	0.32	0.18	0.22		0.32	0.39	0.37	0.43
SSM	0.6	0.11	0.15	0.15	0.17		0.18	0.21	0.19	0.21
SSM	1	0.08	0.10	0.09	0.12		0.16	0.17	0.18	0.24
SSM	1.6	0.09	0.14	0.12	0.18		0.27	0.33	0.38	0.43

Table 2.5: Medians of the mean depletion error (MDE) for the three estimation models with β fixed at one and the three estimation models with β estimated using different prior assumptions for the level of true nonlinearity. Negative values indicate that the estimated relative depletion trajectory was on average more depleted than the true relative depletion trajectory (see Equation 2.7). Numbers in italics indicate the true scenario which most closely matches the assumption in the estimation model.

Model	True	0.15		0.45		<i>Depletion</i>	
	β	0.1	0.3	0.1	0.3	<i>CPUEcv</i>	
<i>DDD</i>	0.6	9.8%	0.3%	10.3%	6.0%		
<i>DDD</i>	1	-0.3%	-1.5%	-1.4%	-0.9%		
<i>DDD</i>	1.6	-7.4%	-5.2%	-12.4%	-5.5%		
<i>AWA</i>	0.6	9.8%	3.0%	10.0%	6.6%		
<i>AWA</i>	1	-0.1%	-0.3%	0.2%	0.2%		
<i>AWA</i>	1.6	-6.2%	-3.4%	-9.5%	-5.0%		
<i>SSM</i>	0.6	15.8%	12.6%	12.6%	8.7%		
<i>SSM</i>	1	2.8%	3.6%	1.9%	1.3%		
<i>SSM</i>	1.6	-8.2%	-2.4%	-11.0%	-5.4%		

Model	True	<i>Uniform Prior</i>				<i>Hicks Prior</i>			
		0.15		0.45		0.15		0.45	
		0.1	0.3	0.1	0.3	0.1	0.3	0.1	0.3
<i>DDD</i>	0.6	-2.9%	-1.5%	2.5%	2.2%	-1.9%	-1.4%	8.0%	7.2%
<i>DDD</i>	1	-2.2%	-1.2%	2.7%	0.3%	-2.8%	-0.6%	3.8%	1.8%
<i>DDD</i>	1.6	-3.8%	-2.7%	-3.7%	1.4%	-3.8%	-2.3%	-2.4%	1.9%
<i>AWA</i>	0.6	-1.5%	-1.5%	2.1%	2.2%	-1.3%	-1.3%	6.5%	6.1%
<i>AWA</i>	1	-2.1%	-0.8%	2.2%	0.3%	-1.9%	-0.4%	3.4%	1.2%
<i>AWA</i>	1.6	-2.9%	-1.2%	-1.4%	1.4%	-2.9%	-1.1%	-0.4%	2.1%
<i>SSM</i>	0.6	4.1%	5.8%	2.8%	4.8%	5.2%	7.2%	6.5%	7.1%
<i>SSM</i>	1	3.2%	4.9%	1.1%	1.9%	4.2%	4.1%	3.9%	4.4%
<i>SSM</i>	1.6	3.5%	4.4%	1.8%	1.8%	3.0%	4.4%	1.9%	1.2%

Model	True	<i>Hicks Prior1</i>				<i>Harley Prior</i>			
		0.15		0.45		0.15		0.45	
		0.1	0.3	0.1	0.3	0.1	0.3	0.1	0.3
<i>DDD</i>	0.6	-2.3%	-1.4%	4.1%	6.4%	-1.7%	-1.5%	3.1%	3.2%
<i>DDD</i>	1	-2.6%	-1.0%	1.3%	1.2%	-4.0%	-0.9%	-4.4%	-1.0%
<i>DDD</i>	1.6	-4.1%	-2.6%	-3.7%	-0.1%	-9.9%	-2.3%	-12.1%	-3.2%
<i>AWA</i>	0.6	-1.4%	-1.2%	4.1%	3.8%	-1.4%	-1.4%	2.7%	2.7%
<i>AWA</i>	1	-2.0%	-0.7%	1.4%	0.3%	-2.1%	-0.8%	-1.3%	-1.1%
<i>AWA</i>	1.6	-3.0%	-1.3%	-2.6%	0.6%	-3.1%	-2.1%	-6.1%	-3.3%
<i>SSM</i>	0.6	4.9%	6.7%	4.7%	5.3%	5.6%	6.9%	5.0%	5.3%
<i>SSM</i>	1	3.4%	4.2%	1.7%	2.3%	2.6%	3.4%	0.2%	0.4%
<i>SSM</i>	1.6	2.5%	4.2%	-0.8%	-0.3%	0.2%	1.8%	-4.4%	-3.9%

Table 2.6: Medians of the mean absolute depletion error (*MADE*) for the three estimation models with β fixed at one under assumptions of different levels of true nonlinearity. Larger values indicate increased estimation error (see Equation 2.8).

Model	True	0.15		0.45		<i>Depletion CPUEcv</i>
	β	0.1	0.3	0.1	0.3	
<i>DDD</i>	0.6	10.2%	6.4%	10.7%	9.5%	
<i>DDD</i>	1	5.0%	6.4%	8.8%	7.9%	
<i>DDD</i>	1.6	8.1%	6.8%	13.2%	8.6%	
<i>AWA</i>	0.6	10.2%	5.7%	10.6%	8.8%	
<i>AWA</i>	1	4.9%	5.2%	6.3%	7.0%	
<i>AWA</i>	1.6	7.2%	5.6%	10.5%	7.6%	
<i>SSM</i>	0.6	15.9%	12.6%	12.6%	9.6%	
<i>SSM</i>	1	4.3%	4.7%	4.8%	6.4%	
<i>SSM</i>	1.6	9.0%	4.9%	11.3%	7.7%	

Model	True β	<i>Uniform Prior</i>				<i>Hicks Prior</i>			
		0.15		0.45		0.15		0.45	
		0.1	0.3	0.1	0.3	0.1	0.3	0.1	0.3
<i>DDD</i>	0.6	6.1%	5.5%	8.9%	8.5%	5.9%	5.5%	12.1%	10.8%
<i>DDD</i>	1	6.6%	5.5%	10.5%	10.0%	6.6%	5.4%	9.5%	9.2%
<i>DDD</i>	1.6	7.6%	5.9%	11.5%	8.7%	7.6%	5.8%	9.8%	7.6%
<i>AWA</i>	0.6	5.7%	5.4%	8.7%	8.2%	5.7%	5.5%	11.1%	10.6%
<i>AWA</i>	1	6.5%	5.4%	8.5%	9.8%	6.4%	5.4%	9.1%	8.4%
<i>AWA</i>	1.6	7.4%	5.8%	10.2%	8.5%	7.4%	5.8%	9.3%	7.4%
<i>SSM</i>	0.6	5.6%	6.5%	6.7%	8.2%	5.6%	7.4%	7.9%	9.2%
<i>SSM</i>	1	4.4%	6.0%	5.5%	7.8%	4.9%	5.0%	6.5%	7.3%
<i>SSM</i>	1.6	4.7%	5.5%	5.1%	6.0%	4.6%	4.9%	4.7%	5.7%

Model	True β	<i>Hicks Prior1</i>				<i>Harley Prior</i>			
		0.15		0.45		0.15		0.45	
		0.1	0.3	0.1	0.3	0.1	0.3	0.1	0.3
<i>DDD</i>	0.6	5.9%	5.4%	9.6%	9.6%	5.7%	5.4%	8.6%	8.5%
<i>DDD</i>	1	6.5%	5.4%	8.3%	8.3%	6.5%	5.4%	9.3%	7.8%
<i>DDD</i>	1.6	7.6%	5.7%	9.4%	6.8%	10.0%	5.4%	13.9%	7.2%
<i>AWA</i>	0.6	5.7%	5.4%	9.6%	9.0%	5.7%	5.4%	8.5%	8.4%
<i>AWA</i>	1	6.4%	5.3%	8.2%	8.1%	6.3%	5.4%	7.3%	7.5%
<i>AWA</i>	1.6	7.3%	5.7%	8.9%	6.7%	6.7%	5.0%	7.8%	7.3%
<i>SSM</i>	0.6	5.6%	7.3%	6.6%	8.0%	5.9%	7.1%	7.3%	8.6%
<i>SSM</i>	1	4.5%	5.3%	5.8%	7.2%	4.1%	4.7%	4.9%	6.4%
<i>SSM</i>	1.6	4.6%	4.9%	4.9%	5.2%	3.7%	4.1%	5.8%	6.0%

2.6 Figures

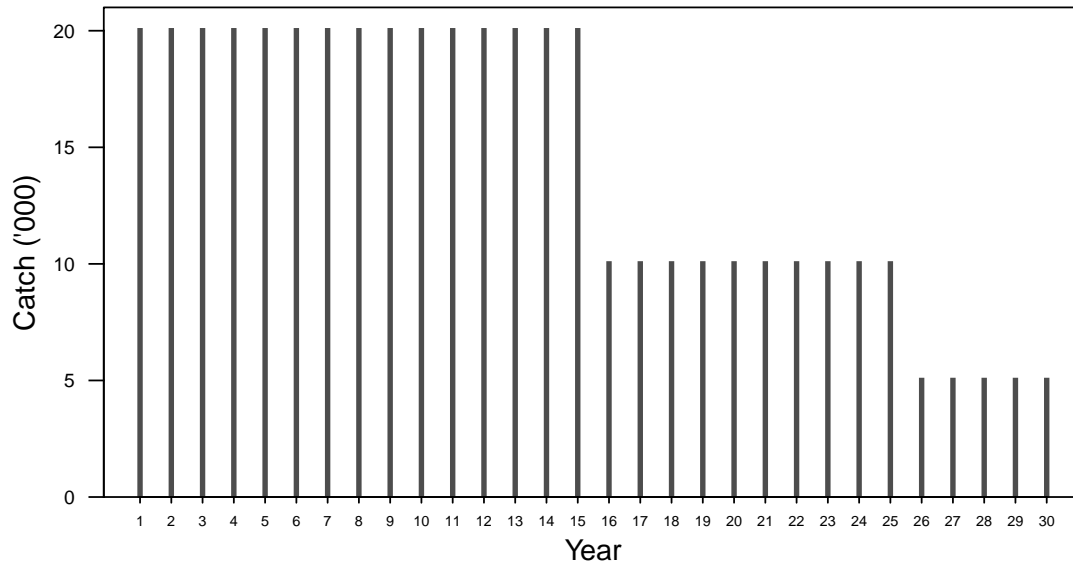


Figure 2.1: The fixed catch (thousands of metric tons) used in the models.

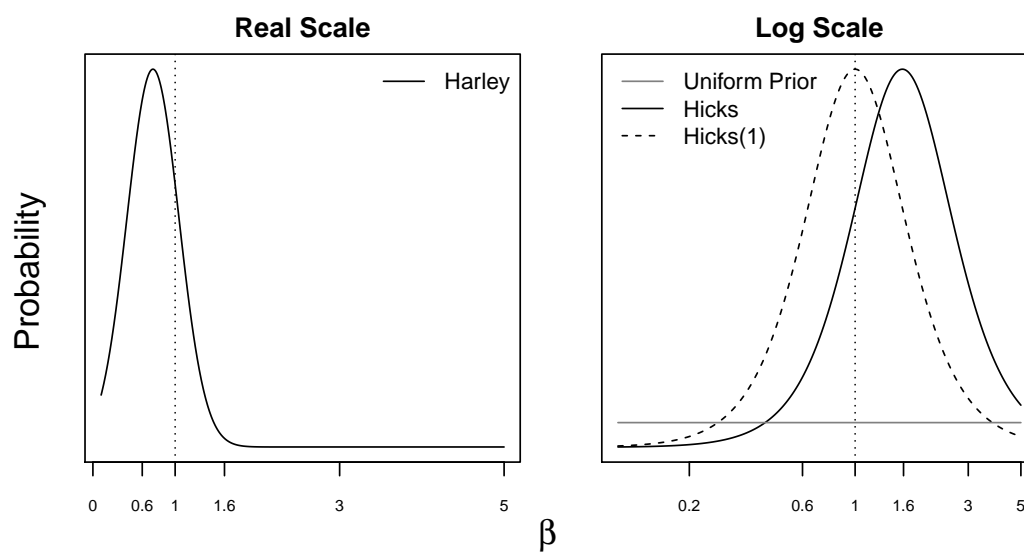


Figure 2.2: The four prior distributions for β used in the estimation models. The *Harley Prior* is a normal distribution in real space (left panel). The *Hicks Prior* and *Hicks(1) Prior* are logistic distributions in log space and the *Uniform Prior* is also in log space (right panel).

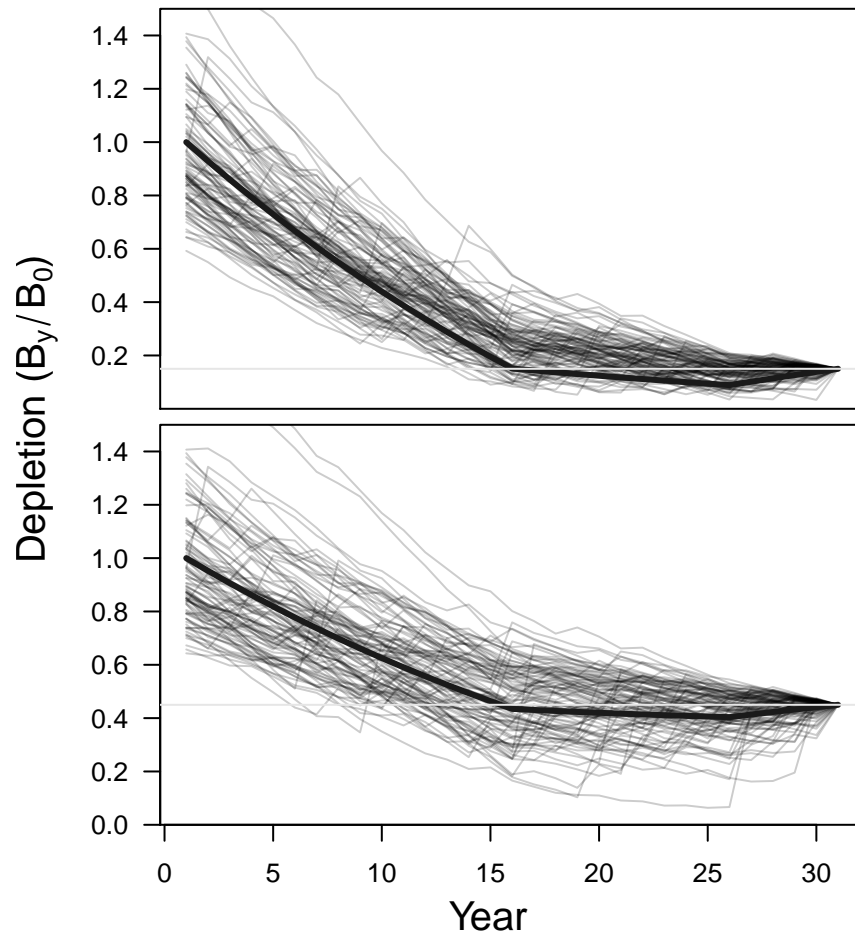


Figure 2.3: Simulated trajectories of beginning of the year spawning biomass from the true population with recruitment variability equal to 1.1 and an ending depletion of 0.15 (top panel) or 0.45 (bottom panel). The thick dark line is the deterministic trajectory ($\sigma_R = 0$) and the light colored horizontal line is the simulated final level of depletion. Data were generated from these "true" trajectories.

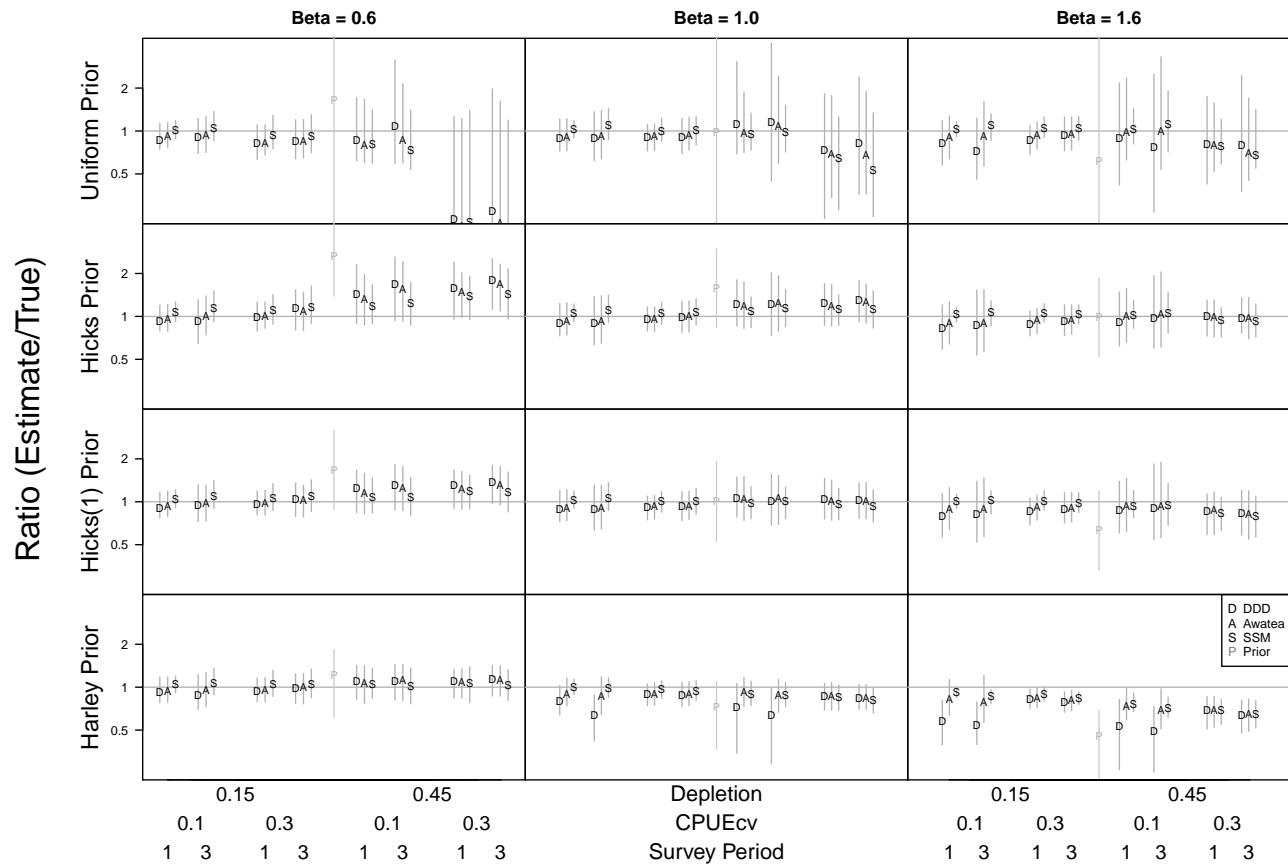


Figure 2.4: Ratio of the estimated β parameter to the true β parameter for the simulations. The four priors are shown down the rows while the three true β parameters are shown across columns. Within each box, the eight combinations of *Depletion*, *CPUEcv*, and *Period* are displayed. The mean ratio for each of the three models is shown for each case with a letter indicating the model and bars encompassing the central 75% of the values observed from the simulations. Random values from the prior distribution, divided by the true β are shown in the center of each plot with the median marked by a “P” for comparison.

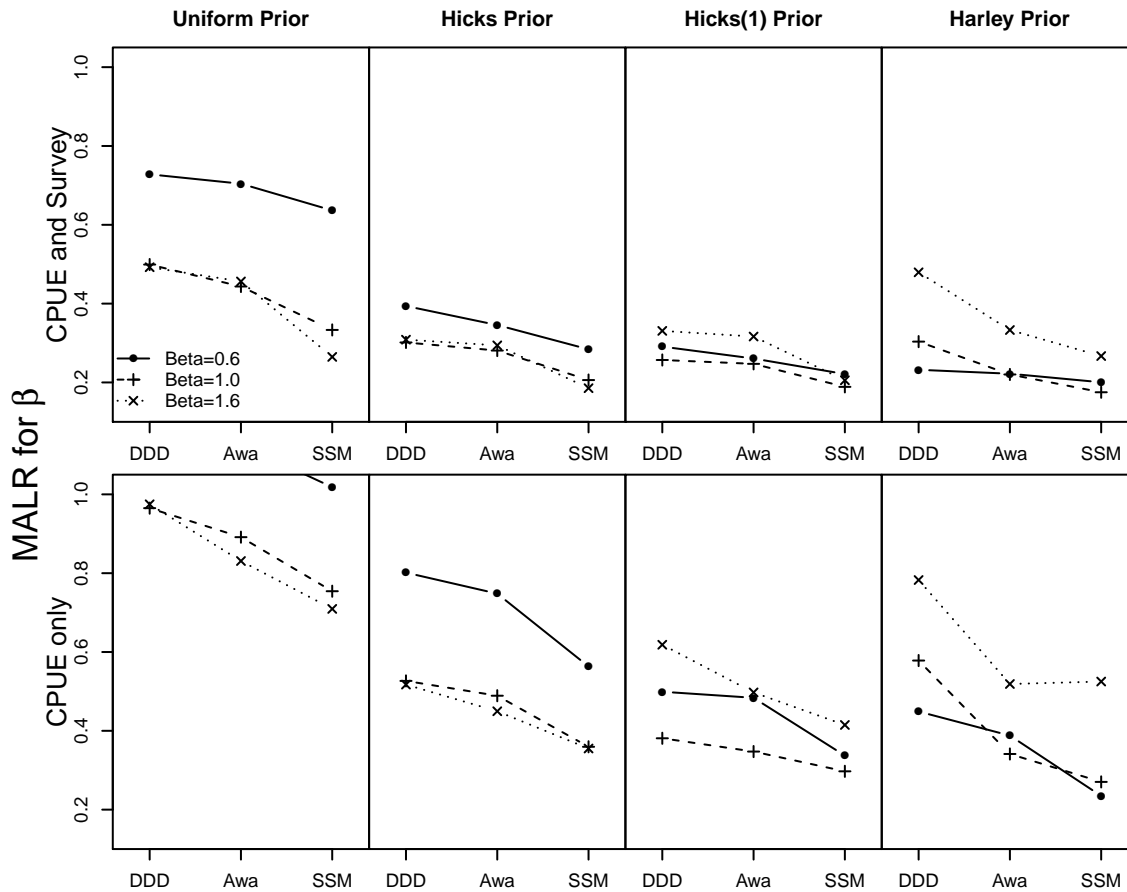


Figure 2.5: MALR for different true values of β (lines) and the three models (x-axis within each subplot) from simulations using CPUE and survey data and estimating β with different prior distributions (subplots), integrated over *Depletion*, *CPUEcv*, and *Period* (top row). Also shown are MALR values for simulations using only CPUE data, integrated over *Depletion* and *CPUEcv* (bottom row). The results for the true β equal to 0.6 estimated with a uniform prior and only CPUE data in the *DDD* and *AWA* models (bottom left plot) are higher than the upper limit of the plot.

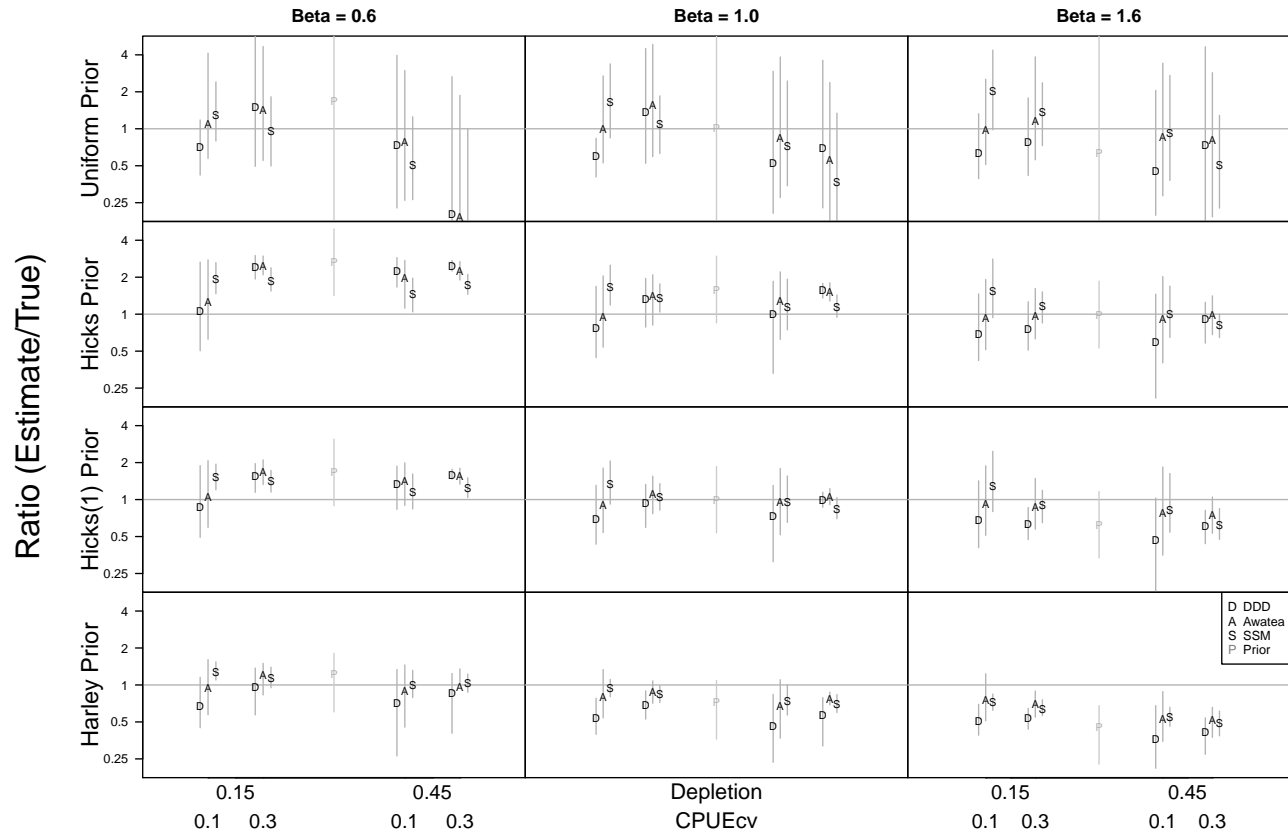


Figure 2.6: Ratio of the estimated β parameter to the true β parameter for the simulations **with only CPUE data**. The four priors are shown down the rows while the three true β parameters are shown across columns. Within each box, the four combinations of *Depletion* and *CPUEcv* are displayed. The mean ratio for each of the three models is shown for each case with a letter indicating the model and bars encompassing the central 75% of the values observed from the simulations. Random values from the prior distribution, divided by the true β are shown in the center of each plot with the median marked by a “P” for comparison.

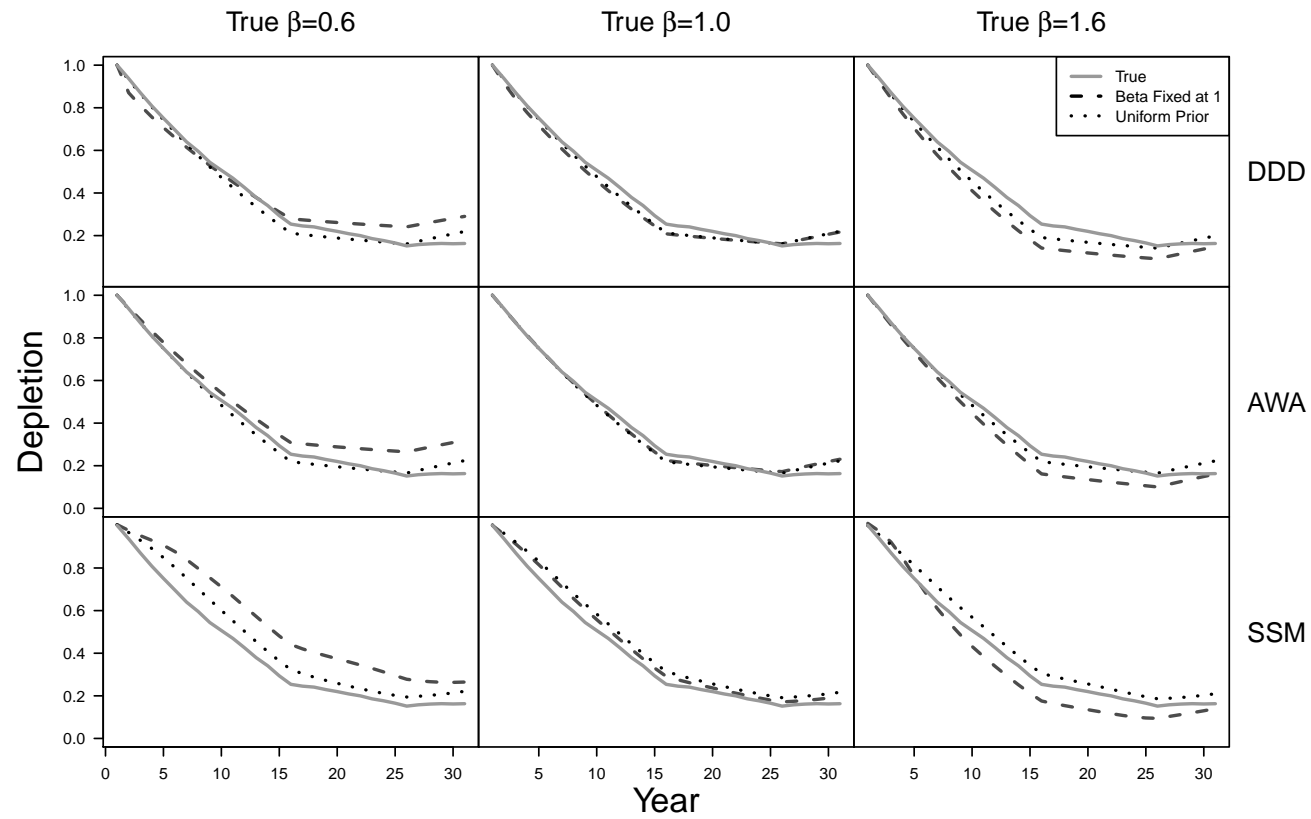


Figure 2.7: The mean true depletion trajectory (solid line) with a final depletion of 0.15. Mean estimated depletion trajectories are shown where β was fixed at 1 (dashed line) or estimated with a uniform prior distribution (dotted line) in the three estimation models (rows) with the three levels of true nonlinearity (columns).

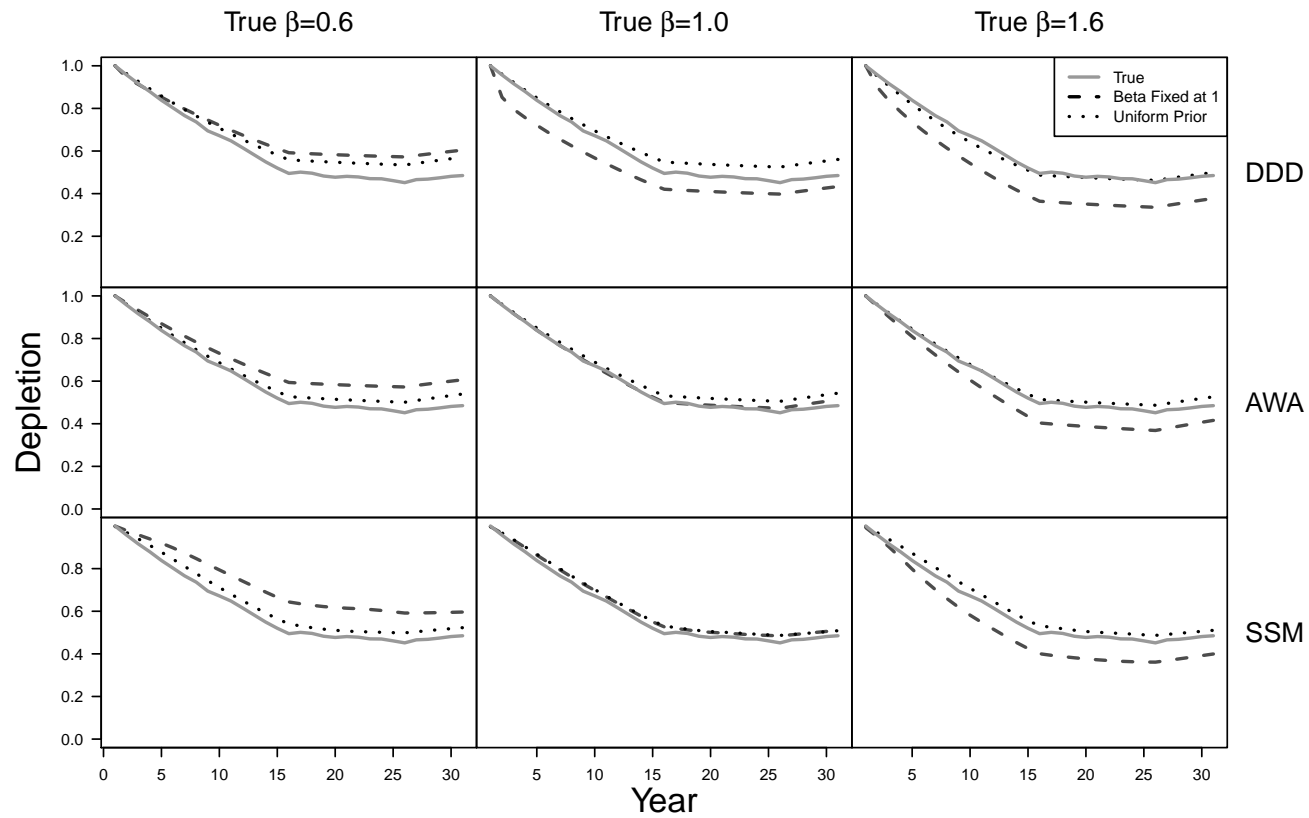


Figure 2.8: The mean true depletion trajectory (solid line) with a final depletion of 0.45. Mean estimated depletion trajectories are shown where β was fixed at 1 (dashed line) or estimated with a uniform prior distribution (dotted line) in the three estimation models (rows) with the three levels of true nonlinearity (columns).

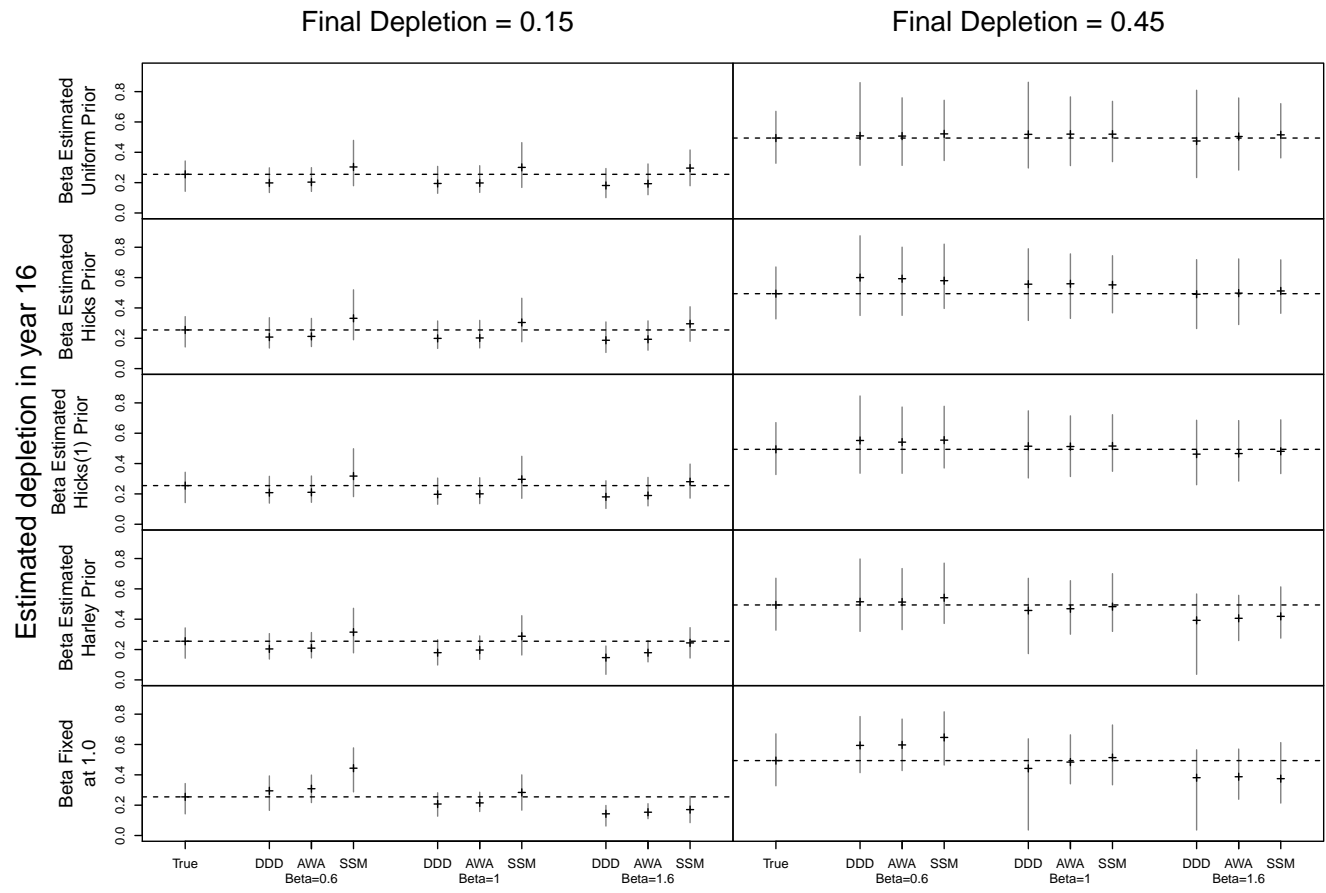


Figure 2.9: Estimated depletion in year 16 from the operating model (True) and the three models given different levels of nonlinearity (β), depletion (columns), and priors (rows). The median value is shown with a '+' and the 75% probability interval is shown with the vertical line. The horizontal dashed line indicates the median of the true depletion.

Chapter 3

**MANAGING A LONG-LIVED FISH STOCK WHEN THERE IS A
NONLINEAR RELATIONSHIP BETWEEN CPUE AND
ABUNDANCE*****Abstract***

Most modern fisheries management systems rely on assessments of trend in stock status, and these assessments are highly dependent on indices of stock size. Such indices are commonly research surveys or catch-per-unit-effort (CPUE) from fishing operations. CPUE data are commonly assumed to be proportional to abundance, but are often not. This analysis investigates whether accounting for nonlinearity between CPUE and abundance in the management of long-lived species can improve the outcomes. An age-structured operating model was used to simulate a true population from which CPUE and survey data were generated and alternative estimation models were used to estimate population parameters from the simulated data. Three alternative assumptions about the relationship between CPUE and abundance were considered in the operating model: 1) hyperstability (CPUE declined slower than abundance), 2) proportional to abundance, and 3) hyperdepletion (CPUE declined faster than abundance). Two-area models with movement dependent on fishing effort or fish density were also investigated. The benefits to estimates of stock status and yield objectives when estimating a nonlinearity parameter were dependent on the true underlying relationship between CPUE and abundance. Hyperstable scenarios were especially risky and should always be accounted for, or at least acknowledged, in a management strategy. Hyperdepletion scenarios, on the other hand, led to reduced conservation risk, reduced yield in the short term, and a pessimistic view of the stock, and thus the management system. In the long-term, yield was similar whether or not nonlinearity was estimated, estimating nonlinearity reduced the risk to the stock when CPUE data were hyperstable and although risk was increased when CPUE showed hyperdepletion, stock status was typically always higher than the hyperstable scenarios.

3.1 Introduction

Many fisheries are managed by regulating catch or effort based on the productivity and abundance of the stock as estimated from an assessment. Regulations are often chosen with the joint objectives of achieving a low probability that the stock will fall below a threshold value and maximizing the yield. A stock assessment may involve a complicated statistical model integrating many sources of data (Maunder, 2003), or may use empirical indicators of stock health, such as length-based reference points (Cope and Punt 2009; Froese 2004; Prince *et al.* 2011) or catch-rates from the fishery (Starr *et al.* 1997). Typically, the outputs of the assessment are inputs into a harvest control rule that determines the catch or effort level (Deroba and Bence 2008).

There will always be trade-offs among management objectives of conservation, yield, and the stability of catch targets, both in the long and short term (Cox and Kronlund 2008). Management strategy evaluation (MSE, or management procedure evaluation, MPE) has become a popular tool to investigate these trade-offs given a management system (Bunnefeld *et al.* 2011; Butterworth *et al.* 1997; de la Mare 1998; Hilborn 1979; Martell and Walters 2002; Punt *et al.* 2001; Sainsbury 2000; Walters and Martell 2004). An MSE involves a simulation of the full management cycle, mimicking the underlying fish population, data gathering, analysis, and policy application. MSE's often focus on the harvest control rule, but the approach can also be used to compare the performance of different methods used to estimate the parameters important to setting the fishery policy (Hilborn 1979; Martell and Walters 2002).

Since the 1970's, fisheries have been expanding into deeper water, targeting species that are typically long-lived, slow-growing, late-maturing and often associated with seamounts (Clark 2009). Large fisheries have developed for low productivity species such as orange roughy (*Hoplostethus atlanticus*), oreos (family Oreosomatidae), and black cardinalfish (*Epigonus telescopus*), especially in New Zealand (Cochrane *et al.* 1998). These deepwater species occur mainly deeper than 500 m (Sissenwine and Mace 2007), are less productive than shelf species, have low natural mortality rates (less than 0.065 yr^{-1}), and commonly experience maturity at an age greater than 25 years (Cochrane *et al.* 1998). Additionally,

many deepwater fish have high variability in recruitment, which may be a result of naturally high variability from year to year, or caused by serial or episodic recruitment (Clark 2009; Ianelli 2002).

The low productivity and high vulnerability of many deepwater species, along with rapid declines in catch-rates, variable recruitment, and examples of "boom or bust" fisheries has resulted in uncertainty in whether these fisheries can be managed sustainably (Clark 2001; Koslow 2000; Lack *et al.* 2003b; Sissenwine and Mace 2007). Management strategy evaluations have been conducted or are planned for some of these species (Punt *et al.* 2001; Sissenwine and Mace 2007). Francis (1992) undertook a risk analysis of different rates at which catches of orange roughy were reduced to a target. Wayte, SE (editor) (2009) simulation tested the Australian Tier 1 harvest control rule, which uses outputs from an assessment model and target reference points, for a stock with life history characteristics that are similar to orange roughy. These studies showed there was a high risk that the stock could collapse after which it would take many years to recover.

Fishery-dependent catch-rate data are an important source of information for these species and are often the only information on abundance trends. Catch-rate data are typically standardized (e.g., Maunder and Punt (2004)) to create a catch-per-unit-effort (CPUE) series. CPUE is usually assumed to be proportional to abundance when providing management advice, but it may decline slower than abundance (hyperstability) or decline faster than abundance (hyperdepletion), resulting in a biased assessment of stock status (Beverton and Holt 1957; Harley *et al.* 2001; Hilborn and Walters 1992; Paloheimo and Dickie 1964; Walters 2003; Wilberg *et al.* 2010) as well as biased information presented to managers and the public (Maunder *et al.* 2006; Wilberg and Bence 2006). Orange roughy fisheries have been the focus of much research because of the high value of these fisheries and management concerns, which are exacerbated by the common occurrence of a rapid decline in CPUE during the early years of the fishery (Clark 2009; Japp and Wilkinson 2007; Sissenwine and Mace 2007).

The rapid decline in CPUE often seen in orange roughy fisheries may not be due solely to depletion of populations in response to fishing. Possible hypotheses to explain faster than expected declines in estimated stock size are 1) intermittent aggregating, 2) disruption

due to fishing, and 3) mass emigration or mortality (Clark and Tracey 1992; McAllister and Kirchner 2002). Additionally, a habitat hypothesis (pers. comm., Matthew Dunn, NIWA, New Zealand & Patrick Cordue, ISL, New Zealand) was used by Dunn (2011) to develop a two-area assessment model structure for orange roughy, which was able to explain the steep decline observed in CPUE data at the beginning of the fishery, and a flat trend afterwards. In this model, fish recruit to a secondary habitat (flat areas) and adults migrate slowly to primary habitats (hill or seamount areas). Large removals typical at the start of orange roughy fisheries depletes the population faster than migration from the flat areas can replenish it, thus CPUE declines faster than total abundance. When fishing is reduced, migration to the primary habitat may keep CPUE at stable levels although the total biomass may continue to decline. All four of these hypotheses can be approximated using a two-area model with migration between a fished area and an unfished area.

The consequences of different harvest control rules (Deroba and Bence 2008) and alternative relationships between CPUE and abundance on management outcomes can be investigated using MSE (Maunder *et al.* 2006). Cox and Kronlund (2008) considered hyperstability in their analysis and found that lower than average catches and a more depleted stock were more common when hyperstability was present. Conversely, it is expected that the stock would appear to be more depleted than it actually is given hyperdepletion, and catches would be unnecessarily reduced, at least in the short term. MSE can help to identify a management strategy that is robust to structural uncertainties and meets fishery objectives and conservation goals (Cox and Kronlund 2008; Maunder *et al.* 2006).

In this analysis, we use MSE to investigate the outcomes of three control rules that have been or currently are used for New Zealand fisheries management, under different alternatives of the true relationship between CPUE and abundance. We also examine the impacts of estimating a nonlinearity parameter for the relationship between CPUE and abundance, or assuming a proportional relationship between CPUE and abundance in the estimation model. Two questions were addressed using this MSE: 1) does estimating a nonlinear relationship between CPUE and abundance affect the management of a simulated deepwater stock, and 2) are the control rules considered here robust to nonlinearity between CPUE and abundance. Outcomes of these simulations are presented in terms of risk to the

stock, amount of catch, and stability of catch over short, medium, and long time periods. Results of the simulations are presented separately for each control rule.

3.2 *Materials and methods*

The implementation of an MSE involves simulating a “true” stock through time with a feedback loop between assessment models and management strategies. The “true” stock is simulated (using what is known as the operating model) and typically explores alternative assumptions about the nature of the fish stock and fishery that are consistent with the current data. This “true” stock is not directly observed, but is simulated through time and data are generated that are generally comparable to what would be expected from the actual data collection system, although alternative hypotheses regarding data collection can be tested. Based on the estimated stock productivity and abundance, management measures, such as harvest control rules, are applied and the outcomes (i.e., the catch specified by the control rule) are input into the operating model to feedback into the stock dynamics of the operating model. Iterations of this process are projected forward for a specified duration and the realized performance can be evaluated against various objectives. Further, comparisons can be made to the behavior of the stock in the absence of fishing and to a case where there is no uncertainty; i.e. “perfect information” is always available upon which to base management actions.

3.2.1 Operating model and data

The operating model was an age-structured model with stochastic recruitment, written in the R statistical software (R Development Core Team 2010). The “true” population was based on long-lived, late-maturing, deepwater species in New Zealand waters such as orange roughy (*Hoplostethus atlanticus*) and oreos (family Oreosomatidae) (see Ministry of Fisheries (2010) for biological information on these species). Recruitment was highly variable (based on orange roughy life history) and was the only stochastic element of the operating model (other life-history parameters were assigned a single value and kept fixed throughout the simulations). Parameters and their assumed values are shown in Table 3.1.

Some important assumptions were: selectivity and maturity ogives were equal and knife-edged at age 29 (zero fish of age 28 were mature whereas all fish of age 29 were mature), natural mortality (M) was fixed at 0.045 yr^{-1} , growth was fixed and variability of length-at-age (σ_L) was negligible.

The operating model assumed that a single stock was present, but made alternative sets of assumptions about stock movement and availability. First, a simple model was constructed assuming that the entire stock was available to the fishery and survey throughout its entire range. The other two operating models addressed the disruption hypothesis and the habitat hypothesis by moving mature fish between a fished area and an unfished area with migration rates dependent on either fishing effort or the density of fish in the available area. These two-area models are simplified versions of the two-area model proposed by Dunn (2011) and assumed that a portion of the stock was available to the fishery and the survey (fished area), and a portion was only available to the survey (unfished area). Mature fish were less likely to stay in or move to the available area when higher exploitation rates occurred in the two-area effort-dependent model, similar to the fishing disruption hypothesis proposed by McAllister and Kirchner (2002). The migration rates of mature fish in the two-area density-dependent model were a function of the amount of mature fish in the available area, mimicking the habitat hypothesis mentioned earlier, except that fish not selected by the fishery recruited to the fished area. Additional details for the operating models are given in Appendix C.

The true population was initialized by simulating 200 years of no fishing (to reach equilibrium conditions) followed by a constant exploitation rate of 10% for the first ten years of the fishery. The latter period resembles the phase of fishery development before assessments and the implementation of the specific management strategies began. The management system was then simulated for 60 years. The simulation was repeated 200 times within each case, and each case used the same random recruitment deviates to eliminate confounding effects between cases. In all cases a maximum exploitation rate of 0.67 was implemented when catches were set too high, which is a common assumption in historical orange roughy assessments in New Zealand (Ministry of Fisheries 2007).

The only information on status and trend of the stock that was used in the assessments

was commercial CPUE and a scientific survey series. A single CPUE value for each year that fishing was allowed was drawn from a lognormal distribution with a mean equal to $\alpha V_{i,y}^\beta$ and a coefficient of variation (CV) of 0.2, where $V_{i,y}$ is the mid-year vulnerable biomass from simulation i in year y , β is the nonlinearity parameter, and α is a scalar. Survey observations for every other year, starting 3 years after fishing first occurred, were drawn from a lognormal distribution in a similar manner with a mean equal to $qV_{i,y}$, where the catchability coefficient (q) is a scalar, and the CV was equal to 0.2. CV 's of 0.2 were based on results from Francis *et al.* (2003).

The migration rates in the two-area models determined the amount of nonlinearity between available biomass (which determines CPUE) and the total biomass. The parameters determining migration rates (equations C.9 and C.9) were chosen to satisfy two criteria. First, migration back to the available area was slower than migration from the available area, following the habitat hypothesis mentioned earlier. Second, given an exploitation rate of 10% over the first three years of fishing, the nonlinearity parameter (β) in the relationship between biomass available to the fishery and total biomass was near 1.6 (hyperdepletion). The parameter values are given in Table 3.1, and the probabilities of moving from each area are shown in Figure 3.1. Although the equations for movement rates allowed for curvature (a Type II functional response), the parameters chosen for the simulations resulted in movement rates that were nearly linear over the range of possible effort or density.

The equilibrium reference points presented in Table 3.2 were determined for the single-area and two-area operating models by projecting them forward for 500 years from equilibrium unfished biomass at specified exploitation rates with no recruitment deviations. Additionally, the two-area operating models were projected with no recruitment deviations for 30 years with an exploitation rate of 10% followed by 30 years with no exploitation to investigate the behavior of these models during fishing-down and recovery.

3.2.2 Assessment model

The assessment model was an age-structured, forward-projection model called Awatea, which is a modified version of Coleraine (Hilborn *et al.* 2003) adapted to satisfy some

of the assumptions used in New Zealand orange roughy assessments (Appendix C). The population dynamics were modeled the same as in the single-area operating model, except that recruitment was deterministic. The inputs into Awatea were the generated CPUE series and survey series. Estimated parameters were initial recruitment (R_0), the CPUE scalar (α), and the survey catchability coefficient (q). A nonlinearity parameter (β) for the relationship between CPUE and abundance was also estimated in log space for certain cases with a logistic penalty for the value of β centered on one and a variance equal to 0.3266 (this is the *Hicks(1) Prior* in Chapter 2). Back-transformed 2.5th and 97.5th percent quantiles for this prior distribution are 0.30 and 3.31, respectively. Maximum likelihood was used for the estimation. Descriptions of all parameters in this estimation model are given in Table C.1.

Parameters that were not estimated were fixed at the same values used in the operating model (Table 3.1) except for selectivity parameters, which were jittered from the values in the operating model and fixed at these new values in the assessment. The parameters for the age at 50% selection to the fishery and to the survey were drawn from normal distributions with standard deviations of 3 and 1, respectively. The parameters indicating the number of ages from 50% to 95% selection for CPUE and survey selectivity were drawn from lognormal distributions with CV's of 1.5 and 0.5, respectively. These values were chosen to cover the typical range of selectivity estimates seen in historical orange roughy assessments (see the ORH Introduction in Ministry of Fisheries (2011)).

3.2.3 Management strategies and control rules

Historical model-based control rule

A management strategy based on historical methods used in New Zealand was implemented to investigate the differences of managing a hypothetical low productivity fish stock assuming that 1) CPUE is proportional to abundance, or 2) estimating a nonlinearity parameter, β , for the relationship between CPUE and abundance. In New Zealand, the purpose of the Fisheries Act is “to provide for the utilisation of fisheries resources while ensuring sustainability.” More importantly, the Act states that “[t]he Minister shall set a total allowable

catch that ... [m]aintains the stock at or above a level that can produce the maximum sustainable yield ... will result in the stock moving towards or above a level that can produce the maximum sustainable yield.” These principles, along with experience in the past New Zealand assessment process, were used to define a “simplified historical” management strategy (Table 3.3). It uses the current status (defined as depletion, which is the current spawning biomass divided by the unfished equilibrium biomass, B_0) and 5 year projections to determine the trend in the biomass given different catch levels in 100 ton increments. The catch level that results in a spawning stock size closest to 30% of B_0 (a historical proxy for B_{MSY}) is used as the next catch limit and the status determines when the stock will be assessed next.

Current management strategies

Two management strategies based on the recently implemented harvest strategy standard in New Zealand (Ministry of Fisheries 2008a,b) were tested. A high-information harvest control rule uses an assessment model to define fishing mortality rates, expressed here as an exploitation rate. A medium information harvest strategy uses a CPUE-based control rule. Using terminology from the New Zealand harvest strategy standard (Ministry of Fisheries 2008a), the high information, or model-based, harvest control rule uses “analytical proxies”, while the CPUE-based harvest control rule uses “conceptual proxies”.

The harvest strategy standards define the following reference points.

1. Target: the value around which the stock should fluctuate. This typically is a level analogous to B_{MSY} .
2. Threshold: a value where management action, exploitation rate or total allowable catch (TAC), for example, begins declining from the target level. It is recommended to be the target times one minus natural mortality to allow for natural fluctuation.
3. Soft limit: a value which triggers a rebuilding plan for the stock. This is 20% of equilibrium unfished biomass, $0.2B_0$, for all New Zealand stocks (Ministry of Fisheries 2011).

4. Hard limit: a value where the management action is set to zero. This is 10% of B_0 for all New Zealand stocks (Ministry of Fisheries 2011).

In the absence of detailed information about the stock, the New Zealand harvest strategy standard (Ministry of Fisheries 2008a) suggests proxy targets for B_{MSY} (as a percentage of B_0) and F_{MSY} (the fishing mortality that reduces the spawning-biomass-per-recruit to a percentage of the unfished spawner-per-recruit (SPR) level, F_{SPR}). Recommended default proxies for low productive species are 40% of B_0 for the biomass target and 45% SPR for the F_{SPR} exploitation rate, which is 4.5% given the parameterization of the hypothetical stock. More details of the two current management strategies used in this analysis are given below.

The management strategy used when a large amount of information is available uses a control rule that sets an exploitation rate dependent on the current biomass relative to the unfished equilibrium biomass. This is called the current model-based control rule with analytical proxies. We used a target exploitation rate of 4.5%, which is consistent with the current management of orange roughy in New Zealand (Ministry of Fisheries 2011). The recommended biomass target of 40% would be consistent with most species managed under the quota system in New Zealand (including oreos), but we chose to use the target of 30% B_0 , which is what is currently used for orange roughy stocks. The true B_{MSY} as a percentage of B_0 for our hypothetical stock was 25%, but the Ministry of Fisheries (2008b) recommends that analytical calculations of B_{MSY} from equilibrium models be adjusted upwards to account for natural fluctuations and the goal of managing near or above B_{MSY} . The exploitation rate declined linearly between the threshold of 28.65% B_0 and the hard limit of 10% B_0 . The soft limit (20% B_0) was not used in these simulations since rebuilding was not simulated as part of the management process. Figure 3.2 shows the control rule as well as the various reference points. If the biomass fell below the hard limit, the fishery was closed for five years, and then reassessed with the addition of new survey data, but no new CPUE data.

When the amount of information for the stock does not allow for adequate estimation of the reference points the operational guidelines in New Zealand's harvest strategy standard

(Ministry of Fisheries 2008b) suggests using qualitative surrogates for the reference points, which are called conceptual proxies. This is called the current CPUE-based control rule with conceptual proxies. We used CPUE as a conceptual proxy and tested its performance given various levels of nonlinearity in the true relationship between CPUE and abundance, but with the assumption that CPUE is proportional to abundance when applying the control rule. The operation guidelines (Ministry of Fisheries 2008b) also suggest using a target CPUE and a historical catch from a period when “catches and CPUE were relatively high.” This is an arbitrary decision and we used a CPUE value 0.3 that would correspond to approximately 30% B_0 and low and high catch targets (2,000 and 4,000 metric tons). The hard limit was a CPUE value of 0.1, approximately corresponding to 10% B_0 . The control rule is shown in Figure 3.2 along with the target, threshold, and hard limit.

To reduce catch variability and overreacting to natural variation in the population and in the CPUE data, the CPUE values from the current and previous four years (for the years in which CPUE values were available) were averaged before applying the control rule. If the averaged CPUE value was below the hard limit the fishery was closed for five years until the sixth year when a small fishery was opened (100 tons) to provide CPUE data to invoke the control rule again.

Each of these management strategies began after 10 years of fishing with a fixed exploitation rate, as with the analysis of the historical management strategy.

3.2.4 *Design*

A ‘case’ was a specific set of assumptions about the operating model and data, and for the model-based control rules a case was also related to whether or not β was estimated in the assessment model (Table 3.4). The operating model was either the single-area model, the two-area effort-dependent model, or the two-area density-dependent model. The data assumptions considered three levels of nonlinearity between CPUE and abundance (hyper-depletion, proportional, and hyperstable) for only the single-area model, while CPUE was always proportional to abundance available to the fishery for the two-area models, although nonlinearity may be introduced through migration into or out of the fished area. Perfect

information cases were also considered for all of the control rules and operating models. For example, the current biomass and projected biomass under various constant catch scenarios, if necessary, were known for the model-based control rules, and CPUE was known exactly for the CPUE-based control rule.

3.2.5 Analysis and performance measures

The metrics defined in Table 3.5 were used to compare the cases over short, medium, and long time periods. The short-term was the 10 years following the onset of management (years 11–20). The medium time period consisted of years 21–30, and was chosen to contrast with the short time period and because most deepwater fisheries in New Zealand have been fished for approximately 30 years. Long-term results are presented for the years 51–70 to show the range of possibilities once the population begins to stabilize under the management paradigm. Metrics for status are conservation measures and indicate the risk to the stock through the mean and minimum depletion, as well as the probability of being below a threshold. Metrics for catch are utilization measures and indicate the average catch and the variability (or conversely stability) in the catch. These metrics attempt to characterize the trade-offs between conservation risk, catch level, and catch stability.

3.3 Results

The population did not start at unfished, equilibrium biomass due to stochastic recruitment, but the end of the initial 200 year simulation produced a stable median spawning biomass. The unfished population showed a considerable amount of variability without fishing even though low natural mortality resulted in many age classes (Figure 3.3). This was due to the high amount of recruitment variability ($\sigma_R = 1.1$), which resulted in probabilities of 13% and 4% that recruitment events 5 and 10 times the average recruitment, respectively, could occur. Coupled with knife-edged maturity, large recruitments were quickly included in the spawning stock biomass resulting in sudden spikes or declines. The 2.5% and 97.5% quantiles of depletion (defined as current biomass divided by unfished, equilibrium biomass) with no fishing were 69% and 149% on average (over time), respectively. Trajectories for the two-area models were similar to those for the single-area operating model when no fishing

occurred, but showed less overall decline when fishing with a constant exploitation rate since some fish were unavailable to the fishery.

Deterministic equilibrium reference points from the single-area and both two-area operating models are shown in Table 3.2. The resulting equilibrium depletion when taking MSY in the single-area and two-area density-dependent model was approximately 25%, which is slightly lower than the New Zealand 30% target for orange roughy. The equilibrium depletion at MSY for the two-area effort-dependent model was slightly higher at 35%. The exploitation rate that would result in MSY is higher than the natural mortality rate, and fishing at an exploitation rate equal to natural mortality would reduce the stock to near 40%, 41%, and 45% of unfished equilibrium biomass for the single-area, two-area effort-dependent, and two-area density-dependent models, respectively.

The ten year simulated fishing-down phase, without management, reduced the total mature biomass to near 45%, 50%, and 60% of unfished equilibrium spawning biomass for the single-area, two-area effort-dependent, and two-area density-dependent models, respectively. The high recruitment variability resulted in a variable depletion level in year 10. The 5th and 95th percent quantiles for the single-area model were 32% and 67%, for the two-area effort-dependent model were 39% and 77%, and for the two-area density-dependent model were 45% and 88%.

Deterministic simulations were used to further investigate the effects of fishing within the two-area models (Figure 3.4). When fishing first began, the two-area models showed hyperdepletion ($\beta \approx 1.6$) in the relationship between available spawning biomass and total spawning biomass, but after 10 to 20 years, the relationship was hyperstable (Figure 3.4, plots b and d). When fishing stopped, the effort-dependent two-area model showed hyperdepletion until the available and total spawning biomass levels were equal. The density-dependent two-area model showed hyperdepletion immediately after fishing stopped, but the buildup of available spawning biomass slowed in comparison to the total spawning biomass as the population approached equilibrium levels.

3.3.1 Historical model-based control rule

The median true trajectory of depletion when using the historical model-based control rule (Figure 3.5, panels a–e, Table 3.6) was below the target depletion (30% B_0) in the long-term for nearly all of the operating models and whether or not β was estimated. Exceptions were when β was fixed at 1 in the single-area operating model where the true relationship between CPUE and abundance showed hyperdepletion (Figure 3.5, panel c), and β was fixed at 1 in the two-area effort-dependent model (Figure 3.5d). Estimating β made little difference to the true biomass when hyperstability was present (Figure 3.5a) and larger true values of β resulted in larger differences between median true biomass when β was or was not estimated (e.g., Figure 3.5, panels b–c). Median biomass was mostly above or near 30% in the perfect knowledge cases.

The probability that the true depletion level was below the threshold of 30% or 10% in the single area model increased quickly when management first began, and then tended to decline slightly before increasing and stabilizing (Figure 3.6, panels a & d). In the long-term, all cases commonly showed a probability greater than 0.3 of being below 30% depletion and a probability greater than 0.1 of being below 10% depletion. Estimating β resulted in higher probabilities of falling below the reference point except for the single-area hyperstable case, which was similar whether or not β was estimated (solid lines in panels a & d of Figure 3.6).

The two-area models showed an increasing probability of falling below the threshold values in the long-term (Figure 3.6, panels b–c & e–f), suggesting that the dynamics had not stabilized. Estimating β resulted in an increased chance that the spawning biomass was below the threshold. The density-dependent model showed higher probabilities than the effort-dependent model, and the maximum probability that the spawning biomass was lower than 10% B_0 was 0.13 for the effort-dependent model and 0.33 for the density-dependent model, both of which occurred in the final simulated year. With perfect information, the probability that the stock was below 30% B_0 fluctuated between 0.3 and 0.6 (Figure 3.6, panels b–c).

The median values for depletion, AAC, and SDAC in the long-term were less than the

median values from the ten years following the implementation of the historical control rule (Table 3.6 and Figure 3.7). Average annual catches quickly declined and were similar for all cases in the late time period, ranging from 1400 to 1800 tons (Figure 3.7, panels a, d, & g). When β was estimated, the AAC was slightly greater in the medium-term (Figure 3.7d) and slightly less in the long-term (Figure 3.7g) than when β was fixed at one, except for the hyperstable case. Variability in catches (median SDAC) quickly declined after the first ten years of management to values near 600 and was slightly higher for all cases, other than the two-area density-dependent model, when β was estimated (700–900). The perfect knowledge cases were able to keep the long-term median depletion near the target of 30% with median average annual catches less than the AAC's when using the historical control rule with the single-area operating model, and above the AAC's when using the same control rule in the two-area models. The long-term variability in the annual catches was higher in the perfect knowledge cases (900–1400 in the long-term).

3.3.2 *Current management strategies*

Model-based control rule

The current model-based control rule resulted in a stock that was less depleted when compared to the historical control rule (Figure 3.5, panels f–j). The probability that depletion was less than 30% never exceeded 0.8, and the probability that depletion was less than 10% never exceeded 0.3 (Figure 3.8). Estimating β in the single-area hyperstable case reduced the probabilities of depletion falling below 30% by an absolute amount of 0.14, on average in the last 20 years of the simulations, while in the single-area hyperdepleted case, the probability increased by 0.14, on average in the last 20 years of the simulations (Figure 3.8a). However, the increase in the probability that depletion was less than 30% in the middle years of the simulations when estimating β was approximately 0.17 for the hyperdepleted case. Estimating β in the two-area effort-dependent model (Figure 3.8b) resulted in the largest increase in the probability that depletion was less than 30% (0.33 on average over the last twenty years), but the two-area density-dependent model (Figure 3.8c) resulted in little difference (0.08 on average over the last twenty years). The probability that depletion

was less than 10% was zero in the two-area models until late in the time-series (Figure 3.8, panels e–f). Perfect knowledge of the stock size to apply to the model-based control rule resulted in probabilities less than 0.16, 0.07, and 0.03 that depletion would fall below 30% for the single-area, two-area effort-dependent, and two-area density-dependent models, respectively. The depletion was never lower than 10% when using perfect knowledge.

The performance metrics for the model-based control rule (Table 3.7) show that when compared to the historical control rule, the catches were smaller at the onset of management, and the catches were less variable throughout the times series. Estimating β , compared to when β was fixed at one, resulted in small differences to depletion in the short term, even though the AAC's were 1.6 times and 1.4 times the AAC's for the hyperdepleted model and the two-area effort-dependent model, respectively (Table 3.7 & Figure 3.9). Over the long-term, larger differences were seen in depletion when β was estimated and the AAC's were more similar whether or not β was estimated (1400–1800 tons). The standard deviation of the annual catches was low throughout the time series and ranged between 100 and 500. Median minimum depletion was never less than 0.18. Using perfect information kept the median depletion above 30% and median AAC slightly below $C_{30\%}$ (Figure 3.9).

CPUE-based control rule

The median depletion in the low catch and perfect knowledge cases using the CPUE-based control rule stayed above 30% over the time simulated, but was slowly declining at the end of the modeled time period (Figure 3.5, panels k–o). The high catch scenario resulted in a steeper decline once management began and a lower depletion at the end of the 70 years. The probability of falling below the depletion threshold of 30% with catches near $C_{30\%}$, as seen in Figure 3.10a, was highest for the hyperstable scenario (a maximum of 0.45) and just slightly less for the proportional case (a maximum of 0.35). When the relationship between CPUE and abundance showed hyperdepletion, the probability of dropping below the 30% threshold decreased significantly and was highest at the beginning of the series (a maximum of 6%). Doubling the catch target to 4000 tons resulted in a probability near 1 that the population would drop below the 30% threshold in the hyperstable and

proportional scenarios (Figure 3.10a), 0.65 to 0.75 in the two-area model scenarios (Figure 3.10, panels b–c), and was significantly less for the hyperdepletion case (a maximum of 0.3, Figure 3.10a). The only scenario that had a probability greater than 0.06 of falling below 10% depletion was the hyperstable scenario with the high catch control rule (Figure 3.10a).

The performance metrics for the current CPUE-based control rule are shown in Table 3.8. Median AAC in the low catch case was always near the 2000 ton target (which could not be exceeded) in the short and long term when the true β was 0.6 or 1.0 (Table 3.8 & Figure 3.11, panels a, d, & g). The AAC was lower (1600 to 1900 tons) and more variable (standard deviations from 100 to 300) with the hyperdepletion and the two-area operating model cases (Table 3.8 & Figure 3.11). The median AAC decreased by less than 200 tons in the long-term for these same cases and median SDAC increased slightly for the two-area models. Long-term median depletion decreased for all cases except the hyperdepletion case, but was above the target of 30% for all cases. Doubling the catch target to 4000 tons resulted in much more risk to the stock (Figure 3.10), higher catches in the short term (Figure 3.11, panels a–c) and much more variability in the annual catch (Table 3.8). The stock was much more depleted in the long-term with a high catch target, and the median depletion was less than 10% for the hyperstable scenario (Figure 3.11, panels g–i). Perfect information resulted in little difference compared to the low catch case using uncertain CPUE data (Figure 3.11).

3.3.3 *Estimates of the nonlinearity parameter*

Estimates of β for the cases using the current model-based control rule were variable across simulations and the median estimate changed over time (Figure 3.12). The prior distribution used for β , which was centered around one, pulled the estimates towards one when few years of data were available. When the true relationship between CPUE and abundance was hyperstable, the medians of the estimates of β were closer to one early in the time series, and centered closer to the true value later in the time-series. When the true relationship was proportional, the medians of the estimates were near one early on, increased slightly until approximately year 30, and then decreased back down to one. The medians of the

estimates of β were close to the true value early in the time-series when the relationship between CPUE and abundance showed hyperdepletion until later in the time series when the median of the estimates were slightly below the true value. Assessments were typically conducted every five years unless the stock was perceived to be in poor shape. Therefore, more estimates of β from the simulations were available in every fifth year, and estimates of β in the years between every fifth year showed a different pattern to the estimates of β in every fifth year, especially early on when it was less likely to have assessments out of the five year cycle.

3.4 Discussion

There is a trade-off between conservation and utilization objectives with regard to the choice of estimating a nonlinearity parameter, β , for the relationship between CPUE and abundance, or assuming that CPUE is proportional to abundance. These trade-offs depend on the underlying true relationship. A hyperstable relationship results in a high risk to the stock because changes in abundance are more difficult to detect and abundance is perceived to remain high when it is not, often resulting in catches that are too high to meet conservation objectives. Estimating β in a hyperstable scenario reduces the risk to the stock because catches are often lower, although the risk remained higher than a proportional or hyperdepletion scenario, which is likely due to lack of contrast in the CPUE data. Conversely, with hyperdepletion, the risk to the stock was low because the perception of the stock was more pessimistic and catches were less than optimal for the depletion target. Estimating β when hyperdepletion was present increased the yield, but also increased the conservation risk to the stock. Compared to the case where CPUE was proportional to abundance and was assumed proportional in model-based assessments, the hyperdepletion scenario showed a similar risk to the stock when β was estimated, but the hyperstable scenario always had more risk regardless if β was estimated or not. Overall, estimating β brought the catches and depletion levels closer to target when nonlinearity was present, but increased variability in catches.

These trade-offs also depend on whether the goals are short- or long-term. In the short-term (immediately following implementation of the control rule) catches were variable among

scenarios with highest catches in the hyperstable scenarios and lowest catches in the hyperdepletion scenarios. In the long-term, catches were much less variable across scenarios, but the depletion was much more variable. Estimating β resulted in little difference in the long-term catches when compared to not estimating β .

The two-area operating models showed hyperdepletion and hyperstability, depending on the status of the stock and the amount of fishing, but results were similar to the single-area operating model. A major difference between the single-area and two-area stock assumptions is that there is an unavailable portion of the stock that is only accessible by lowering catches. The higher standard deviation in average annual catch for the two-area operating models shows that a strategy may be to vary catch so that fish become available in periods when catches are low and then are taken when available abundance is high. This would likely result in a complicated relationship between CPUE and abundance, which would not be a simple function of biomass as assumed in the assessment model.

The power function, $\alpha V_{i,y}^\beta$, may not be the best choice for modeling the relationship between CPUE and abundance, especially if catchability is not a simple function of biomass. Other modeling techniques, such as time-varying catchability, may improve estimation performance and management goals (Wilberg *et al.* 2010). For example, catchability may increase over time through experience, knowledge, or increases in technology (Maunder *et al.* 2006). Refugia may play a role in changing catchability, as was seen in the two-area models (Rindorf and Andersen 2008). Or, catchability may have a different relationship with biomass depending on whether the stock is increasing or decreasing. Regardless, there are many reasons why catchability may change over time, and even though the power model used here is parsimonious and simple, more complicated methods may be warranted when the appropriate data are available.

The current model-based control rule was more precautionary than the historical model-based control rule because the target exploitation rate was equal to $E_{45\%}$, which is nearly half of the exploitation rate that would produce MSY. However, both control rules were similar in that when estimating β , differences in yields were greater in the short-term than in the long-term, while the difference in stock status was greater in the long-term even though long-term catches were similar. These conflicting results show why it is important

to define an objective function that combines the conservation and yield results into a measurable quantity that can be maximized, which likely takes cooperation between managers, scientists, and stakeholders (Cox and Kronlund 2008).

Using a harvest control rule that specifically uses a CPUE index rather than a model-based assessment ignores the issue of estimating a nonlinearity parameter and is useful for fish stocks without sufficient data to properly conduct a model-based stock assessment (Cox and Kronlund 2008; McAllister *et al.* 1999; Rademeyer *et al.* 2007). However, setting the catch target at a level that maximizes yield yet reduces the long-term risk to the stock can be difficult (McAllister *et al.* 1999). As Little *et al.* (2011) concluded, setting the parameters of the harvest control rule (i.e., catch target and reference points) can be difficult with limited information about the fish stock. These issues are exacerbated in the presence of nonlinearity. The risk to the stock can be very high when the relationship between CPUE and abundance is hyperstable or proportional, but hyperdepletion reduces the risk, as well as the yield in the short term, and works as a precautionary buffer, although this would be unknown in practice. This is, however, dependent on setting the catch target and reference points correctly since reference points that are too low may result in the stock reaching critically low levels, and reference points that are too high may result in lost yield, regardless of the relationship between CPUE and abundance. New fisheries with few years of fishing to base a target catch on are especially problematic and may require an adaptive approach of monitoring the stock closely for several years to see how catch-rates respond to the catch target before a model-based assessment could be conducted (Rademeyer *et al.* 2007).

The estimates of a parameter for the relationship between CPUE and abundance occasionally incorrectly classified the relationship as hyperstable or hyperdepleted, and surprisingly, the probability of estimating a hyperstable relationship increased in the hyperdepletion case with additional years and more data due to biases in the model. In the presence of hyperdepletion, the deterministic models often overestimate the decline in biomass which is followed by an increase in estimated biomass when catches are reduced (Chapter 2). The results in this study showed that trajectories that were perceived to be more depleted had lower estimates of β , which was likely a result of the biases of applying a deterministic model

to data from a stochastic population (Chapter 2). However, because β was estimated at a lower value and the stock status was estimated at a lower level than reality, there was no additional risk to the stock, although potential yields were reduced and the perception of the stock was unduly pessimistic.

An important factor that is often not included in the objectives of the management of a fish stock is the perception of the stock. It is obviously important to maintain a stock at healthy levels while also providing fishing opportunities, but the perception of a stock can have unfavorable consequences. In the case of hyperstability, it is a major concern that the stock can be perceived to be large, yet is potentially below target and at risk of collapse (e.g., Rose and Kulka 1999). When hyperdepletion is present, the stock may be healthy, but perceived to be at risk of collapse, which can lead to lower catch rates, closures of fisheries, and negative public perception (see Hampton *et al.* (2005) and Polacheck (2006) in response to Myers and Worm (2003)). These misperceptions can be very frustrating to stakeholders, environmentalists, managers, and scientists, resulting in conflicts between the different groups, and pressure to manage the stock at non-target levels.

Estimating a nonlinearity parameter can improve the management of a long-lived species and provide a more accurate perception of the true status of the stock, as well as alleviate concerns about conflicting data. Nonlinearity in the relationship between CPUE and abundance can often result in contradictory information on stock status from a CPUE series and a survey series (for example, see the description given by Hilborn and Walters (1992, page 533) of the northern cod fishery). Hilborn and Walters (1992) warn against averaging across datasets and suggest presenting a decision table to managers with alternative hypotheses. Francis (2011) also suggests presenting alternative models to managers with and without potentially unrepresentative datasets. Estimating β is a modeling method that can be used in addition to alternative models to understand why two datasets may be in conflict.

Fishery-independent catch-rate data are more likely to be proportional than fishery-dependent CPUE because surveys are typically well designed and appropriate for the stock being surveyed, and it may seem appropriate to simply omit the questionable fishery-dependent CPUE. However, there is a benefit to using CPUE data in an assessment. CPUE data are often available for more years than survey data and can provide insight into his-

torical time periods. Fishers are most familiar with catch-rates and often appreciate their use in assessments. Survey data may not be proportional to abundance (Davies and Jonsen 2011) and simply omitting CPUE would imply that the survey provides the only representative dataset. Finally, it is useful to use CPUE and survey data in an assessment to further understand the relationship between CPUE and abundance, which can then be applied to the assessment and management of stocks that have only CPUE data or are using a CPUE-based control rule.

Management strategy evaluation, like any modeling approach, involves simplifications of reality. In this study, we used the maximum likelihood estimates, which correspond to the mode of the posterior distribution when uninformative priors are used in a Bayesian analysis, and likely result in negatively-biased estimates of biomass with skewed distributions (Stewart *et al.* 2013). We also did not account for uncertainty in the estimates. The Pacific Management Council in the U.S. reduces recommended catches based on scientific uncertainty (Ralston *et al.* 2011), and the New Zealand harvest strategy standard states that a stock is not rebuilt until there is a 70% probability that it is greater than the soft limit of the management target. Performing Bayesian analyses and accounting for uncertainty may slightly modify the results of this study, but we feel that it would not affect the general conclusions.

Another common source of uncertainty in management strategy evaluations that was not accounted for in this study was implementation error of the management decision (McAlister *et al.* 1999). The assumption that the exact catch is taken every year is questionable. For example, New Zealand regulations specify an annual catch entitlement (ACE) for each fisher, and if the fisher exceeds their ACE, they can either buy more if it is available, or pay a deemed value for the amount of catch that exceeded their ACE. Additionally, due to precautionary, economic, or social concerns, managers may make the decision to alter the exact catch as specified by the control rule. A common management decision is to cap the total allowable catch as a precautionary measure when the stock is predicted to be very large or limit the amount of change in catch from one year to the next (Butterworth *et al.* 1997, *i.e.*). Implementation error could be modeled as a probability distribution with a possible truncation to limit unrealistically high predicted catches. Adding a cap on the catch may

also be implemented specifically as part of a control rule, and it would likely decrease the risk to the stock.

This study could also be expanded by investigating the effects of alternative life-history parameters on the results. We used proxies for reference points as they are currently used in New Zealand (Ministry of Fisheries 2011), but the true reference points and stock risk are greatly influenced by the stock-recruitment relationship (Cox and Kronlund 2008; Maunder 2012; Punt *et al.* 2008). The value of steepness used here, 0.75, may be higher than typical for long-lived, low productivity species such as orange roughy (Sissenwine and Mace 2007) and future MSE work could investigate the robustness of the management strategy to various values of steepness and other life-history parameters. Additionally, Clark (1993) found that higher SPR_{MSY}/SPR_0 ratios might be needed due to serially correlated recruitment, which was not investigated here. An even less productive species with serial recruitment may need more precautionary reference point proxies.

It is useful to investigate the relationship between CPUE and abundance for a better understanding of the risks that may be present. An investigation may specifically look at the relationship between CPUE and abundance (Harley *et al.* 2001; Wilberg and Bence 2006) or draw conclusions by examining fish and fisher behavior (Paloheimo and Dickie 1964; Rose and Kulka 1999; Winters and Wheeler 1985). However, making inference of the relationship between CPUE and abundance based solely on life-history characteristics or fish behavior may be inconclusive. For example, orange roughy aggregate in dense spawning and feeding aggregations which are targeted by the fishery which has been thought to lead to a hyperstable relationship, but could also lead to hyperdepletion if small localized aggregations are fished out (Francis and Clark 2005). Examination of additional data sources (i.e., age or length data), or indicators of the population status (Cope and Punt 2009; Froese 2004; Prince *et al.* 2011) can assist in verifying that the management strategy is effectively managing the population.

Overall, the decision of whether or not to account for nonlinearity is based on the assumptions and risks one is willing to make, the potential loss in yield, and the misperceptions that may result. Hyperstable scenarios are especially risky and should always be accounted for, or at least acknowledged. Hyperdepletion scenarios, on the other hand, may

appear to be desirable due to reduced conservation risk, but the negative consequences of reduced yield, at least in the short term, and a pessimistic view of the stock status, and thus the management system, make it worthwhile to at least acknowledge the potential for hyperdepletion and that not accounting for it is chosen as part of the management strategy.

3.5 Tables

Table 3.1: Parameters used in the single-area and two-area operating models, and for data generation.

Parameter	Value
Natural mortality (M , yr^{-1})	0.045
Recruitment variability (σ_R)	1.1
Steepness (h)	0.75
Knife-edge selectivity (age)	29
Knife-edge maturity (age)	29
<i>Growth</i>	
t_0	-0.491
k	0.059
L_∞ (cm)	37.78
<i>Length-weight</i>	
Intercept (a)	0.08
Exponent (b)	2.75
<i>Movement</i>	
Effort-dependent ρ_1	0.6
Effort-dependent ρ_2	0.06
Density-dependent ρ_1	0.02
Density-dependent ρ_2	0.01
<i>CPUE</i>	
α	$(1 \times 10^5)^\beta$
β	0.6, 1.0, 1.6
CV	0.2
<i>Survey</i>	
q	0.25
CV	0.2
<i>Periodicity</i>	Biennial

Table 3.2: Equilibrium reference points for the single area and two-area operating models.

Quantity	Single area	Two area effort-dependent	Two area density-dependent
B_0	100,180	100,180	100,180
E_{MSY}	0.081	0.067	0.080
$E_{35\%SPR}$	0.068	0.125	0.070
$E_{45\%SPR}$	0.045	0.065	0.046
MSY	1956	1574	1925
Depletion at MSY	24.70%	35.3%	25.5%
$C_{30\%}$	1930	1547	1907

Table 3.3: Simplified historical control rule. Each box corresponds to the current biomass (B_{curr}) and the rows corresponds to the five-year projected biomass (B_{+5}).

$B_{curr} > B_{30\%}$	
$B_{+5} > B_{curr}$	Set catch level at the predicted catch where $B_{+5} = B_{30\%}$. Assess in 5 years.
$B_{30\%} < B_{+5} \leq B_{curr}$	Set catch level at the predicted catch where $B_{+5} = B_{30\%}$. Assess in 5 years.
$B_{20\%} < B_{+5} \leq B_{30\%}$	Keep catch level at the current catch level. Assess in 3 years.
$B_{+5} \leq B_{20\%}$	Set catch level at the predicted catch where $B_{+5} = B_{30\%}$. Assess in 3 years.
$B_{20\%} < B_{curr} \leq B_{30\%}$	
$B_{+5} > B_{30\%}$	Keep catch level at the current catch level. Assess in 3 years.
$B_{curr} < B_{+5} \leq B_{30\%}$	Keep catch level at the current catch level. Assess in 3 years.
$B_{20\%} < B_{+5} \leq B_{curr}$	Set catch level at the predicted catch where $B_{+5} = B_{30\%}$. Assess in 3 years.
$B_{+5} \leq B_{20\%}$	Set catch level at the predicted catch where $B_{+5} = B_{30\%}$. Assess in 1 year.
$B_{curr} \leq B_{20\%}$	
$B_{+5} > B_{30\%}$	Keep catch level at the current catch level. Assess in 3 years.
$B_{20\%} < B_{+5} \leq B_{30\%}$	Keep catch level at the current catch level. Assess in 3 years.
$B_{curr} < B_{+5} \leq B_{20\%}$	Set catch level at the predicted catch where $B_{+5} = B_{30\%}$. Assess in 1 year.
$B_{+5} \leq B_{curr}$	Set catch level at the predicted catch where $B_{+5} = B_{30\%}$. Assess in 1 year.

Table 3.4: Cases used for each control rule. Data generation refers to the nonlinear relationship between CPUE and abundance. Perfect means that perfect information was available when applying the control rule (biomass for model-based control rules and CPUE for CPUE-based control rules). Low catch is 2000 tons and high catch is 4000 tons.

Model-based control rules		
Operating Model	Data generation	Assessment
Single area	$\beta = 0.6$	Fix β at 1.0
Single area	$\beta = 1.0$	Fix β at 1.0
Single area	$\beta = 1.6$	Fix β at 1.0
Single area	$\beta = 0.6$	Estimate β
Single area	$\beta = 1.0$	Estimate β
Single area	$\beta = 1.6$	Estimate β
Two-area density-dependent	$\beta = 1.0$	Fix β at 1.0
Two-area density-dependent	$\beta = 1.0$	Estimate β
Two-area effort-dependent	$\beta = 1.0$	Fix β at 1.0
Two-area effort-dependent	$\beta = 1.0$	Estimate β
Single area	Perfect	—
Two-area density-dependent	Perfect	—
Two-area effort-dependent	Perfect	—

CPUE-based control rule		
Operating Model	Data generation	Catch level
Single area	$\beta = 0.6$	Low & high
Single area	$\beta = 1.0$	Low & high
Single area	$\beta = 1.6$	Low & high
Two-area density-dependent	$\beta = 1.0$	Low & high
Two-area effort-dependent	$\beta = 1.0$	Low & high
Single area	Perfect, $\beta = 0.6$	Low
Single area	Perfect, $\beta = 1.0$	Low
Single area	Perfect, $\beta = 1.6$	Low
Two-area density-dependent	Perfect, $\beta = 1.0$	Low
Two-area effort-dependent	Perfect, $\beta = 1.0$	Low

Table 3.5: Metrics used to investigate performance of the simulations.

Metric	Description	Formula
Median status	Status of the stock in terms of median depletion over a defined period of time	$Median \left(\frac{B_t}{B_0}, \frac{B_{t+1}}{B_0}, \dots, \frac{B_{t+n}}{B_0} \right)$
Minimum status	Minimum depletion over a defined period of time.	$Min \left(\frac{B_t}{B_0}, \frac{B_{t+1}}{B_0}, \dots, \frac{B_{t+n}}{B_0} \right)$
P(B<Threshold)	The probability that depletion will be below the threshold value at any point of the defined period of time	$\frac{\sum_{i=t}^{t+n} I_i}{n+1}$ where $I = 1$ if $\frac{B_i}{B_0} < \text{Threshold}$
Mean catch	The mean catch over the time period defined.	$\bar{C} = \sum_{i=t}^{t+n} \frac{C_i}{n+1}$
Catch variability	The standard deviation of the catch over the time period defined.	$\sum_{i=t}^{t+n} \frac{(C_i - \bar{C})^2}{n}$

Table 3.6: Medians of the minimum depletion, median depletion, average annual catch rounded to the nearest 100 tons (AAC), and the standard deviation of the annual catch rounded to the nearest 100 tons (SDAC) for the first 10 years of management (years 11 to 20 after fishing began) using the historical model-based control rule. The operating model assumptions are shown as rows for each metric, and the assessment assumptions are shown as columns within each time period.

		Years 11–20			Years 21–30			Years 51–70		
		Perfect	β	Est	Perfect	β	Est	Perfect	β	Est
		info	fixed	β	info	fixed	β	info	fixed	β
Minimum Depletion	$\beta = 0.6$	0.25	0.05	0.06	0.28	0.06	0.08	0.26	0.02	0.02
	$\beta = 1.0$	0.25	0.14	0.12	0.28	0.18	0.13	0.26	0.11	0.04
	$\beta = 1.6$	0.25	0.31	0.21	0.28	0.30	0.18	0.26	0.24	0.09
	Effort	0.26	0.36	0.28	0.27	0.35	0.25	0.27	0.25	0.14
	Density	0.26	0.32	0.28	0.27	0.27	0.21	0.26	0.16	0.07
Median Depletion	$\beta = 0.6$	0.30	0.18	0.20	0.31	0.14	0.16	0.31	0.09	0.09
	$\beta = 1.0$	0.30	0.28	0.25	0.31	0.28	0.21	0.31	0.22	0.16
	$\beta = 1.6$	0.30	0.38	0.31	0.31	0.37	0.25	0.31	0.35	0.21
	Effort	0.30	0.44	0.39	0.31	0.43	0.33	0.31	0.34	0.21
	Density	0.31	0.45	0.43	0.30	0.36	0.29	0.31	0.27	0.16
AAC	$\beta = 0.6$	3400	5500	5200	1400	1800	1900	1800	1600	1700
	$\beta = 1.0$	3400	4100	4600	1400	1700	2000	1800	1800	1600
	$\beta = 1.6$	3400	2200	3700	1400	1900	2100	1800	1700	1600
	Effort	4000	2600	3600	1400	1700	2100	1100	1600	1400
	Density	4800	3700	4400	1300	1500	2100	1600	1700	1700
SDAC	$\beta = 0.6$	2100	3200	3000	800	600	700	1400	600	700
	$\beta = 1.0$	2100	2400	2300	800	500	700	1400	600	800
	$\beta = 1.6$	2100	900	1700	800	500	900	1400	500	900
	Effort	3200	1200	1600	800	500	700	900	500	600
	Density	4000	2000	1900	800	600	800	1200	700	600

Table 3.7: Medians of the minimum depletion, median depletion, average annual catch rounded to the nearest 100 tons (AAC), and the standard deviation of the annual catch rounded to the nearest 100 tons (SDAC) for the first 10 years of management (years 11 to 20 after fishing began) using the current model-based control rule. The operating model assumptions are shown as rows for each metric, and the assessment assumptions are shown as columns within each time period.

		Years 11–20			Years 21–30			Years 51–70		
		Perfect	β	Est	Perfect	β	Est	Perfect	β	Est
		info	fixed	β	info	fixed	β	info	fixed	β
Minimum Depletion	$\beta = 0.6$	0.36	0.27	0.31	0.36	0.22	0.27	0.31	0.13	0.19
	$\beta = 1.0$	0.36	0.34	0.34	0.36	0.32	0.31	0.31	0.26	0.24
	$\beta = 1.6$	0.36	0.38	0.36	0.36	0.40	0.34	0.31	0.35	0.26
	Effort	0.46	0.42	0.39	0.45	0.38	0.31	0.37	0.28	0.18
	Density	0.53	0.49	0.48	0.50	0.42	0.40	0.40	0.27	0.25
Median Depletion	$\beta = 0.6$	0.42	0.35	0.37	0.41	0.28	0.33	0.39	0.23	0.28
	$\beta = 1.0$	0.42	0.40	0.41	0.41	0.39	0.38	0.39	0.37	0.33
	$\beta = 1.6$	0.42	0.45	0.43	0.41	0.47	0.41	0.39	0.45	0.36
	Effort	0.51	0.49	0.46	0.50	0.45	0.37	0.45	0.38	0.26
	Density	0.60	0.56	0.55	0.56	0.48	0.47	0.49	0.37	0.34
AAC	$\beta = 0.6$	1800	3000	2600	1800	2200	2100	1700	1800	1700
	$\beta = 1.0$	1800	1900	2100	1800	1800	2000	1700	1700	1600
	$\beta = 1.6$	1800	1100	1800	1800	1400	1800	1700	1400	1600
	Effort	1400	1800	2600	1600	1700	2200	1500	1500	1400
	Density	1400	1800	2000	1500	1600	1900	1600	1600	1600
SDAC	$\beta = 0.6$	200	500	500	200	200	200	200	200	200
	$\beta = 1.0$	200	300	300	200	100	100	200	100	200
	$\beta = 1.6$	200	200	300	200	100	100	200	100	300
	Effort	100	300	400	200	100	300	200	200	400
	Density	100	300	400	200	100	200	200	200	200

Table 3.8: Medians of the minimum depletion, median depletion, average annual catch rounded to the nearest 100 tons (AAC), and the standard deviation of the annual catch rounded to the nearest 100 tons (SDAC) for the first 10 years of management (years 11 to 20 after fishing began) using the current CPUE-based control rule. The operating model assumptions are shown as rows for each metric, and the assessment assumptions are shown as columns within each time period.

		Years 11–20			Years 21–30			Years 51–70		
		Perfect info	Low catch	High catch	Perfect info	Low catch	High catch	Perfect info	Low catch	High catch
Minimum Depletion	$\beta = 0.6$	0.36	0.36	0.22	0.34	0.34	0.08	0.24	0.24	0.01
	$\beta = 1.0$	0.36	0.36	0.23	0.34	0.34	0.16	0.26	0.26	0.12
	$\beta = 1.6$	0.37	0.37	0.30	0.39	0.39	0.29	0.36	0.36	0.27
	Effort	0.46	0.43	0.33	0.45	0.42	0.31	0.37	0.32	0.22
	Density	0.53	0.50	0.39	0.50	0.44	0.32	0.40	0.32	0.18
Median Depletion	$\beta = 0.6$	0.42	0.42	0.33	0.40	0.40	0.17	0.34	0.34	0.07
	$\beta = 1.0$	0.42	0.42	0.33	0.40	0.41	0.23	0.36	0.37	0.19
	$\beta = 1.6$	0.43	0.43	0.36	0.45	0.45	0.36	0.45	0.45	0.35
	Effort	0.51	0.50	0.41	0.50	0.48	0.38	0.45	0.41	0.29
	Density	0.60	0.57	0.49	0.56	0.51	0.39	0.49	0.42	0.26
AAC	$\beta = 0.6$	2000	2000	4000	2000	2000	4000	2000	2000	1800
	$\beta = 1.0$	2000	2000	4000	2000	2000	2600	2000	1900	1900
	$\beta = 1.6$	1700	1700	2700	1600	1600	1900	1600	1600	1700
	Effort	1400	1800	3200	1600	1800	2000	1500	1600	1600
	Density	1400	2000	3500	1500	1900	2300	1600	1800	2000
SDAC	$\beta = 0.6$	0	0	0	0	0	100	0	0	1300
	$\beta = 1.0$	0	0	0	0	0	700	100	100	900
	$\beta = 1.6$	200	300	900	200	200	600	300	300	900
	Effort	100	100	900	200	100	800	200	200	900
	Density	100	100	600	200	100	600	200	200	900

3.6 Figures

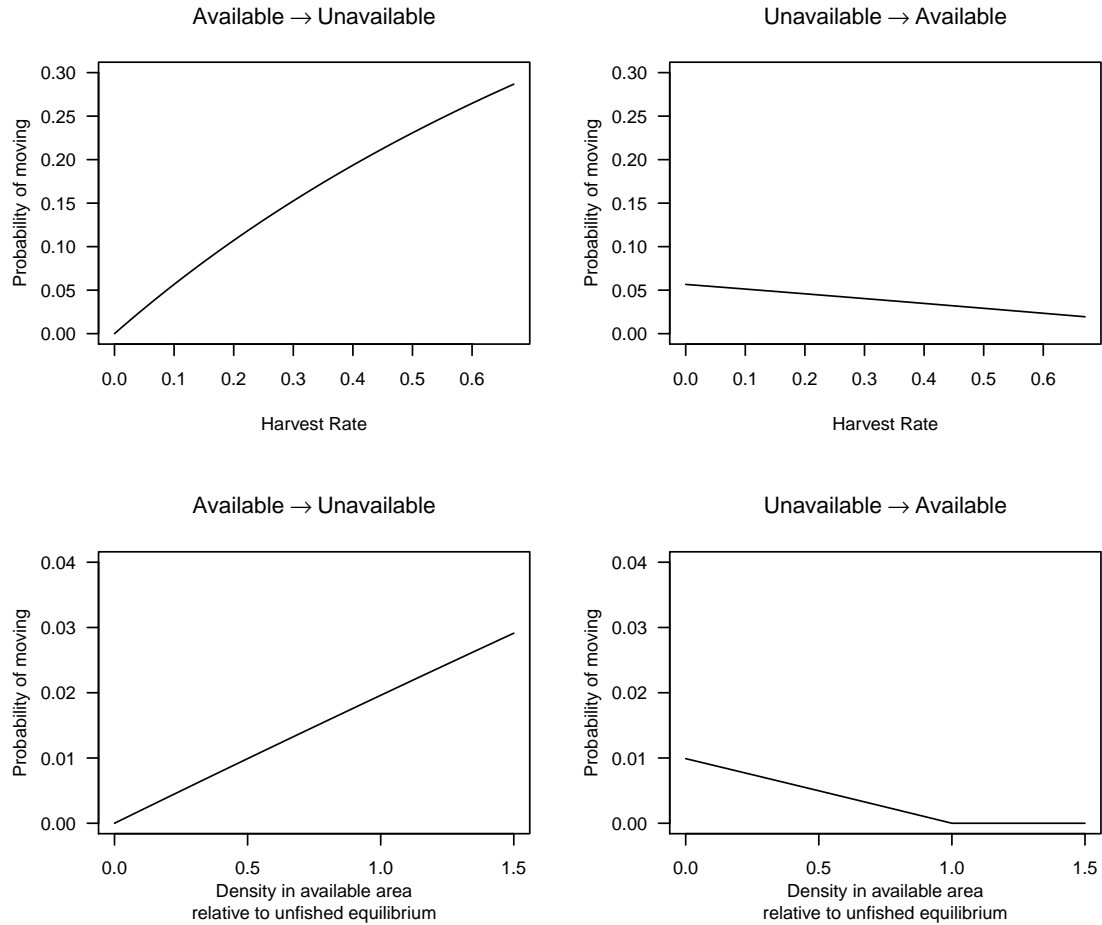


Figure 3.1: Movement rates from the available area to unavailable area and the unavailable area to available area as a function of harvest rate for the effort-dependent two-area model (top row) and as a function of density in the available area for the density-dependent two-area model (bottom row).

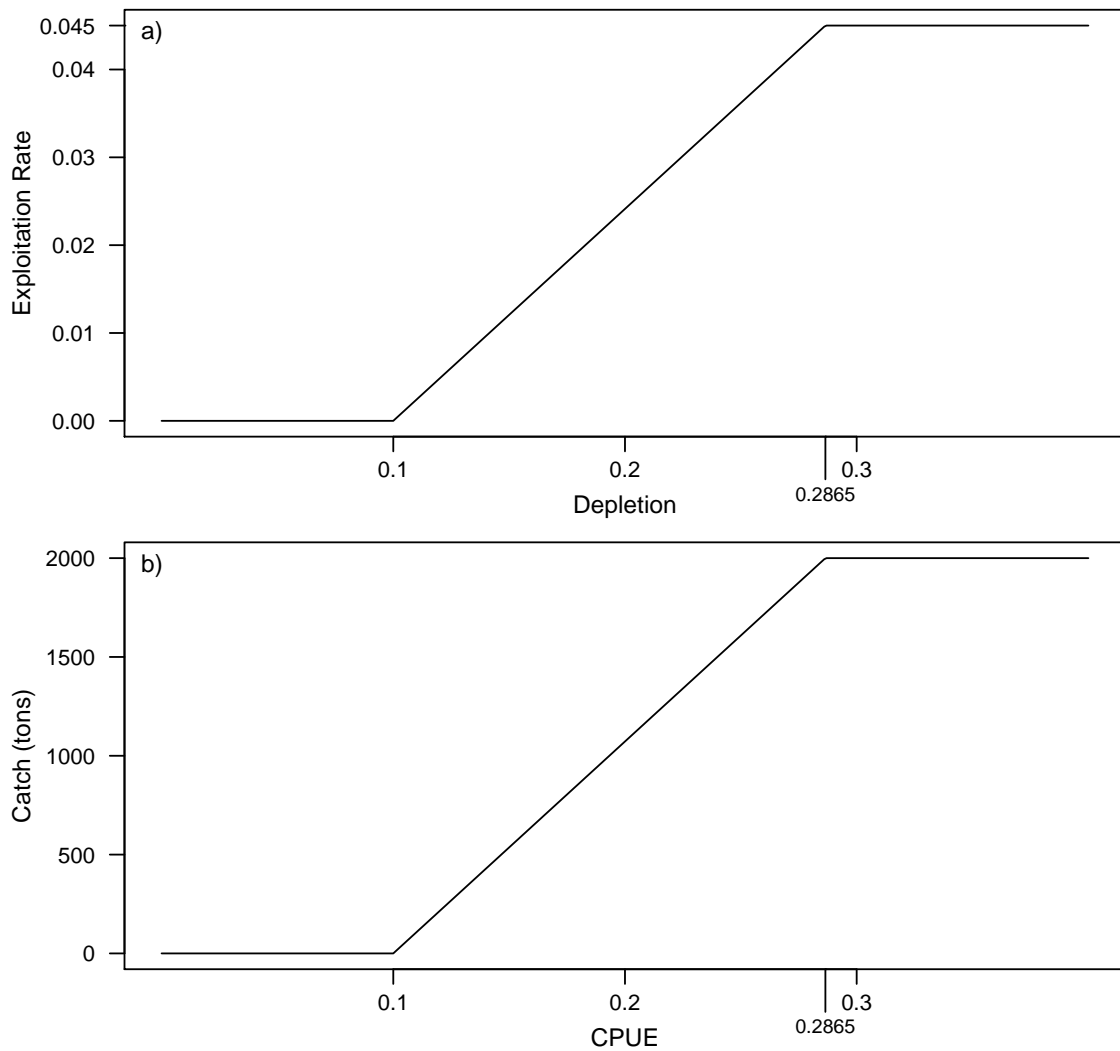


Figure 3.2: The current control rules based on the New Zealand harvest strategy standard (Ministry of Fisheries 2008a). The model-based control rule (a) is dependent on depletion. The CPUE-based control rule (b) is dependent on CPUE. The target is 0.3, the threshold is 0.2865, the soft limit is 0.2 (although it was not used), and the hard limit is 0.1.

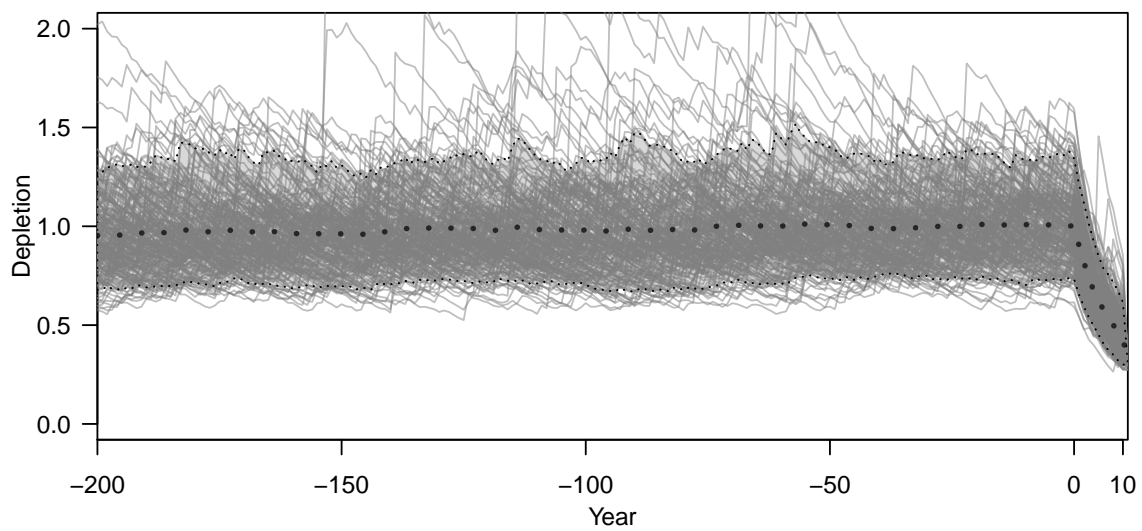


Figure 3.3: Simulated trajectory for the single area model and a constant exploitation rate for the last 10 years. The mean trajectory is shown as the dark dotted line and the light dotted lines represent the 5th and 95th quantiles. The light gray lines are individual simulated trajectories.

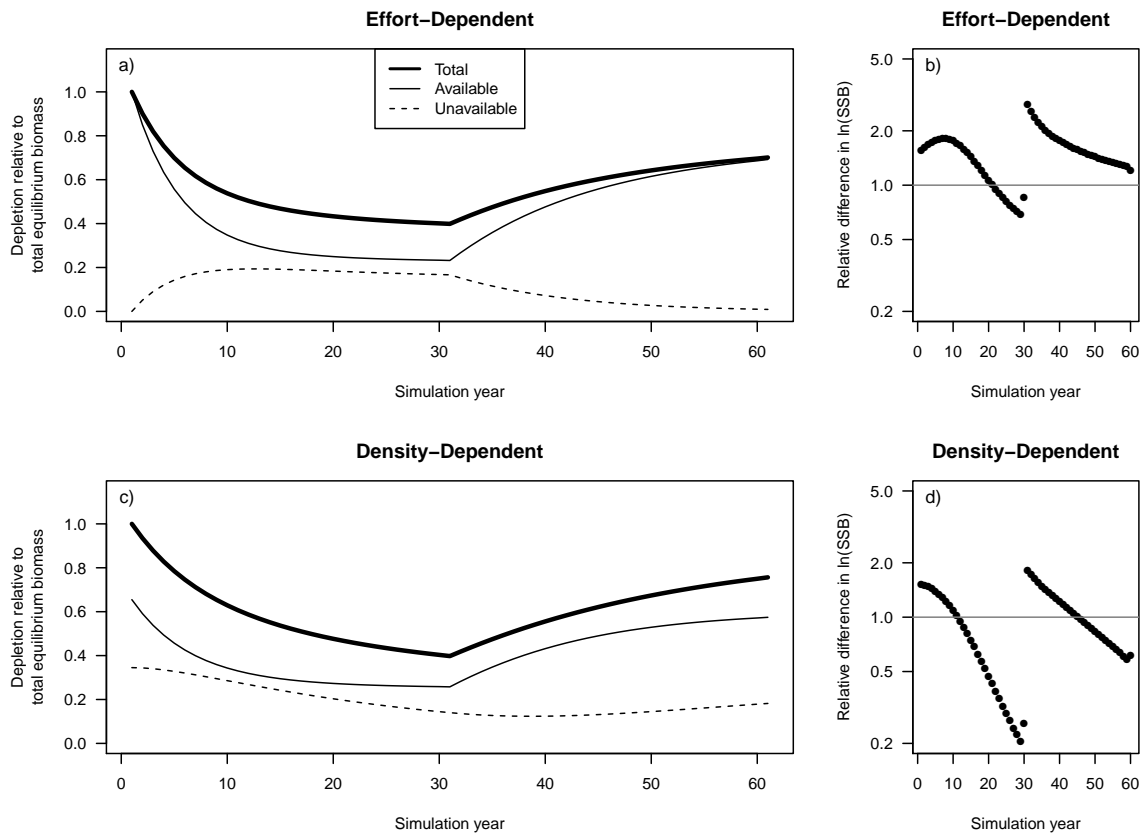


Figure 3.4: Trajectories of depletion for total, available, and unavailable spawning biomass relative to the total unfished equilibrium spawning biomass from deterministic two-area effort-dependent (a) and two-area density-dependent (c) models. Shown on the right (plots b and d) are the differences of the natural log of the available spawning biomass from one year to the next divided by the difference in the natural log of the total spawning biomass for the same years. Values above one indicate that available biomass was changing faster than total biomass (hyperdepletion) while values below one indicate the opposite (hyperstability).

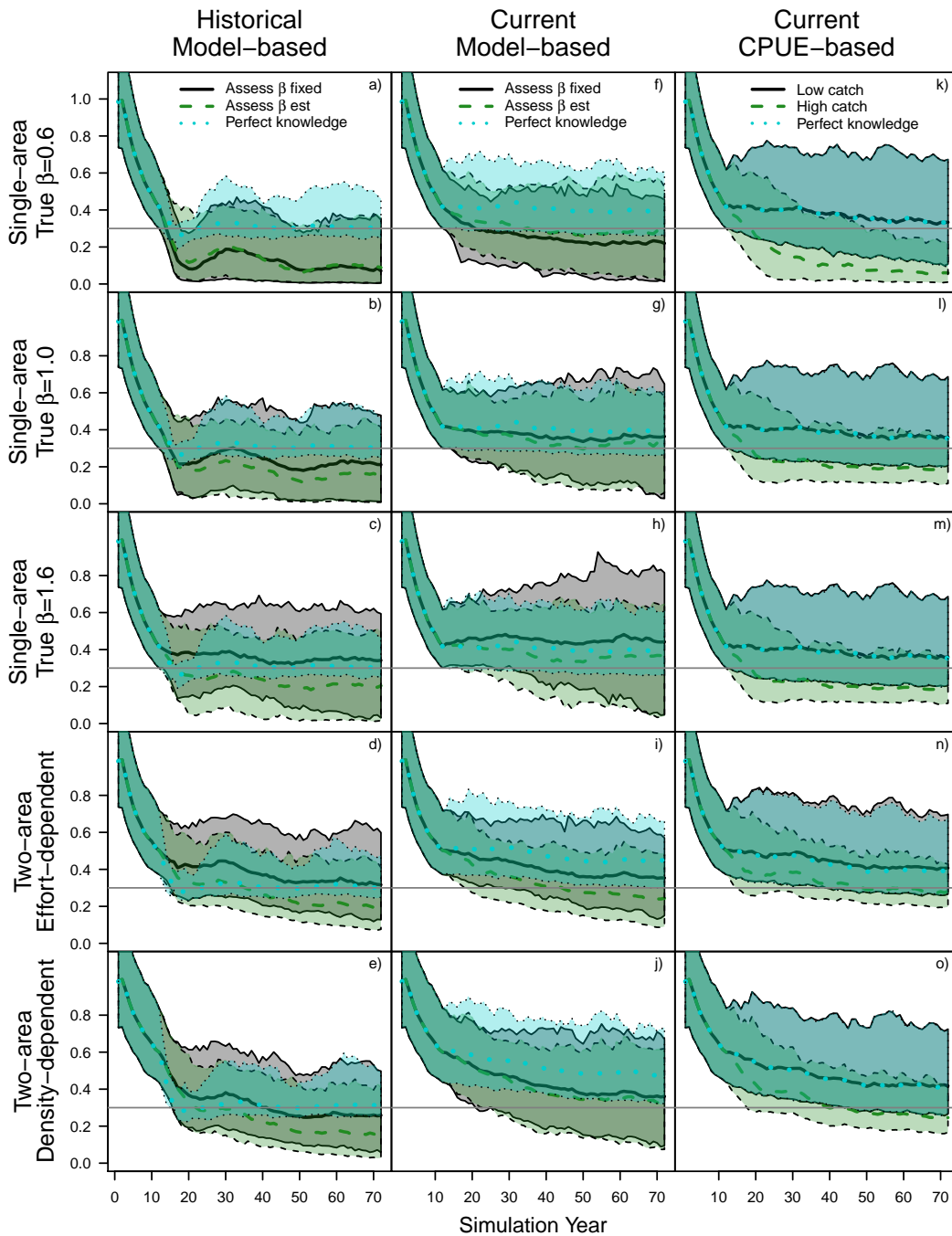


Figure 3.5: Median depletion trajectories with 5th and 95th quantiles from simulations using different operating model assumptions (rows) using the historical model-based (left), current model-based (middle), and current CPUE-based (right) control rules. The vertical line shows when management using the control rule began, and the horizontal dashed line is 30% B_0 for reference.

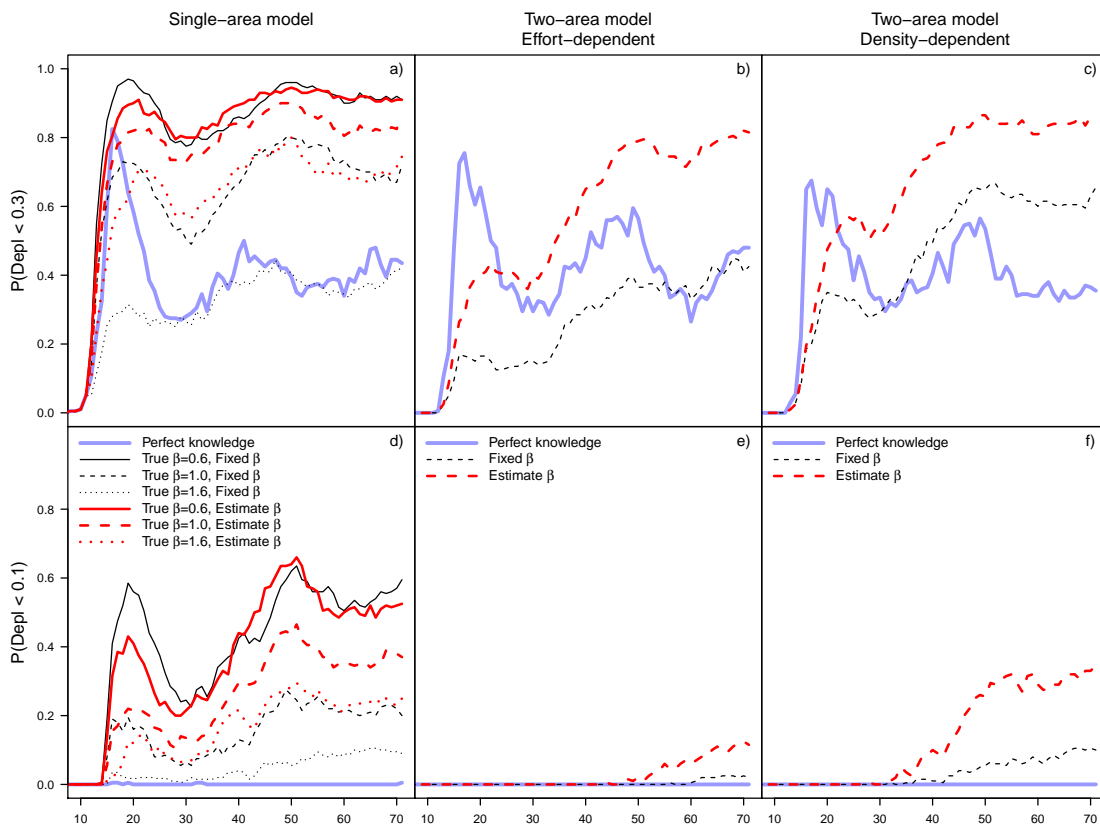


Figure 3.6: The probability of the true depletion for the single-area (left column) and two-area models (middle and right columns) being below the 30% (top) and 10% (bottom) for each year when using the historical model-based control rule. The assessment-based control rules, with and without estimating β , are shown along with perfect knowledge of abundance applied to the control rule.

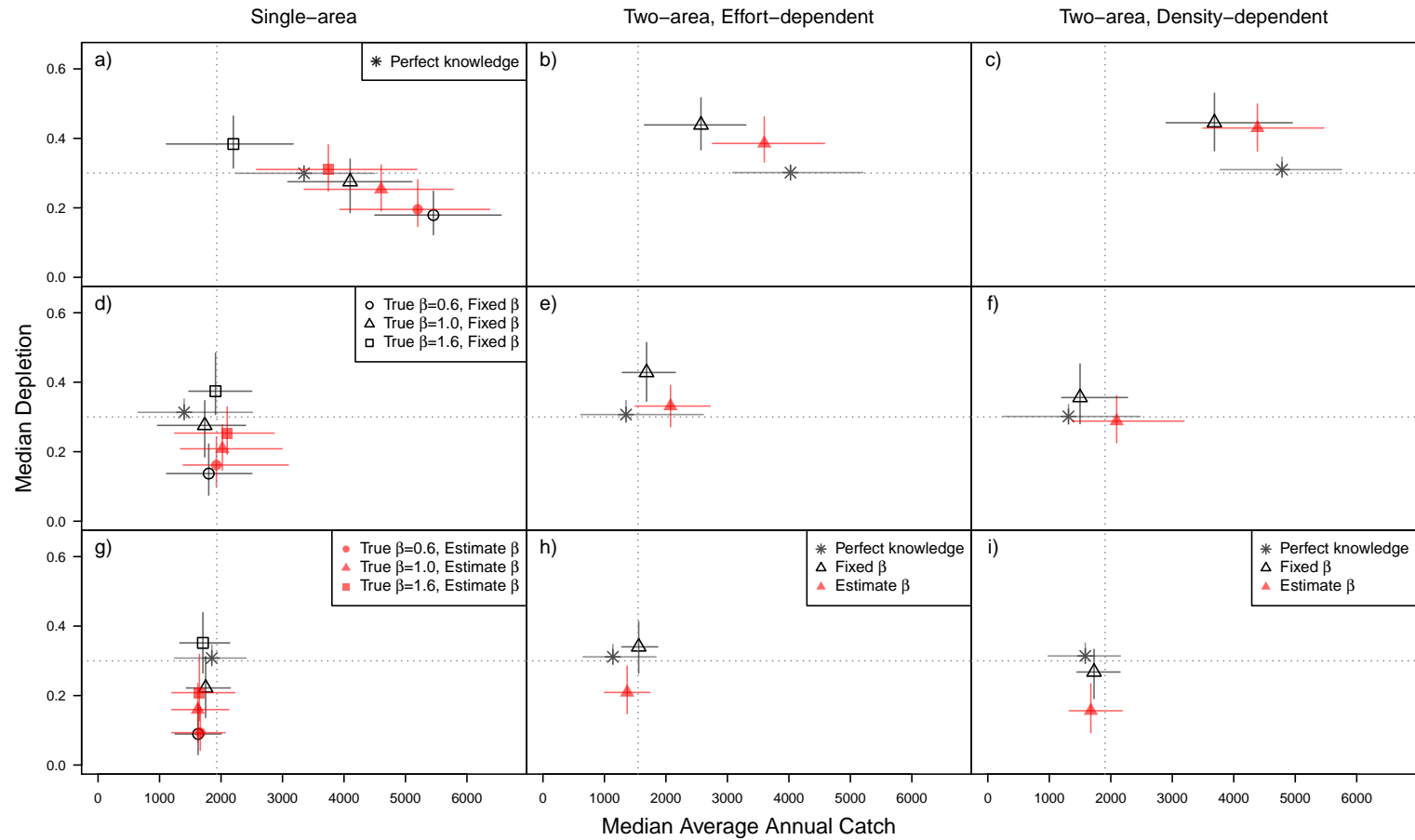


Figure 3.7: Median of the median depletion vs. median average annual catch with bars indicating the 25th and 75th percent quantiles for different periods of the historical control rule analysis: a–b) first 10 years after management began (years 11–20), d–f) years 21–30, and g–i) years 51–70. The horizontal dashed line is the 30% depletion target and the vertical dashed line is $C_{30\%}$.

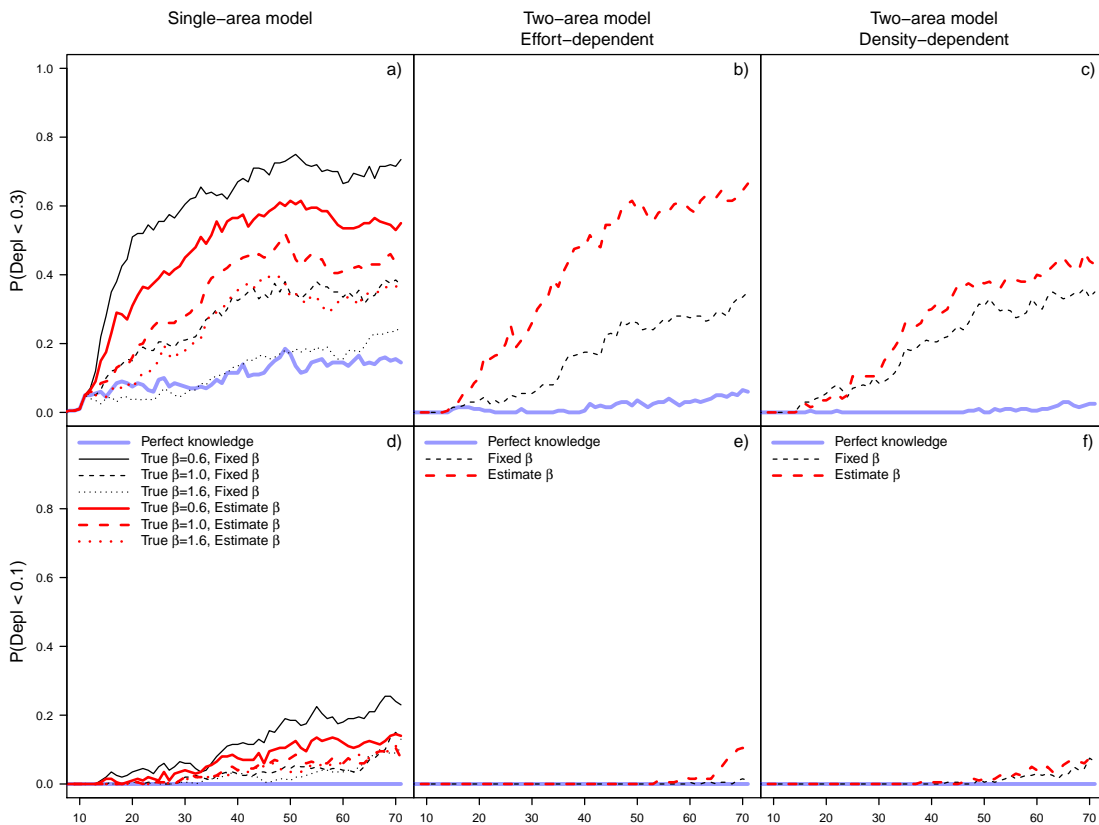


Figure 3.8: The probability of the true depletion for the single-area (left column) and two-area models (middle and right columns) being below the 30% (top) and 10% (bottom) for each year when using the current model-based control rule. The assessment-based control rules, with and without estimating β , are shown along with perfect knowledge of abundance applied to the control rule.

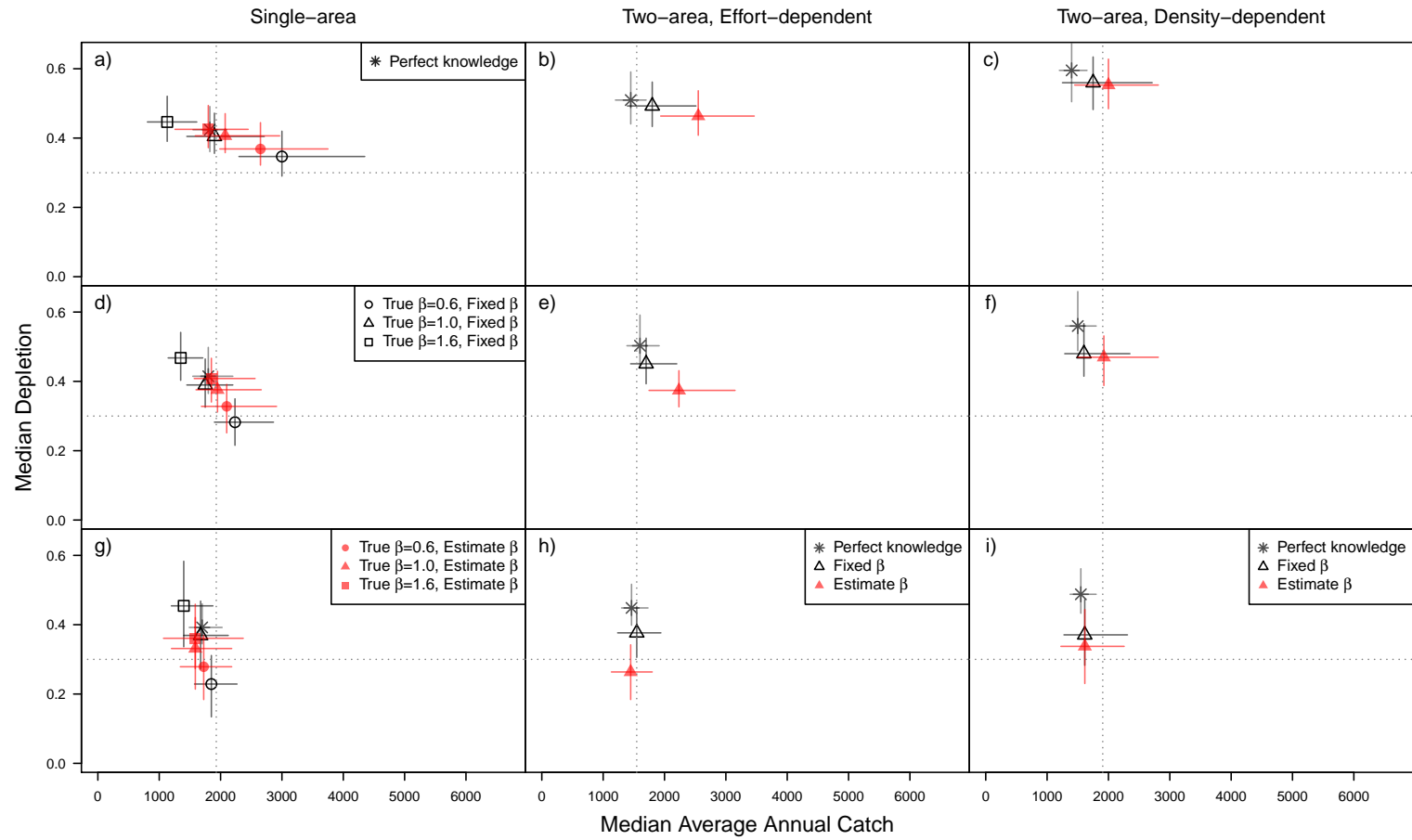


Figure 3.9: Median of the median depletion vs. median average annual catch with bars indicating the 25th and 75th percent quantiles for different periods of the current model-based control rule analysis: a–c) first 10 years after management began (years 11–20), d–f) years 21–30, and g–i) years 51–70. The horizontal dashed line is the 30% depletion target and the vertical dashed line is $C_{30\%}$.

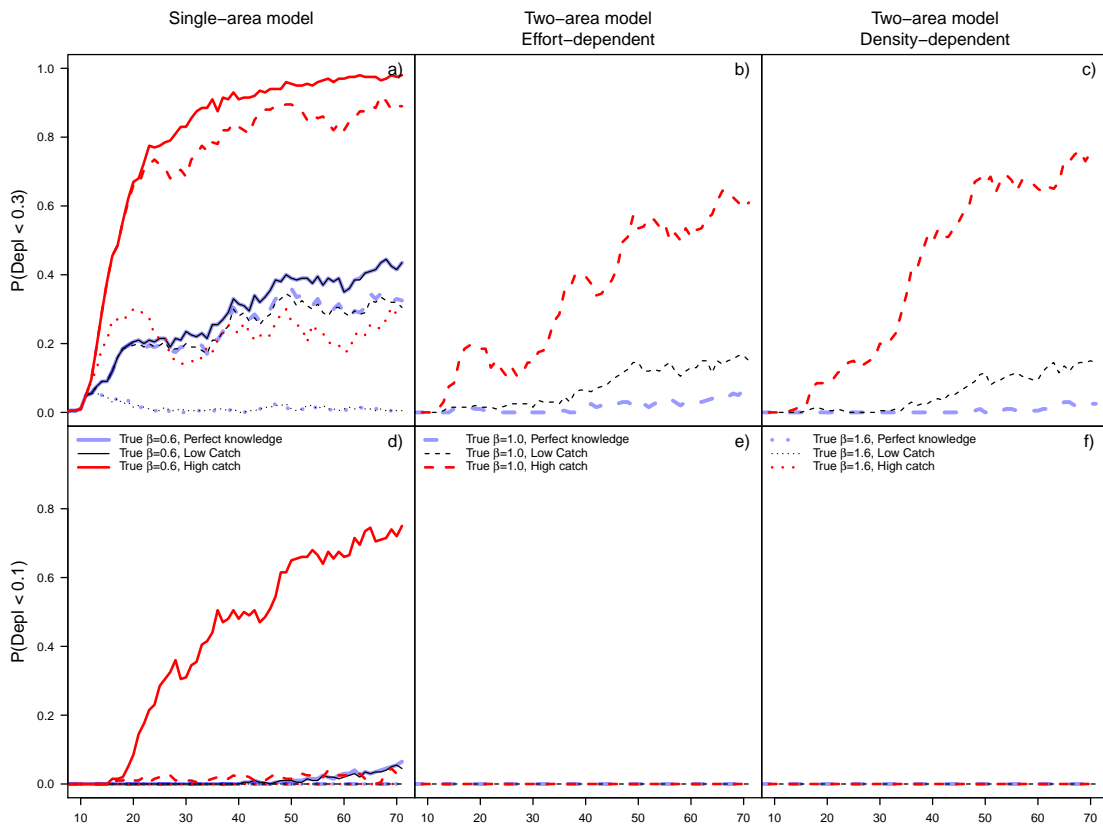


Figure 3.10: The probability of the true depletion being below the targets of 30% (top) and 10% (bottom) for each year that fishing occurred in the future analysis when using the CPUE-based control rule with the single-area and two-area operating models (columns). The low catch is 2000 metric tons and is near the MSY catch target and the high catch is 4000 metric tons. Perfect knowledge assumes that CPUE is exactly known and the catch target is 2000 metric tons.

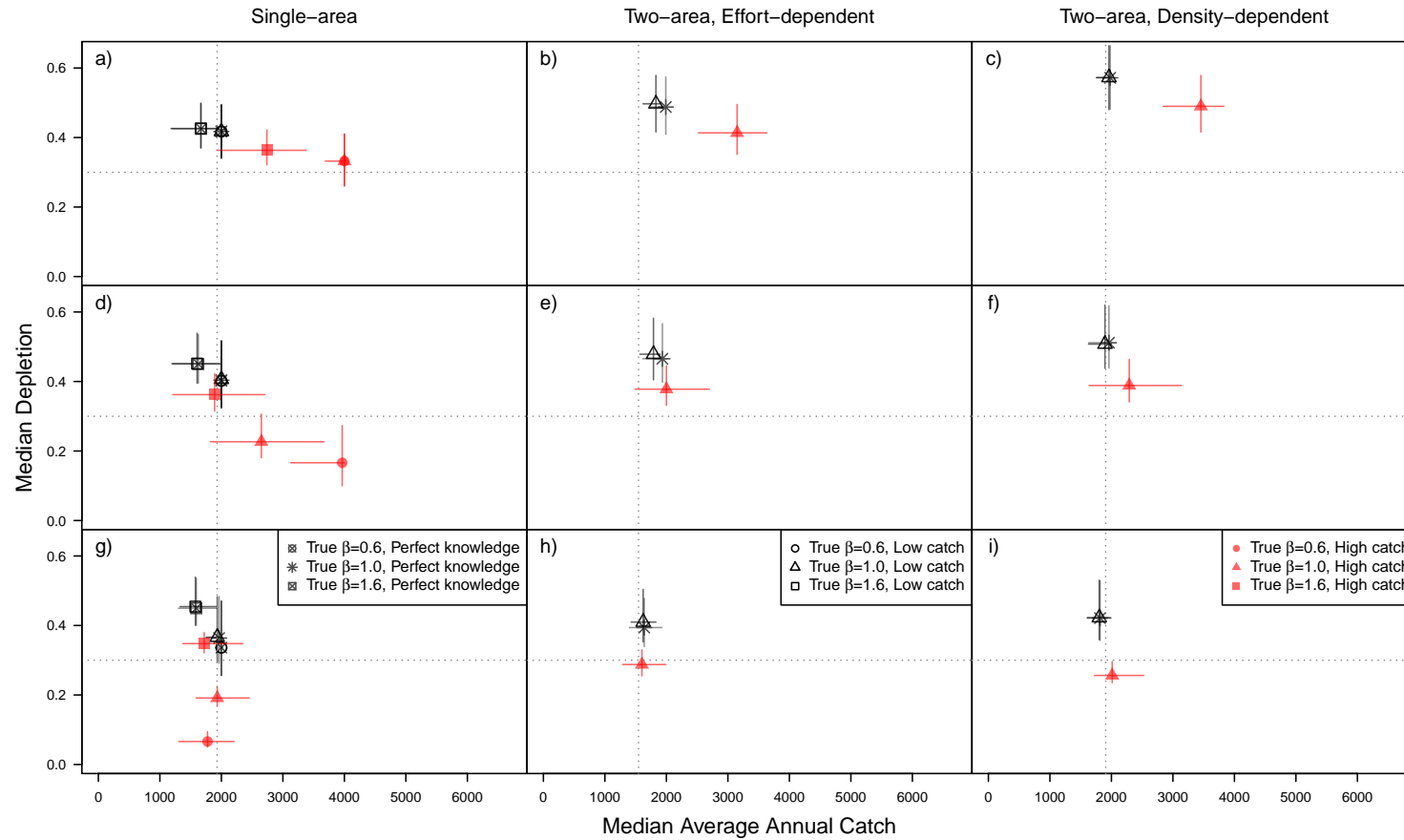


Figure 3.11: Median of the median depletion vs. median average annual catch with bars indicating the 25th and 75th percent quantiles for different periods of the current CPUE-based control rule analysis: a–c) first 10 years after management began (years 11–20), d–f) years 21–30, and g–i) years 51–70. The horizontal dashed line is the 30% depletion target and the vertical dashed line is $C_{30\%}$. The “low catch” target was 2000 metric tons and the “high catch” target was 4000 metric tons. The perfect knowledge scenarios almost exactly overlap the corresponding low catch scenarios.

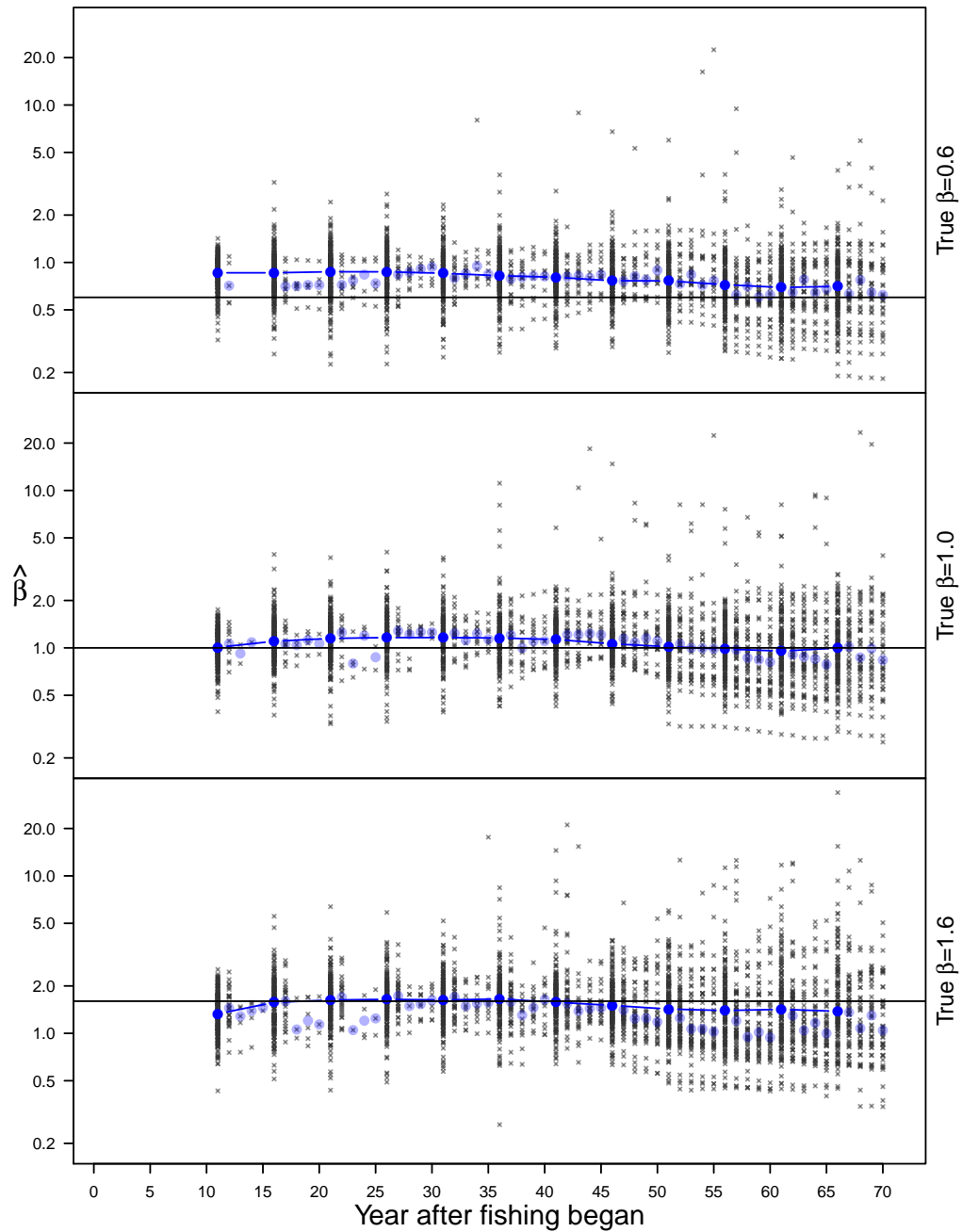


Figure 3.12: Estimates of β in each year that had an assessment for the single-area operating model. The "x" points denote estimates from individual simulations. The blue dots are the median of the estimates for that year. The line connects the blue dots in every 5th year, which are the years with most assessments since that is the default assessment period in the control rule.

CONCLUSIONS

The three main chapters of research in this dissertation focused on the relationship between CPUE and abundance for long-lived species by investigating real data from orange roughy fisheries, examining assessment models that estimate the nonlinear relationship, and finally exploring the outcomes of different management systems when choosing to estimate a nonlinear relationship between CPUE and abundance. Many studies to date have focused on the hyperstable relationship between CPUE and abundance, which is considered to be risky due to a false impression that the stock is remaining at a higher abundance (Bannerot and Austin 1983; Cox and Kronlund 2008; Crecco and Overholtz 1990; Crecco and Savoy 1985; Harley *et al.* 2001; MacCall 1976; Peterman and Steer 1981; Rose and Leggett 1991; Swain and Sinclair 1994; Ulltang 1980; Winters and Wheeler 1985). Fewer studies have investigated or found hyperdepletion, which gives a false impression that the stock is more depleted than it actually is when being fished down (Ahrens and Walters 2005; Davies and Jonsen 2011; Hilborn and Walters 1992; Sosa-Lopez and Manzo-Monroy 2002; Walters 2003). The research in the dissertation equally investigated hyperstability and hyperdepletion in simulation studies using a power function to model the relationship between CPUE and abundance

$$U = \alpha N^\beta \tag{3.1}$$

Chapter 1 used data from four orange roughy fisheries in New Zealand and Australia to investigate the relationship between CPUE and abundance and estimate β . The results indicated that CPUE is likely to decline faster than abundance in the early part of a fishery for orange roughy, which may lead to a pessimistic view of the stock status as well as the fishery after a number of years of fishing. Hyperdepletion was unexpected for an aggregating species, and these results can not only be used to more accurately determine the historical biomass trend, but may also be applicable to other species of fish, such as oreos (family Oreosomatidae), which are commonly associated with orange roughy in catches and also

form feeding and spawning aggregations near seamounts. This study provided a realization of the potential bias in an assessment due to the nonlinear relationship between CPUE and abundance if a nonlinear parameter modeling density-dependent catchability was not incorporated into the assessment. Furthermore, the results from Chapter 1 provided a range of possible values for β and also presented a prior distribution which may be used in a Bayesian analysis relating CPUE to abundance for orange roughy or similar species.

Chapter 2 showed that assessment models perform differently when estimating β in the relationship between CPUE and abundance, and priors may improve estimation error but may also lead to bias. In addition, fishery-independent surveys improve estimates of β , and there is more information about the nonlinearity in CPUE when a stock is more depleted. An unintuitive result was that additional uncertainty in the CPUE data improved estimates of β . Increasing the variability on the CPUE data lessened the influence of those data, allowing the model to put more weight on the prior distribution (if it was informative) and the survey data, which was proportional to abundance. This result was most prevalent in the proportional and hyperdepletion scenarios using models that assumed deterministic recruitment.

Supplying information on the amount of nonlinearity in the relationship between CPUE and abundance to the estimation model in the form of an informative prior distribution resulted in fewer extreme values and more precise estimates of β , but resulted in some bias. With CPUE data providing the only information in an assessment, the estimates of β degraded, but an informative prior distribution improved the estimates. An informative prior distribution was useful when estimating nonlinearity in the CPUE, especially when limited data were available, but it must be appropriate, justifiable, and wide enough to support all possible values of β .

The management strategy evaluation from Chapter 3 showed that there is a trade-off between conservation and utilization management objectives with regard to the choice of estimating a nonlinearity parameter, β , for the relationship between CPUE and abundance, or assuming that CPUE is proportional to abundance. These trade-offs were dependent on the underlying true relationship. A hyperstable relationship resulted in a high risk to the stock because changes in abundance were more difficult to detect and abundance was

perceived to remain high, often resulting in catches that were too high to meet conservation objectives. Estimating β in a hyperstable scenario reduces the risk to the stock because catches are often lower, although the risk remained higher than a proportional or hyperdepletion scenario, which is likely due to lack of contrast in the CPUE data. Conversely, with hyperdepletion, the risk to stock status was low because the perception of the stock was more pessimistic and catches were less than optimal for the depletion target. Estimating β when hyperdepletion was present increased the yield, but also increased the conservation risk to the stock. Compared to the case where CPUE was proportional to abundance and was assumed proportional in model-based assessments, the hyperdepletion scenario showed a similar risk to stock status when β was estimated, but the hyperstable scenario always had more risk regardless if β was estimated or not. Overall, estimating β brought the catches and depletion levels closer to target when nonlinearity was present, but increased variability in catches. In the short-term (immediately following implementation of the control rule) catches were variable among scenarios with highest catches in the hyperstable scenarios and lowest catches in the hyperdepletion scenarios. In the long-term, catches were much less variable across scenarios, but the depletion was much more variable. Estimating β reduced the differences in catch across scenarios, but the hyperstable case still resulted in the most depleted stock, and the hyperdepletion case resulted in the least depleted stock. Estimating β resulted in little difference in the long-term catches when compared to not estimating β .

It is useful to investigate the relationship between CPUE and abundance for a better understanding of the risks that may be present. An investigation may specifically look at the relationship between CPUE and abundance (Harley *et al.* 2001; Wilberg and Bence 2006) or draw conclusions by examining fish and fisher behavior (Paloheimo and Dickie 1964; Rose and Kulka 1999; Winters and Wheeler 1985). However, making inference of the relationship between CPUE and abundance based solely on life-history characteristics or fish behavior may be inconclusive. For example, orange roughy aggregate in dense spawning and feeding aggregations which are targeted by the fishery which has been thought to lead to a hyperstable relationship, but could also lead to hyperdepletion if small localized aggregations are fished out (Francis and Clark 2005).

Nonlinearity in the relationship between CPUE and abundance can often result in con-

tradiictory information on stock status from a CPUE series and a survey series (for example, see the description given by Hilborn and Walters (1992, page 533) of the northern cod fishery). Francis (2011) suggested that if survey and fishery abundance data appear to be contradictory, then separate assessments should be done using only subsets of the abundance data, unless a data set is obviously unrepresentative. Hilborn and Walters (1992) warn against averaging across datasets and suggests presenting a decision table to managers with alternative hypotheses. As noted by Francis (2011), it may be difficult to portray an accurate level of uncertainty when presenting multiple assessments, and furthermore, detecting unrepresentative data is not straightforward. The simulations in this dissertation took an additional approach to conducting two separate assessments, and introduced a slightly more complicated model to explain the differences between two abundance indices. I showed that estimating a nonlinearity parameter resulted in improved estimates of depletion and trend in abundance. In addition, estimating this parameter allowed for a better representation of the uncertainty that would otherwise be difficult to portray using two separate assessments. The key is to understand the processes that may require a particular data set to be modeled differently. That understanding can also help create useful prior distributions for certain parameters.

Caveats and future work

The power function may not be the best choice for modeling the relationship between CPUE and abundance, especially if catchability is not a simple function of biomass. Other modeling techniques, such as time-varying catchability (Wilberg *et al.* 2010), may improve estimation performance and management goals. For example, catchability may increase over time through experience, knowledge, and increases in technology, refugia may play a role in changing catchability, or catchability may have a different relationship with biomass depending on whether the stock is decreasing or increasing. Regardless, there are many reasons why catchability may change over time, and even though the power model used here is simple and parsimonious, more complicated methods may be warranted when the appropriate data are available.

Developing a prior distribution for β in Chapter 1 used only survey and CPUE data from

orange roughy fisheries and made some simplifying assumptions about selectivity. Data from other orange roughy stocks, when available, or from additional deepwater species with similar behavior to orange roughy, such as oreos, could be combined into a meta-analysis of nonlinearity between CPUE and abundance. Also, a more complicated age-structured model could incorporate length or age data in addition to the index data already used. However, the results from Chapter 1 captured a wide uncertainty that is present due to uncertainties in the data.

The estimation models used for the simulations in Chapters 2 and 3 made some assumptions that may have limited the analyses. Deterministic recruitment was assumed for two of the estimation models, and all three models fixed many parameters at the true values of the population. Francis (2012) points out that assuming the same parameter values in the operating and estimation models is a weakness in simulation studies because there will always be misspecification, at least in fish stock assessment models. The MSE in Chapter 3 varied the selectivity parameters in the estimation to introduce more realistic error, but other parameters remained fixed. It is unknown how the estimates of β would change when other parameters are incorrect or estimated, but it is likely that estimates of β will likely be more uncertain and biased as this parameter attempts to correct for other misspecifications.

Another common source of uncertainty in management strategy evaluations that was not accounted for in this study was implementation error in the management decision. The assumption that the exact catch is taken every year is an unlikely assumption. For example, New Zealand regulations specify an annual catch entitlement (ACE) for each fisher, and if the fisher exceeds their ACE, they can either buy more if it is available, or pay a deemed value for the amount of catch that exceeded their ACE. Additionally, due to precautionary, economic, or social concerns, managers may make the decision to alter the exact catch as specified by the control rule. A common management decision is to cap the total allowable catch as a precautionary measure when the stock is predicted to be very large or limit the amount of change in catch from one year to the next (i.e., Butterworth *et al.* 1997). Implementation error could be modeled as a probability distribution with a possible truncation to limit the high predicted catches. Adding a cap on the catch may also be implemented specifically as part of a control rule, and it would likely decrease the risk

to the stock.

This dissertation could be further expanded by investigating other species. For example, the West Coast of the United States manages deepwater species that are also long-lived and show a wide range of life-histories and productivity (e.g., Hilborn *et al.* 2002; Punt *et al.* 2008; Ianelli 2002). We used proxies for reference points as they are currently used in New Zealand (Ministry of Fisheries, 2011), but the true reference points and stock risk are greatly influenced by the stock-recruit relationship (Cox and Kronlund 2008; Maunder 2012; Punt *et al.* 2008). The value of steepness used here, 0.75, may be higher than typical for long-lived, low productivity species like orange roughy (Sissenwine and Mace 2007) and future management strategy evaluations may want to investigate the robustness of the management strategy to various values of steepness and other life-history parameters. Additionally, Clark (1993) found that higher SPR_{MSY}/SPR_0 ratios might be needed due to serially correlated recruitment, which was not investigated here. An even less productive species with serial recruitment may need more precautionary reference point proxies (Koslow 1989).

Overall, the decision of whether or not to account for nonlinearity is based on the assumptions and risks one is willing to make, the potential loss in yield, and the misperceptions that may result. Hyperstable scenarios are especially risky and should always be accounted for, or at least acknowledged. Hyperdepletion scenarios, on the other hand, may appear to be of less concern, due to reduced conservation risk, but the negative consequences of reduced yield, at least in the short term, and a pessimistic view of the stock status, and thus the management system, make it worthwhile to at least acknowledge the potential for hyperdepletion and that not accounting for it is chosen as part of the management strategy.

BIBLIOGRAPHY

- Adkison MD. 2009. Drawbacks of complex models in frequentist and Bayesian approaches to natural-resource management. *Ecological Applications* 19:198–205.
- Ahrens R, Walters C. 2005. Why are there still large pelagic predators in the oceans? Evidence of severe hyper-depletion in longline catch-per-effort. Owner: Hicks Added to JabRef: 2008.08.26.
- Anderson OF, Francis RICC, Hicks AC. 2002. CPUE analysis and assessment of the Mid-East Coast orange roughy stock (ORH 2A South, 2B, 3A). New Zealand Fisheries Assessment Report 2003/56. 23 pp.
- Bannerot SP, Austin CB. 1983. Using frequency distributions of catch per unit effort to measure fish-stock abundance. *Transactions of the American Fisheries Society* 112:608–617.
- Baranov TI. 1918. On the question of the biological basis of fisheries. Translated by W. E. Ricker, 1945.
- Bell JD, Lyle JM, Bulman CM, Graham KJ, Newton GM, Smith DC. 1992. Spatial variation in reproduction, and occurrence of non-reproductive adults, in orange roughy, *Hoplostethus atlanticus* Collet (*Trachichthyidae*), from south-eastern Australia. *Journal of Fish Biology* 40:107–122.
- Beverton RJH, Holt SJ. 1957. On the dynamics of exploited fish populations. The Blackburn Press. Owner: Hicks Added to JabRef: 2008.07.14.
- Branch TA, Hilborn R, Haynie AC, Fay G, Flynn L, Griffiths J, Marshall KN, Randall JK, Scheuerell JM, Ward EJ, Young M. 2006. Fleet dynamics and fishermen behavior: lessons for fisheries managers. *Canadian Journal of Fisheries and Aquatic Sciences* 63:1647–1668.
- Bull JT, Shine R. 1979. Iteroparous animals that skip opportunities for reproduction. *The American Naturalist* 114:296–303.
- Bunnefeld N, Hoshino E, Milner-Gulland EJ. 2011. Management strategy evaluation: a powerful tool for conservation? *Trends Ecol Evol* 26:441–7. Bunnefeld, Nils Hoshino, Eriko Milner-Gulland, Eleanor J England *Trends Ecol Evol*. 2011 Sep;26(9):441-7. Epub 2011 Jun 15.
- Burnham KP, Anderson DR. 2002. Model selection and multimodel inference : a practical information-theoretic approach. Springer, New York.
- Butterworth DS, Cochrane KL, De Oliveira JAA. 1997. Management procedures: A better way to manage fisheries? The South African experience. In EK Pikitch, DD Huppert,

- MP Sissenwine, editors, *Global Trends: Fisheries Management*, American Fisheries Society Symposium 20, pp. 83–90.
- Carlin BP, Louis TA. 2000. *Bayes and empirical bayes methods for data analysis*. 2 edition. Chapman & Hall, New York.
- Chen Y, Breen PA, Andrew NL. 2000. Impact of outliers and mis-specifications of priors on Bayesian fisheries-stock assessment. *Can J Fish Aquat Sci* 57:2293–2305.
- Clark M. 2001. Are deepwater fisheries sustainable?—the example of orange roughy (*Hoplostethus atlanticus*) in New Zealand. *Fisheries Research* 51:123–135.
- Clark MR. 1995. Experience with the management of orange roughy *Hoplostethus atlanticus* in New Zealand, and the effects of commercial fishing on stocks over the period 1980–1993. In AG Hopper, editor, *Deep-water fisheries of the North Atlantic oceanic slope*, Kluwer Academic Publishers, Dordrecht, pp. 251–266.
- Clark MR. 1996. Biomass estimation of orange roughy: a summary and evaluation of techniques for measuring stock size of a deep-water fish species in New Zealand. *Journal of Fish Biology* 49 (Supplement A):114–131.
- Clark MR. 2009. Deep-sea seamount fisheries: a review of global status and future prospects. *Latin American Journal of Aquatic Research* 37:501–512.
- Clark MR, Tracey DM. 1992. Changes in a population of orange roughy, *Hoplostethus atlanticus*, with commercial exploitation on the Challenger Plateau, New Zealand. *Fishery Bulletin* 92:236–253.
- Clark MR, Tracey DM. 1994. Changes in a population of orange roughy, *Hoplostethus atlanticus*, with commercial exploitation on the Challenger Plateau, New Zealand. *Fishery Bulletin* 92:236–253.
- Clark WG. 1993. The effect of recruitment variability on the choice of a target level of spawning biomass per recruit. In G. Kruse, D. M. Eggers, R. Marasco, C. Pautze, and T. J. Quinn II, editors, *Proceedings of the International Symposium on Management Strategies for Exploited Fish Populations*, pp 233–246, Alaska Sea Grant College Program, University of Alaska, Fairbanks.
- Cochrane KL, Butterworth DS, De Oliveira JAA, Roel BA. 1998. Management Procedures in a fishery based on highly variable stocks and with conflicting objectives: experiences in the South African pelagic fishery. *Reviews in Fish Biology and Fisheries* 8:177–214.
- Cooke J. 1985a. On the relationship between catch per unit effort and whale abundance (SC/35/O7). Annual Report International Whaling Commission [REP INT WHALING COMM] 35:511–519. Database Name: ASFA: Aquatic Sciences and Fisheries Abstracts.
- Cooke JG. 1985b. Trends in abundance of sperm whales in the western-North Pacific (SC/36/Sp6). Annual Report International Whaling Commission [REP INT WHALING COMM] 35:205–208. Owner: Hicks Added to JabRef: 2008.05.20.

- Cooke JG, Beddington JR. 1984. The relationship between catch rates and abundance in fisheries. *Mathematical Medicine and Biology* 1:391–405. URL <http://imamb.oxfordjournals.org/cgi/content/abstract/1/4/391>.
- Cope J, Punt A. 2009. Length-Based Reference Points for Data-Limited Situations: Applications and Restrictions. *Marine and Coastal Fisheries: Dynamics, Management, and Ecosystem Science* 1:169–186.
- Cox SP, Kronlund AR. 2008. Practical stakeholder-driven harvest policies for groundfish fisheries in British Columbia, Canada. *Fisheries Research* 94:224–237.
- Crecco V, Overholtz WJ. 1990. Causes of density-dependent catchability for Georges Bank haddock *Melanogrammus aeglefinus*. *Canadian Journal of Fisheries and Aquatic Sciences* 47:385–394.
- Crecco VA, Savoy TF. 1985. Density-dependent catchability and its potential causes and consequences on Connecticut River American shad, *Alosa sapidissima*.
- Davies TD, Jonsen ID. 2011. Identifying nonproportionality of fishery-independent survey data to estimate population trends and assess recovery potential for cusk (*Brosme brosme*). *Canadian Journal of Fisheries and Aquatic Sciences* 68:413–425.
- de la Mare WK. 1998. Tidier fisheries management requires a new MOP (management-oriented paradigm). *Reviews in Fish Biology and Fisheries* 8:349–356.
- de Valpine P, Hilborn R. 2005. State-space likelihoods for nonlinear fisheries time-series. *Canadian Journal of Fisheries and Aquatic Sciences* 62:1937–1952.
- Delury DB. 1947. On the Estimation of Biological Populations. *Biometrics* 3:145–167.
- Deriso RB. 1980. Harvesting strategies and parameter estimation for an age-structured model. *Canadian Journal of Fisheries and Aquatic Sciences* 37:268–282.
- Deroba JJ, Bence JR. 2008. A review of harvest policies: Understanding relative performance of control rules. *Fisheries Research* 94:210–223.
- Doonan IJ, Hicks AC, Coombs RF, Hart AC, Tracey DM. 2003. Acoustic estimates of the abundance of orange roughy in the Mid-East Coast fishery, June–July 2001. *New Zealand Fisheries Assessment Report 2003/4*. 22 pp.
- Dunn A, Harley S, Doonan I, Bull B. 2000. Calculation and interpretation of catch-per-unit effort (CPUE) indices. *New Zealand Fisheries Assessment Report 2000/01*. 44 pp.
- Dunn M. 2007. CPUE analysis and assessment of the East Chatham Rise orange roughy stock (part of ORH3B) to the end of the 2004–05 fishing year. *New Zealand Fisheries Assessment Report 2007/08*. 76 pp.
- Dunn MR. 2011. Investigation of some alternative stock assessment model structures for Mid-East Coast orange roughy. Technical report.

- Erismann BE, Allen LG, Claisse JT, Pondella DJ, Miller EF, Murray JH. 2011. The illusion of plenty: hyperstability masks collapses in two recreational fisheries that target fish spawning aggregations. *Canadian Journal of Fisheries and Aquatic Sciences* 68:1705–1716.
- Field KD, Francis RICC. 2001. CPUE analysis and stock assessment of the Challenger Plateau orange roughy stock (ORH 7A) for the 2000-01 fishing year. *New Zealand Fisheries Assessment Research Document* 2001/25. 19 pp.
- Fonteneau A, Richard N. 2003. Relationship between catch, effort, CPUE, and local abundance for non-target species, such as billfishes, caught by Indian Ocean longline fisheries. *Marine and Freshwater Research* 54:383–392. Owner: Hicks Added to JabRef: 2008.08.27.
- Fournier DA, Skaug HJ, Ancheta J, Ianelli J, Magnusson A, Maunder MN, Nielsen A, Sibert J. 2011. AD Model Builder: using automatic differentiation for statistical inference of highly parameterized complex nonlinear models. *Optimization Methods and Software* pp. 1–17.
- Francis RICC. 1992. Use of risk analysis to assess fishery management strategies: A case study using orange roughy (*Hoplostethus atlanticus*) on the Chatham Rise, New Zealand. *Can J Fish Aquat Sci* 49:922–930.
- Francis RICC. 2001. Stock assessment for 2001 of orange roughy on the northeast Chatham Rise. *New Zealand Fisheries Assessment Report* 2001/41. 32 pp.
- Francis RICC. 2006. Some recent problems in New Zealand orange roughy assessments. *New Zealand Fisheries Assessment Report* 2006/43. 65 pp.
- Francis RICC. 2011. Data weighting in statistical fisheries stock assessment models. *Canadian Journal of Fisheries and Aquatic Sciences* 68:1124–1138.
- Francis RICC. 2012. The reliability of estimates of natural mortality from stock assessment models. *Fisheries Research* 119-120:133–134.
- Francis RICC, Clark MR. 1998. Inferring spawning migrations of orange roughy (*Hoplostethus atlanticus*) from spawning ogives. *Marine Freshwater Research* 49:103–108.
- Francis RICC, Clark MR. 2005. Sustainability Issues for Orange Roughy Fisheries. *Bull Mar Sci* 76:337–352.
- Francis RICC, Hurst RJ, Renwick JA. 2003. Quantifying annual variation in catchability for commercial and research fishing. *Fishery Bulletin* 101:293–304.
- Froese R. 2004. Keep it simple: three indicators to deal with overfishing. *Fish and Fisheries* 5:86–91.
- Fuller WA. 1987. *Measurement Error Models*. John Wiley & Sons, New York, 440 pp.
- Garstang W. 1900. The impoverishment of the sea. *J Mar Biol Assoc UK* 6:1–69.

- Gelman A. 2006. Prior distributions for variance parameters in hierarchical models. *Bayesian Analysis* 1:515–533.
- Gelman A, Carlin JB, Stern HS, Rubin DB. 1995. *Bayesian Data Analysis*. Chapman & Hall/CRC, Boca Raton, FL, 526 pp.
- Geweke. 1992. Evaluating the accuracy of sampling-based approaches to the calculation of posterior moments. In JM Bernardo, JO Berger, AP Dawid, AFM Smith, editors, *Bayesian statistics 4 : proceedings of the Fourth Valencia International Meeting, April 15-20, 1991*. Clarendon Press – Oxford University Press, Oxford; New York, pp. 169–193.
- Gillis DM, Peterman RM. 1998. Implications of interference among fishing vessels and the ideal free distribution to the interpretation of CPUE. *Canadian Journal of Fisheries and Aquatic Sciences* 55:37–46.
- Hampton J, Sibert JR, Kleiber P, Maunder MN, Harley SJ. 2005. Fisheries: decline of Pacific tuna populations exaggerated? *Nature* 434:E1–E2. URL <http://dx.doi.org/10.1038/nature03581>.
- Hanchet SM, Blackwell RG, Dunn A. 2005. Development and evaluation of catch per unit effort indices for southern blue whiting (*Micromesistius australis*) on the Campbell Island Rise, New Zealand. *ICES Journal of Marine Science* 62:1131–1138.
- Harley SJ, Myers RA, Dunn A. 2001. Is catch-per-unit-effort proportional to abundance. *Canadian Journal of Fisheries and Aquatic Sciences* 58:1760–1772.
- Harvey AC. 1990. *Forecasting, structural time series models and the Kalman filter*. Cambridge University Press, Cambridge.
- Hilborn R. 1979. Comparison of fisheries control systems that utilize catch and effort data. *Can J Fish Aquat Sci* 36:1477–1489. Owner: Hicks Added to JabRef: 2008.03.06.
- Hilborn R, Maunder M, Parma A, Ernst B, Payne J, Starr PJ. 2003. A generalized age-structured stock assessment model. User's Manual Version 2.0. Technical report. FRI/UW Owner: Hicks Added to JabRef: 2008.03.22.
- Hilborn R, Parma A, Maunder M. 2002. Exploitation rate reference points for West Coast rockfish: Are they robust and are there better alternatives? *North American Journal of Fisheries Management* 22:365–375.
- Hilborn R, Peterman RM. 1996. The development of scientific advice with incomplete information in the context of the precautionary approach, United Nation Food and Agriculture Organization, Rome, Italy, volume *Fisheries Technical Paper 350/2*, pp. 77–101.
- Hilborn R, Walters CJ. 1992. *Quantitative fisheries stock assessment: choice, dynamics, and uncertainty*. Chapman and Hall, New York, 570 pp.

- Holland DS, Bentley N, Lallemand P. 2005. A bioeconomic analysis of management strategies for rebuilding and maintenance of the NSS rock lobster (*Jasus edwardsii* stock in southern New Zealand. Canadian Journal of Fisheries and Aquatic Sciences 62:1553–1569.
- Holt SJ, Gulland JA, Taylor C, Kurita S. 1959. A Standard Terminology and Notation for Fishery Dynamics. J Cons int Explor Mer 24:239–242.
- Ianelli JN. 2002. Simulation Analyses Testing the Robustness of Productivity Determinations from West Coast Pacific Ocean Perch Stock Assessment Data. North American Journal of Fisheries Management 22:301–310.
- Japp D, Wilkinson S. 2007. Deep-sea resources and fisheries, volume 838 of *FAO Fish Rep.*, pp. 39–59.
- Kleiber P, Maunder MN. 2008. Inherent bias in using aggregate CPUE to characterize abundance of fish species assemblages. Fish Res 93:140–145.
- Kloser R, Koslow J, Williams A. 1996. Acoustic assessment of the biomass of a spawning aggregation of orange roughy (*Hoplostethus atlanticus*, Collett) off south-eastern Australia, 1990-93. Marine Freshwater Research 47:1015–1024. URL <http://www.publish.csiro.au/paper/MF9961015>.
- Koslow J. 2000. Continental slope and deep-sea fisheries: implications for a fragile ecosystem. ICES Journal of Marine Science 57:548–557.
- Koslow JA. 1989. Managing nonrandomly varying fisheries. Canadian Journal of Fisheries and Aquatic Sciences 46:1302–1308. URL <http://www.nrcresearchpress.com/doi/abs/10.1139/f89-167>.
- Koslow JA, Bell J, Virtue P, Smith DC. 1995a. Fecundity and its variability in orange roughy: effects of population density, condition, egg size, and senescence. Journal of Fish Biology 47:1063–1080.
- Koslow JA, Kloser R, Stanley CA. 1995b. Avoidance of a camera system by a deepwater fish, the orange roughy (*Hoplostethus atlanticus*). Deep-Sea Research I 42:233–244.
- Lack M, Short K, Willock A. 2003a. Managing risk and uncertainty in deep-sea fisheries: lessons from Orange Roughy. TRAFFIC Oceania and WWF Endangered Seas Programme.
- Lack M, Short K, Willock A. 2003b. Managing risk and uncertainty in deep-sea fisheries: lessons from Orange Roughy.
- Little LR, Wayte SE, Tuck GN, Smith ADM, Klaer N, Haddon M, Punt AE, Thomson R, Day J, Fuller M. 2011. Development and evaluation of a cpue-based harvest control rule for the southern and eastern scalefish and shark fishery of Australia. ICES Journal of Marine Science: Journal du Conseil 68:1699–1705. URL <http://icesjms.oxfordjournals.org/content/68/8/1699.abstract>. <http://icesjms.oxfordjournals.org/content/68/8/1699.full.pdf+html>.

- Lunn DJ, Thomas A, Best N, Spiegelhalter D. 2000. WinBUGS - A Bayesian modelling framework: concepts, structure, and extensibility. *Statistics and Computing* 10:325–337. URL <http://www.mrc-bsu.cam.ac.uk/bugs/>.
- MacCall AD. 1976. Density-dependence of catchability coefficient in the California sardine, *Sardinops sagax caerulea*, purse-seine fishery. *Mar Res Comm Calif Coop Oceanic Fish Invest Rep* 18:136–148. Owner: Hicks Added to JabRef: 2008.08.26.
- Martell SJ, Walters CJ. 2002. Implementing harvest rate objective by directly monitoring exploitation rates and estimating changes in catchability. *Bulletin of Marine Science* 70:695–713.
- Maunder MN. 2012. Evaluating the stockrecruitment relationship and management reference points: Application to summer flounder (*Paralichthys dentatus*) in the U.S. mid-Atlantic. *Fisheries Research* 125-126:20–26.
- Maunder MN, Punt AE. 2004. Standardizing catch and effort data: a review of recent approaches. *Fisheries Research* 70:141–159.
- Maunder MN, Sibert JR, Fonteneau A, Hampton J, Kleiber P, Harley SJ. 2006. Interpreting catch per unit effort data to assess the status of individual stocks and communities. *ICES Journal of Marine Science* 63:1373–1385.
- McAllister MK, Kirchner C. 2002. Accounting for structural uncertainty to facilitate precautionary fishery management: illustration with Namibian orange roughy. *Bulletin of Marine Science* 70:499–540.
- McAllister MK, Starr PJ, Restrepo VR, Kirkwood GP. 1999. Formulating quantitative methods to evaluate fishery-management systems: what fishery processes should be modelled and what trade-offs should be made? *ICES J Mar Sci* 56:900–916.
- Methot RD, Taylor IG. 2011. Adjusting for bias due to variability of estimated recruitments in fishery assessment models. *Canadian Journal of Fisheries and Aquatic Sciences* 68:1744–1760.
- Meyer R, Millar RB. 1999a. Bayesian stock assessment using a state-space implementation of the delay difference model. *Canadian Journal of Fisheries and Aquatic Sciences* 56:37–52.
- Meyer R, Millar RB. 1999b. BUGS in Bayesian stock assessments. *Canadian Journal of Fisheries and Aquatic Sciences* 56:1078–1086.
- Millar RB, Meyer R. 2000. Bayesian State-Space Modeling of Age-Structured Data: Fitting a Model is Just the Beginning. *Canadian Journal of Fisheries and Aquatic Sciences* 57:43–50.
- Ministry of Fisheries. 2007. Report from the fishery assessment plenary, May 2007: stock assessments and yield estimates. Ministry of Fisheries, Wellington, New Zealand., 1015 pp. URL <http://fs.fish.govt.nz/>.

- Ministry of Fisheries. 2008a. Harvest Strategy Standard of New Zealand Fisheries. Technical report. URL <http://fs.fish.govt.nz/Page.aspx?pk=104>.
- Ministry of Fisheries. 2008b. Operational guidelines for New Zealand's harvest strategy standard p. 68. URL <http://fs.fish.govt.nz/Page.aspx?pk=104>.
- Ministry of Fisheries. 2010. Report from the fishery assessment plenary, May 2010: stock assessments and yield estimates. Ministry of Fisheries, Wellington, New Zealand., 1158 pp. URL <http://fs.fish.govt.nz/>.
- Ministry of Fisheries. 2011. Report from the fishery assessment plenary, May 2011: stock assessments and yield estimates. Ministry of Fisheries, Wellington, New Zealand., 1158 pp. URL <http://fs.fish.govt.nz/>.
- Minte-Vera CV, Branch TA, Stewart IJ, Dorn MW. 2005. Practical application of meta-analysis results: avoiding the double use of data. *Canadian Journal of Fisheries and Aquatic Sciences* 62:925–929.
- Myers RA, Worm B. 2003. Rapid worldwide depletion of predatory fish communities. *Nature* 423:280–283.
- National Research Council. 1998. Improving fish stock assessments. National Academy Press, Washington, D.C., 188 pp.
- Newman KB. 1998. State-space modeling of animal movement and mortality with application to salmon. *Biometrics* 54:1290–1314.
- Newman KB. 2000. Hierarchic modeling of salmon harvest and migration. *Journal of Agricultural, Biological, and Environmental Statistics* 5:430–455.
- Newman KB, Buckland ST, Lindley ST, Thomas L, Fernández C. 2006. Hidden process models for animal population dynamics. *Ecological applications* 16:74–86.
- Paloheimo JE, Dickie LM. 1964. Abundance and fishing success. In *ICES Rapports et Procès-verbaux des réunions vol 155*.
- Paulin CD. 1979. New Zealand roughies (Pisces: Berycomorphii: Trachichthyidae). *New Zealand Journal of Zoology* 6:69–76.
- Peterman RM, Steer GJ. 1981. Relation Between Sport-Fishing Catchability Coefficients and Salmon Abundance. *Transactions of the American Fisheries Society* 110:585–593. Owner: Hicks Added to JabRef: 2008.03.02.
- Polacheck T. 2006. Tuna longline catch rates in the Indian Ocean: did industrial fishing result in a 90% rapid decline in the abundance of large predatory species? *Marine Policy* 30:470–482.
- Prince JD, Dowling NA, Davies CR, Campbell RA, Kolody DS. 2011. A simple cost-effective and scale-less empirical approach to harvest strategies. *ICES Journal of Marine Science* 68:947–960.

- Punsly R. 1987. Estimation of the relative annual abundance of yellowfin tuna, *Thunnus albacares*, in the eastern Pacific Ocean during 1970–1985. *Inter-American Tropical Tuna Commission Bulletin* 19:263–306.
- Punt AE, Dorn MW, Haltuch MA. 2008. Evaluation of threshold management strategies for groundfish off the U.S. West Coast. *Fisheries Research* 94:251–266.
- Punt AE, Hilborn R. 1997. Fisheries stock assessment and decision analysis: the Bayesian approach. *Reviews in Fish Biology and Fisheries* 7:35–63. Owner: Hicks Added to JabRef: 2008.02.28.
- Punt AE, Smith ADM, Cui G. 2001. Review of progress in the introduction of management strategy evaluation (MSE) approaches in Australia’s South East Fishery. *Mar Freshwater Res* 52:719–726.
- Quinn, Deriso. 1999. *Quantitative Fish Dynamics*. Biological Resource Management Series. Oxford University Press, New York.
- R Development Core Team. 2010. *R: A Language and Environment for Statistical Computing*. R Foundation for Statistical Computing, Vienna, Austria. URL <http://www.R-project.org>. ISBN 3-900051-07-0.
- Rademeyer RA, Plagnyi vE, Butterworth DS. 2007. Tips and tricks in designing management procedures. *ICES Journal of Marine Science: Journal du Conseil* 64:618–625.
- Ralston S, Punt AE, Hamel OS, DeVore JD, Conser RJ. 2011. A meta-analytic approach to quantifying scientific uncertainty in stock assessments. *Fishery Bulletin* 109:217–231.
- Richards LJ, Schnute JT. 1986. An experimental and statistical approach to the question: Is CPUE an index of abundance? *Canadian Journal of Fisheries and Aquatic Sciences* 43:1214–1227.
- Ricker. 1940. Relation of Catch per Unit Effort to Abundance and Rate of Exploitation. *J Fish Res Bd Can* 5:43–70.
- Ricker WE. 1944. Further Notes on Fishing Mortality and Effort. *Copeia* 1944:23–44.
- Rindorf A, Andersen BS. 2008. Do North Sea cod (*Gadus morhua*) fisheries maintain high catch rates at low stock size? *Canadian Journal of Fisheries and Aquatic Sciences* 65:1800–1813.
- Rose GA, Kulka DW. 1999. Hyperaggregation of fish and fisheries: how catch-per-unit-effort increased as the northern cod (*Gadus morhua*) declined. *Canadian Journal of Fisheries and Aquatic Sciences* 56(Suppl. 1):118–127.
- Rose GA, Leggett WC. 1991. Effects of Biomass–Range Interactions on Catchability of Migratory Demersal Fish by Mobile Fisheries: An Example of Atlantic Cod (*Gadus morhua*). *Canadian Journal of Fisheries and Aquatic Sciences* 48:843–848.

- Rothschild BJ. 1977. Fishing effort. In JA Gulland, editor, *Fish Population Dynamics*, John Wiley & Sons, Ltd., chapter 5.
- Sainsbury K. 2000. Design of operational management strategies for achieving fishery ecosystem objectives. *ICES Journal of Marine Science* 57:731–741.
- Salthaug A, Aanes S. 2003. Catchability and the spatial distribution of fishing vessels. *Canadian Journal of Fisheries and Aquatic Sciences* 60:259–268.
- Schaefer MB. 1954. Some aspects of the dynamics of populations important to the management of the commercial marine fisheries. *IATTC Bull* 1:25–56. Owner: Hicks Added to JabRef: 2008.08.29.
- Schnute J. 1985. A General Theory for Analysis of Catch and Effort Data. *Canadian Journal of Fisheries and Aquatic Sciences* 42:414–429.
- Schnute JT. 1994. A general framework for developing sequential fisheries models. *Canadian Journal of Fisheries and Aquatic Sciences* 51:1676–1688.
- Sissenwine MP, Mace PM. 2007. Can deep water fisheries be managed sustainably?, volume 838 of *FAO Fish Rep.*, pp. 61–111.
- Smith TD. 1994. *Scaling fisheries: the science of measuring the effects of fishing, 1855–1955*. Cambridge University Press. Owner: Hicks Added to JabRef: 2006.12.19.
- Sosa-Lopez A, Manzo-Monroy HG. 2002. Spatial patterns of the yellowfin tuna *Thunnus albacares* in the Eastern Pacific Ocean: an exploration of concentration profiles. *Ciencias marinas* 28:331–346. Owner: Hicks Added to JabRef: 2008.08.27.
- Starr PJ, Breen PA, Hilborn RH, Kendrick TH. 1997. Evaluation of a management decision rule for a New Zealand rock lobster substock. *Marine Freshwater Research* 48:1093–1101.
- Stewart IJ, Hicks AC, Taylor IG, Thorson JT, Wetzel C, Kupschus S. 2013. A comparison of stock assessment uncertainty estimates using maximum likelihood and Bayesian methods implemented with the same model framework. *Fisheries Research* 142:37–46.
- Sullivan PJ. 1992. A Kalman filter approach to catch-at-length analysis. *Biometrics* 48:237–257.
- Swain DP, Sinclair AF. 1994. Fish distribution and catchability: what is the appropriate measure of distribution? *Canadian Journal of Fisheries and Aquatic Sciences* 51:1046–1054.
- Thompson JR, Carter RL. 2007. An overview of normal theory structural measurement error models. *International Statistical Review* 75:183–198.
- Ulltang A. 1980. Factors affecting the reaction of pelagic fish stocks to exploitation and requiring a new approach to assessment and management. *Rapp P-v Run Cons, Int Explor Mer* 177:489–504.

- Walters C. 2003. Folly and fantasy in the analysis of spatial catch rate data. *Canadian Journal of Fisheries and Aquatic Sciences* 60:1433–1436.
- Walters CJ, Martell SJD. 2004. *Fisheries ecology and management*. Princeton University Press, 399 pp. Owner: Hicks Added to JabRef: 2006.12.19.
- Wayte S, Bax N. 2002. Stock assessment report 2002. Orange roughy (*Hoplostethus atlanticus*). 57 p. Report for the South East Fishery Stock Assessment Group. CSIRO Marine Research, Hobart, Tasmania.
- Wayte, SE (editor). 2009. Evaluation of new harvest strategies for SESSF species. Technical report.
- Wilberg MJ, Bence JR. 2006. Performance of time-varying catchability estimators in statistical catch-at-age analysis. *Canadian Journal of Fisheries and Aquatic Sciences* 63:2275–2285.
- Wilberg MJ, Thorson JT, Linton BC, Berkson J. 2010. Incorporating time-varying catchability into population dynamic stock assessment models. *Reviews in Fisheries Science* 18:7–24.
- Winters GH, Wheeler JP. 1985. Interaction between stock area, stock abundance, and catchability coefficient. *Canadian Journal of Fisheries and Aquatic Sciences* 42:989–998.
- Ye Y, Dennis D. 2009. How reliable are the abundance indices derived from commercial catch-effort standardization? *Canadian Journal of Fisheries and Aquatic Sciences* 66:1169–1178.
- Zeldis JR, Francis RIC, Clark MR, Ingerson JKV, Grimes PJ, Vignaux M. 1997. An estimate of orange roughy, *Hoplostethus atlanticus*, biomass using the daily fecundity reduction method. *Fishery Bulletin* 95:576–597.

Appendix A

STOCK-SPECIFIC DATA FOR THE META-ANALYSIS (CHAPTER 1)

The four stocks used in the meta-analysis are described below. The catches for these four stocks, adjusted for overruns due to misreporting and lost fish from burst nets, are shown in Figure A.1.

East Chatham Rise (ECR)

The East Chatham Rise orange roughy stock (ECR) is represented by a rotated “L” shaped area on the eastern most portion of the Chatham Rise and has historically produced very large catches (greater than 15 000 tonnes in some years), as seen in Figure A.1. The early years of the fishery on the Chatham Rise consisted of catches mainly from the Spawning Box sub-area, where a large aggregation of orange roughy forms each spawning season (Ministry of Fisheries 2007). After 1992, catches declined in this sub-area due to catch-limits imposed by an agreement between industry and the New Zealand Minister of Fisheries. Fishing shifted eastward to the East Hills and Andes sub-areas during that time, but catches in the Spawning Box sub-area have recently increased, although they are not as large as in the 1980s.

Previous stock assessments have assumed that orange roughy migrate from the East Chatham Rise to spawn in the Spawning Box, and indices of abundance from the Spawning Box are indicative of changes in the entire East Chatham Rise orange roughy stock (Francis 2001). However, recent analyses of CPUE in the hillier East Rise areas showed different CPUE trends that could not be accounted for in a single stock assessment, thus the 2007 assessment split the ECR area into three independent sub-areas to account for these different trends, even though the sub-areas are not likely to be unique stocks (Ministry of Fisheries 2007). Recent stock assessments have indicated that the biomass may currently be increasing in this area (Ministry of Fisheries 2007) and stock status is currently estimated around

40% of the unfished stock size. However, many scientists and managers are skeptical of the recent increase in biomass shown in the assessment because there are no data that explicitly support this.

Three CPUE series were included for the East Chatham Rise: Spawning Box, Eastern Flats, and East Hills (Table A.1). Details of these analyses can be found in Dunn (2007). The CPUE series for the East Rise was calculated using catches from the Spawning Box during the spawning season and covers the fishing years 1982–83 through 1987–88, 1989–90 through 1991–92, and 1995–96 through 1998–99. The last four years were considered unreliable because they were based on few tows and the trend was dissimilar to the trend in CPUE seen on the East Rise. Therefore, these years were also removed from this analysis to be consistent with the 2007 assessment (Ministry of Fisheries 2007), and because the data were considered unreliable on issues not related to modeling catch-rates and abundance.

The fishery-independent abundance data for the ECR stock consisted of a trawl survey series and two acoustic estimates (Table A.2). The trawl survey series was performed by three different vessels and prior distributions have been developed linking the catchability for the three vessels. The two acoustic surveys included for this stock were fit using a lognormal prior for a single estimated catchability.

Mid-East Coast (MEC)

The Mid-East Coast (MEC) orange roughy stock stretches from Cape Runaway to Banks Peninsula, east of New Zealand, and is composed of orange roughy management areas ORH 2A South, ORH 2B, and ORH 3A. Catches began in the Wairarapa region in 1981–82 where small spawning aggregations have been observed, but the majority of catches since 1988 have been taken from the Ritchie Hill and Rockgarden regions in ORH 2A South, which appears to be the main spawning area. Some fishing has occurred outside of the spawning season on the flats of Madden Bank to the southwest of Ritchie Hill (Anderson *et al.* 2002). Catches exceeded 10 000 tonnes for a number of years until catch limits were agreed upon by the fishing industry and the Ministry of Fisheries in 1994–95 (Figure A.1). Recent stock assessments predicted the 2003–04 biomass to be between 14 and 41% of unfished biomass, depending on how CPUE data were used (Ministry of Fisheries 2007).

The “2007 early” CPUE series from Ministry of Fisheries (2007) was used in this analysis, except that the first four observations (1983–84 to 1986–87) were removed (Table A.3). These observations were removed *a priori* because of reasons associated with the underlying data collection. Unreported catches in this area, typically due to fish lost from burst nets with very large catches, were believed to be greater than 30% until 1988, area 2AS became the main area in 1987 and has remained the main area since, an assessment in 2002 Anderson *et al.* (2002) stated that the indices prior to 1990 were “less reliable,” the unstandardized catch rate in area 2AS increased until 1988, and the percent of catch by area stabilized in 1987 and onwards. This left nine years of CPUE data, as reported in Table A.3.

Fishery-independent abundance data for this stock consisted of three relative abundance estimates: a spring trawl survey series, one absolute abundance estimate from an egg survey (the catchability coefficient is fixed at one), and two relative abundance estimates from acoustic surveys (Table A.3). The acoustic surveys were carried out using different designs, but priors for the catchability coefficients have been developed to allow for each catchability coefficient to be estimated with a single survey point (New Zealand Ministry of Fisheries Deepwater Working Group, pers. comm.).

Northwest Chatham Rise (NWCR)

The Northwest Chatham Rise is directly west of the Spawning Box on the East Chatham Rise and contains an area of seamounts near 180 degrees longitude known as the Graveyard. The NWCR fishery is composed of hill and flat tows with historic annual catches typically less than 4 000 tonnes and catches have leveled at about 2 400 tonnes since the mid 1990’s (Figure A.1). The most recent stock assessment estimated stock status between 9 and 39 percent of unfished biomass, depending on the assumptions made and data included (Ministry of Fisheries 2007).

The standardized CPUE series for the NWCR was calculated from catch and effort data that excluded short tows on aggregations around hills in the Graveyard complex (Table A.4). It was believed that tows on flat ground (represented by a longer tow time) were more representative of the abundance of orange roughy for this stock (Ministry of Fisheries New Zealand Deepwater Working Group, pers. comm.). The assessment for the stock in this area

(Ministry of Fisheries 2007) omitted the first three years of CPUE in an attempt to reduce the effects of the common quick reduction in CPUE seen in orange roughy fisheries, even though no issues with the CPUE data were determined. All years of data were included for this stock in the meta-analysis because the purpose of this analysis is to determine how the quick initial decline in CPUE relates to the abundance and if it can be accounted for.

Fishery independent biomass estimates are available from an egg survey in 1996 and acoustic surveys in 1999, 2002, and 2005 (Ministry of Fisheries 2007, Table A.4). The egg survey was assumed to be absolute with a large amount of error. The catchability coefficient for each acoustic survey was estimated, but with a prior (Ministry of Fisheries 2007).

Eastern Zone (AUS)

The Eastern Zone in Australia contains two major seamounts, St. Helen's Hill and St. Patrick's Head, which have supported large spawning aggregations of orange roughy. The 2002 assessment (Wayte and Bax 2002) assumed that the area was a single stock of orange roughy, but they also explored the hypothesis that St. Helen's Hill and St. Patrick's Head may contain separate stocks. Estimates of depletion in 2001 ranged from 7% to 13%, depending on the assumptions of stock structure and the data used. For the hierarchical meta-analysis done here, we assumed that orange roughy in the Eastern Zone are from a single stock.

A CPUE series was available for the years 1989–1999 and was created from catch-per-shot data using vessels that reported catches in the Eastern Zone (containing St. Helen's Hill and St. Patrick's Head) for at least 5 years, including at least 2 of the last 4 years (Wayte and Bax 2002). Records with zero effort, zero catch, depth less than 500 m, or effort greater than 10 hours were not used in a linear model relating the log of effort, quarter, year, and vessel to the log of catch. Inflated coefficients of variation of 0.4 were assigned to the CPUE estimates when used in previous assessments of Eastern Zone orange roughy (Wayte and Bax 2002), but the original estimates of CV from the linear model were used in the meta-analysis described here (Table A.5).

Fishery-independent abundance estimates for the Eastern Zone stock included an acoustic biomass series and an egg survey estimate (Table A.5). The egg survey was done in 1992

to estimate the spawning biomass off St. Helen's hill and was increased by 5% by Wayte and Bax (2002) to account for possible egg loss. Biomass estimates from hull mounted acoustic surveys were made at St. Helen's Hill by the Australian Commonwealth Scientific and Industrial Research Organization (CSIRO) in 1990, 1991, 1992, 1993, and 1996, with a limited survey of St. Patrick's Head in 1996, and a joint CSIRO/industry survey of St. Helen's Hill and St. Patrick's Head in 1999 (for biomass estimates used in the assessment see Wayte and Bax (2002); for acoustic methodologies see Kloser *et al.* (1996)). A significant proportion of the spawning orange roughy biomass was on St. Patrick's Head in the 1996 and 1999 surveys indicating that St. Helen's Hill may not provide a consistent index for this stock of orange roughy. Therefore, the St. Helen's Hill acoustic biomass was increased by the proportion of total commercial catch taken off St. Patrick's Head in each survey year. In addition, the 1990 acoustic biomass was increased by 30% to account for a decreased proportion of fish spawning in that year compared to other years. A CV of 0.4 was assigned to the acoustic biomass estimates in the 2002 assessment to include the sampling variation estimated from the survey and other uncertainties such as species identification. We assumed that the egg survey was absolute as was done in the 2002 assessment (Wayte and Bax 2002), because although it was designed to estimate the biomass on St. Helen's Hill, the 1992 combined acoustic survey estimate was only 4% larger than the St. Helen's only survey estimate. The combined acoustic series was considered as one consistent time series with a single estimated catchability coefficient (q_{AUS}), and we used the assumed CV of 0.4 because no other values were available.

Table A.1: Catch (mt) and CPUE indices for the Eastern Chatham Rise stock. Year refers to the latter part of the fishing year (i.e, 1979 refers to 1 October 1978 to 30 September 1979). Coefficients of variation (CV) were those used in the 2007 assessment (Ministry of Fisheries 2007) without additional error from unobserved processes added in.

Year	Catch	Spawning Box		Eastern Flats		East Hills	
		Value	CV	Value	CV	Value	CV
1979	15 338						
1980	37 820						
1981	20 930	18.9	0.21				
1982	22 620	17.1	0.21				
1983	6 760	17.7	0.21	1.6	0.12		
1984	21 450	18.0	0.21	1.3	0.08		
1985	25 350	20.9	0.21	1.3	0.09		
1986	27 010	14.3	0.21	1.0	0.06		
1987	28 470	13.7	0.21	0.7	0.06		
1988	19 590	14.4	0.21	0.6	0.07		
1989	24 160						
1990	20 760	5.9	0.21				
1991	14 040	8.6	0.22			5.75	0.21
1992	14 310	6.8	0.23			2.92	0.21
1993	5 290					3.17	0.23
1994	5 400					2.48	0.22
1995	4 210					1.43	0.20
1996	3 990					1.33	0.21
1997	3 790					1.15	0.19
1998	4 830					0.52	0.18
1999	2 790					0.80	0.17
2000	4 840					0.86	0.14
2001	3 680					1.00	0.14
2002	7 040					0.75	0.12
2003	7 460					0.56	0.13
2004	7 240					0.52	0.14
2005	7 440					0.54	0.15

Table A.4: Catch (mt), CPUE indices, and fishery-independent abundance estimates (mt) for the Northwest Chatham Rise stock. Year refers to the latter part of the fishing year (i.e, 1979 refers to 1 October 1978 to 30 September 1979). Coefficients of variation (CV) were those used in assessments reported by Ministry of Fisheries (2007) without additional error from unobserved processes added in.

Year	Catch (mt)	CPUE		Egg		Acoustic	
		Value	CV	Value	CV	Value	CV
1980	1 560						
1981	10 920	1.34	0.28				
1982	9 100	1.61	0.25				
1983	7 020	0.96	0.24				
1984	4 290	0.60	0.24				
1985	2 340	0.89	0.25				
1986	4 736	1.09	0.25				
1987	4 032	0.80	0.24				
1988	1 984	0.58	0.24				
1989	4 636	0.44	0.25				
1990	3 960	0.68	0.24				
1991	1 725	0.67	0.26				
1992	330	0.46	0.33				
1993	4 180	0.38	0.35				
1994	3 850	0.43	0.34				
1995	2 520	0.42	0.27				
1996	2 520	0.22	0.34	49 000	0.80		
1997	2 310	0.40	0.26				
1998	2 415	0.31	0.26				
1999	2 835	0.18	0.28			29 000	0.425
2000	2 205	0.22	0.30				
2001	2 730	0.19	0.27				
2002	2 310	0.17	0.27			42 000	0.63
2003	2 310	0.13	0.28				
2004	2 100	0.16	0.28				
2005	1 680	0.15	0.28			9 100	0.40

Table A.5: Catch (mt), CPUE indices, and fishery-independent abundance estimates (mt) for the Australian Eastern Zone stock. Coefficients of variation (CV) were those used in assessments reported by Wayte and Bax (2002).

Year	Catch (mt)	CPUE		Egg		Acoustic	
		Value	CV	Value	CV	Value	CV
1985	6						
1986	33						
1987	310						
1988	1 949						
1989	26 236	2.66	0.29				
1990	23 200	4.42	0.24			50 180	0.40
1991	12 159	0.52	0.23			31 270	0.40
1992	15 119	1.94	0.23	39 955	0.50	20 904	0.40
1993	5 151	0.35	0.20			8 829	0.40
1994	1 869	1.11	0.22				
1995	1 959	0.74	0.18				
1996	1 998	0.20	0.20			9 372	0.40
1997	2 063	0.60	0.18				
1998	1 968	0.58	0.22				
1999	1 952	0.31	0.23			9 471	0.40
2000	1 996						
2001	1 823						

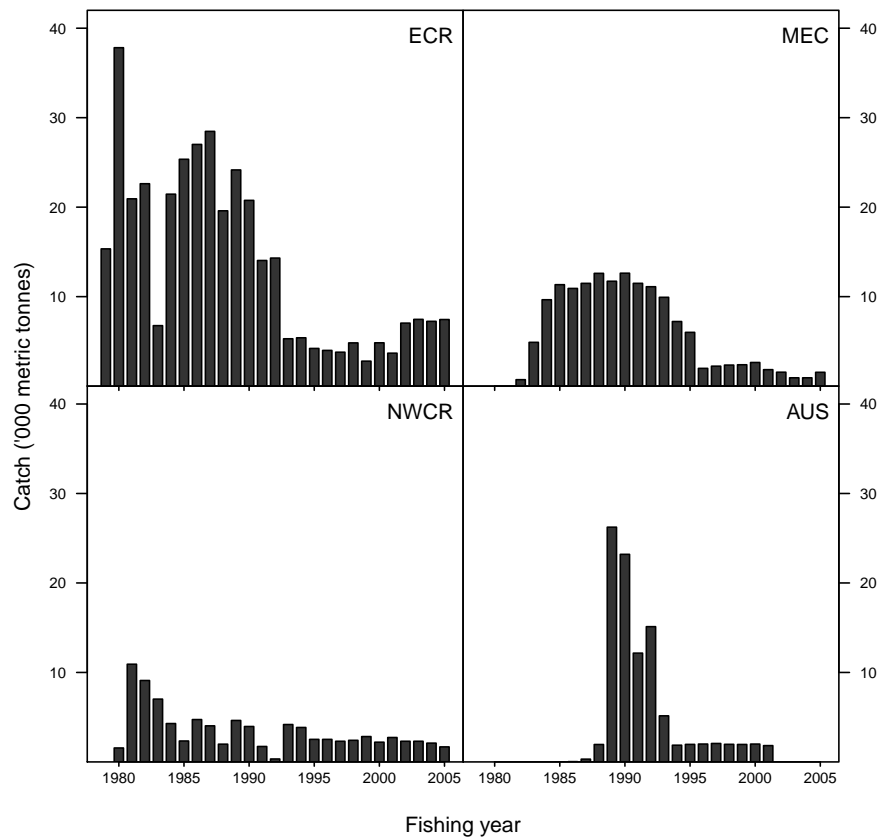


Figure A.1: Catches ('000 mt) by year of orange roughy from four different stocks: East Chatham Rise (ECR), Mid-East Coast (MEC), Northwest Chatham Rise (NWCR), and Australia's Eastern Zone (AUS).

Appendix B

**STOCK SPECIFIC RESULTS FOR THE META-ANALYSIS
(CHAPTER 1)*****East Chatham Rise (ECR)***

The 2007 age-structured assessment of the East Chatham Rise stock (Ministry of Fisheries 2007) was used for comparison to these results, and is labeled as ‘CASAL’, based on the modeling software used. CPUE was assumed proportional to abundance in that assessment, and the ECR area was split into three subareas with each one assessed individually. The overall depletion was 51% and the median unfished biomass was 377 000 metric tonnes when adding up the abundance estimates for the three substocks from runs that used all available data (Table B.1).

The median predicted biomass trajectory from this study for the East Chatham Rise stock and the CPUE and survey data are shown in Figure B.1. The variability of the predicted biomass was large with CV’s ranging from 68% to 80%. The median predicted biomass trajectory fit the CPUE series well, but the trawl survey trends were steeper than this trajectory. The absolute egg survey was much greater than the predicted biomass and the acoustic surveys were both lower than the median predicted biomass trajectory.

The posteriors for depletion (mid-year biomass in 2005 divided by mid-year unfished biomass) and unfished biomass are also shown in Figure B.1. Depletion was lower than that predicted in recent assessments and unfished biomass was generally greater (Table B.1). Uncertainty was large in the state-space model and the 2.5% and 97.5% quantiles from the CASAL model (Ministry of Fisheries 2007) were encompassed within the 2.5% and 97.5% quantiles from the SSM model (quantiles were used for comparison because that is what is reported in the stock assessment reports). The posterior for unfished biomass was highly skewed with a small probability of some very large stock sizes greater than 2 million tonnes. Comparing the CASAL assessment to the state-space model for this stock is difficult because

the CASAL assessment split the area into three sub-areas and assessed each individually. Nevertheless, the CASAL assessments for the Spawning Box area (which contains the bulk of the overall biomass) generally showed a decrease in biomass until the early 1990s, after which the biomass began to increase, resulting in the low amount of depletion. The SSM model for the entire East Chatham Rise area showed a decline until the late 1990s followed by a stabilized level of biomass, resulting in a more depleted stock.

Mid-East Coast (MEC)

Recent assessments of the Mid-East Coast stock were done by two different organizations and are referred to as the CASAL and Awatea assessments, based on the modeling software used (Ministry of Fisheries 2007). The CASAL assessment was done in 2004 and reported 2004 biomass estimates, while the Awatea assessment was updated in 2005 and reported 2004 as well as 2005 biomass estimates. Mid-year biomass estimates for the year 2004 from runs done by both organizations which assumed that CPUE was proportional to abundance and runs done by both organizations which estimated a nonlinearity parameter are reported in Table B.1 for comparison to the SSM results. The overall depletion was near 17% when CPUE was assumed to be proportional to abundance and either 30% or 24% for the CASAL and Awatea runs, respectively, when a nonlinearity parameter was estimated. Unfished spawning biomass from these assessments was estimated near 100,000 metric tonnes.

The median predicted biomass trajectory from the state-space model for the Mid-East Coast stock and the CPUE and survey data are shown in Figure B.2. The variability of the yearly predicted biomass was not as large as for the ECR stock, with CV's ranging from 34% to 63%. The median predicted biomass trajectory fit the CPUE series and trawl surveys well, and the most recent acoustic survey was quite low. The median predicted biomass was also higher than the absolute egg survey, but was well within the confidence bounds.

The posteriors for depletion and unfished biomass are also shown in Figure B.2. Estimated depletion was similar to depletion reported for recent assessment runs where a similar nonlinearity parameter (β) was estimated, but less depleted than runs where CPUE was assumed linear to abundance (Table B.1). Uncertainty was much larger in the state-space

model, which generally encompassed all CASAL and Awatea assessment runs within the 2.5% and 97.5% quantiles of the estimated posterior distributions.

Northwest Chatham Rise (NWCR)

The 2005 assessment of the Northwest Chatham Rise (NWCR) stock (Ministry of Fisheries 2007) was compared to the results from the state-space model. Mid-year biomass estimates are reported in Table B.1 for the year 2006 from runs which used CPUE data only, survey data only, or both together. When used, CPUE was always assumed to be proportional to abundance. The overall depletion was high (9–11%) when CPUE was used, and much less (31%) when CPUE was omitted. Unfished spawning biomass was about 54 000 metric tonnes when CPUE data were included, and 80 000 metric tonnes when omitted.

The median predicted biomass trajectory from the state-space model for the Northwest Chatham Rise stock and the CPUE and survey data are shown in Figure B.3. The variability of the predicted biomass was large with CV's ranging from 65% to 76%. The median predicted biomass trajectory fit the CPUE series relatively well, especially in more recent years. The point estimate of the median predicted biomass was very close to the absolute egg survey even with a large amount of variability assigned to it. The median predicted biomass was above the low estimate from the acoustic survey in 2005 and was nearly outside of the confidence interval calculated from the total variability.

The median depletion from the estimated posterior distribution was 0.21, which was in-between the previous assessment results when only survey or only CPUE data were included (Table B.1). Median unfished biomass was 147 000 tonnes, greater than estimated in the previous assessment. The variabilities for the posterior distributions for depletion and unfished biomass were high and encompassed all of the results from the previous assessment (Figure B.3 and Table B.1).

Eastern Zone (AUS)

Results from the 2002 assessment of the Eastern Zone of Australia stock (Wayte and Bax 2002) were compared to the results from the state-space model (Table B.1). Mid-year biomass estimates are reported in Table B.1 for the year 2001 from runs which assumed

one stock and one fishery, and either included or omitted age data. CPUE was not used in the 2002 assessment. The most recent estimated depletion was low (10–13% of B_0) and unfished spawning biomass was between 87 000 and 110 000 metric tonnes.

The median predicted biomass trajectory for the Eastern Zone of Australia stock and the CPUE and survey data are shown in Figure B.4. The variability of the predicted biomass was very large with CV's ranging from 0.86 to 1.45. Some of this uncertainty was likely due to the inter-annual variability in the CPUE series and the uniform prior on the natural log of the acoustic catchability. The overall trend was a decline in CPUE, but adjacent years showed considerable differences that cannot be explained only by a change in biomass. The absolute egg survey was slightly less than the median predicted biomass, and the acoustic survey showed a faster decline than the median predicted trajectory with all of the last four years being less than the median predicted biomass.

A large amount of uncertainty was present in the estimates of depletion and biomass for the Australian stock. The median depletion in 2001 was 0.20 and the median unfished biomass from the estimated posterior was 175 000 tonnes with a long right tail containing a small probability (Figure B.4). The probability that unfished biomass was less than 500 000 tonnes was 0.85.

Table B.1: The medians of the posterior distributions for the unfished biomass (B_0), last predicted biomass (B_{last}), and depletion (last predicted biomass divided by unfished biomass) from recent assessments (Ministry of Fisheries 2007; Wayte and Bax 2002) and the state-space model with all stocks (SSM results are in bold). The 2.5% and 97.5% quantiles are given in parentheses for comparison because that is what is reported from the stock assessments. For the ECR stock, the assessment results were summed over results from the three sub-areas. B_{last} was the year 2006 from the assessments for ECR and NWCR stocks while the last year was 2005 in the SSM model for these stocks. The last year was 2004 for all models of the MEC stock and 2001 for the AUS stock. Estimates of β are shown for the three CPUE series from the ECR stock and the single CPUE series for each of the other stocks.

Stock	Run	B_0 ('000 mt)	B_{last}	Depletion (%)	$\hat{\beta}$
	CASAL All.W	377 (312–560)	194 (133–377)	51 (—)	fixed at 1
	SSM	624 (274–3471)	107 (37–505)	17 (6–36)	see below
ECR	Spawning Box				1.2 (0.7–2.3)
	Eastern Flats				2.0 (1.1–4.0)
	East Hills				2.3 (1.1–7.1)
	CASAL	94 (91–104)	17 (13–23)	18 (15–23)	fixed at 1
	CASAL (β)	105 (89–126)	31 (22–47)	30 (23–38)	1.9 (1.4–2.5)
MEC	Awatea	99 (87–108)	17 (12–22)	17 (14–21)	fixed at 1
	Awatea (β)	106 (92–119)	25 (16–35)	24 (24–30)	1.5 (1.1–1.7)
	SSM	138 (88–365)	41 (20–117)	30 (16–59)	1.4 (0.8–2.8)
	Alldata	55 (51–60)	6 (4–9)	11 (8–16)	fixed at 1
NWCR	Nobiomass	53 (48–56)	4 (3–7)	9 (6–13)	fixed at 1
	NoCPUE	80 (60–129)	31 (12–78)	39 (21–61)	fixed at 1
	SSM	147 (63–680)	31 (10–117)	21 (8–42)	1.5 (0.8–2.9)
	S1F1	110 (—)	12 (—)	10 (—)	fixed at 1
AUS	S1F1.noAge	87 (—)	12 (—)	13 (—)	fixed at 1
	SSM	175 (71–2114)	38 (9–475)	20 (7–65)	1.4 (0.5–3.5)

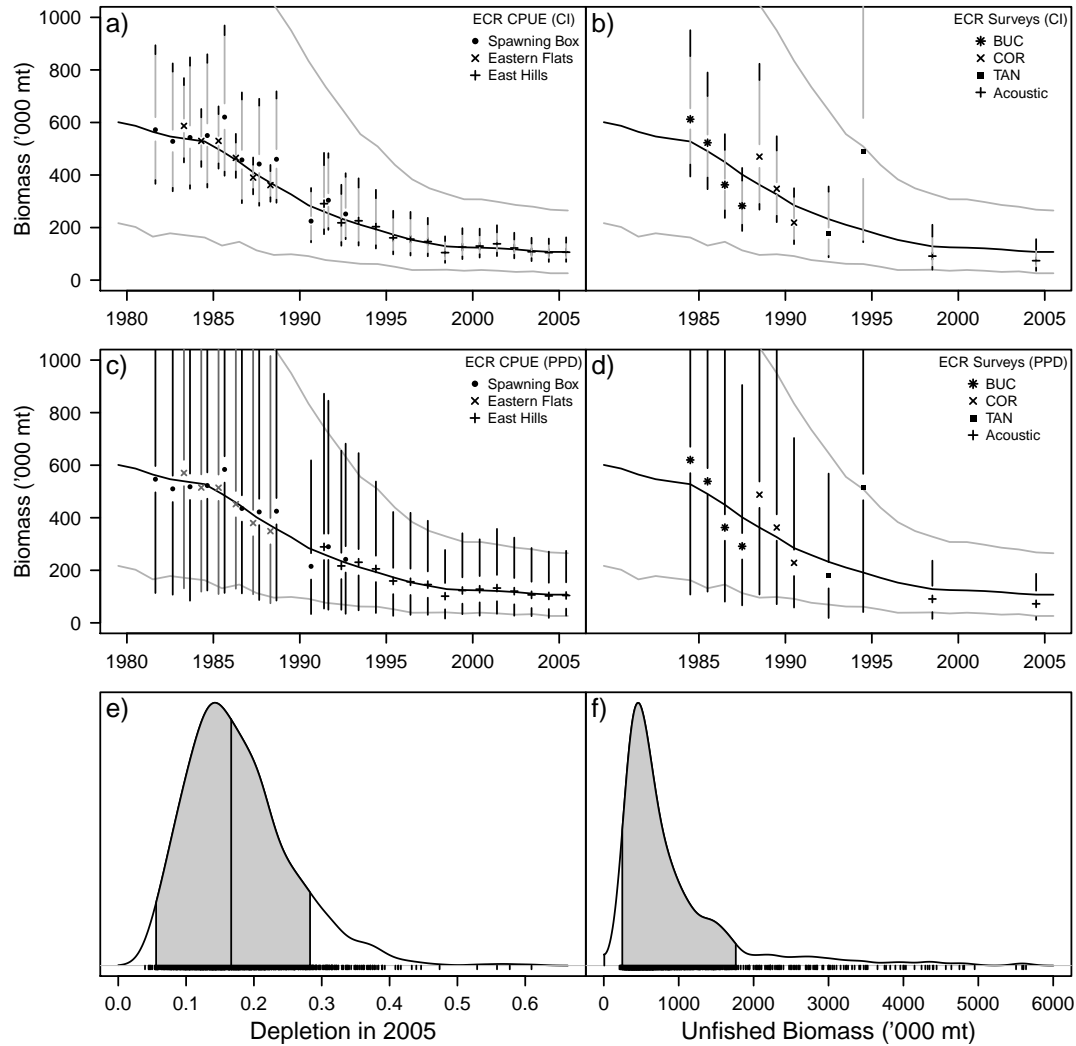


Figure B.1: Median of the posterior distribution for the spawning biomass trajectory of the East Chatham Rise (ECR) stock with a 90% HPD interval in grey (panels a and b). Fitted CPUE (panel a) and survey indices (panel b) are also plotted with 90% confidence intervals calculated from the CV's provided with the data (grey lines) and CV's with the median of the estimated extra variability included (darker extended lines). The same plots are shown in panels c) and d), but with 90% posterior predictive distributions instead of confidence intervals for the data. Posterior distributions for depletion (e) and unfished spawning biomass, B_0 (f) are also shown with the median and the 90% HPD interval. Actual samples from the posterior are indicated immediately below the posterior distributions with small black marks.

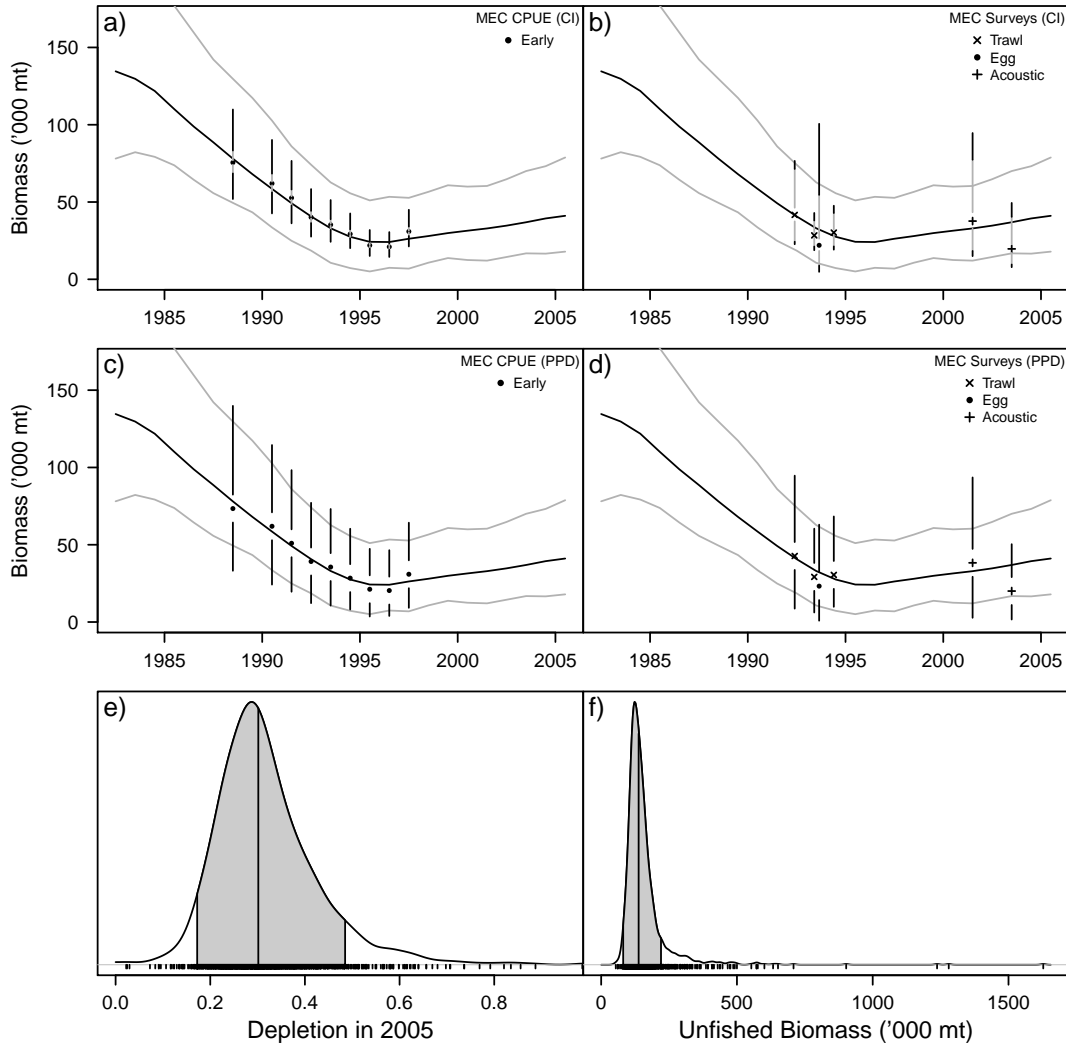


Figure B.2: Median of the posterior distribution for the spawning biomass trajectory of the Mid-East Coast (MEC) stock with a 90% HPD interval in grey (panels a and b). Fitted CPUE (panel a) and survey indices (panel b) are also plotted with 90% confidence intervals calculated from the CV's provided with the data (grey lines) and CV's with the median of the estimated extra variability included (darker extended lines). The same plots are shown in panels c) and d), but with 90% posterior predictive distributions instead of confidence intervals for the data. Posterior distributions for depletion (e) and unfished spawning biomass, B_0 (f) are also shown with the median and the 90% HPD interval. Actual samples from the posterior distribution are indicated with small black marks immediately below the nonparametric density estimate of the posterior distribution.

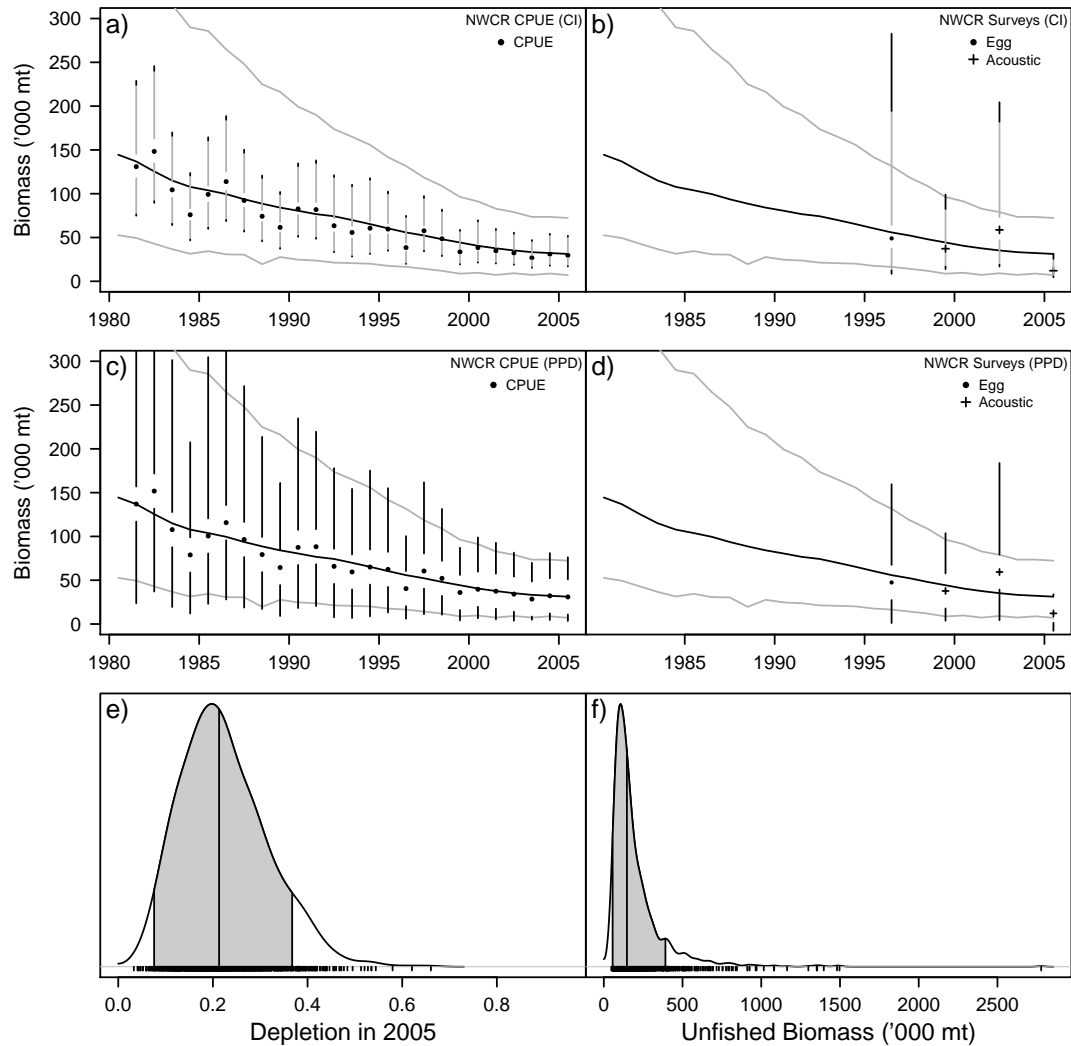


Figure B.3: Median of the posterior distribution for the spawning biomass trajectory of the Northwest Chatham Rise (NWCR) stock with a 90% HPD interval in grey (panels a and b). Fitted CPUE (panel a) and survey indices (panel b) are also plotted with 90% confidence intervals calculated from the CV's provided with the data (grey lines) and CV's with the median of the estimated extra variability included (darker extended lines). The same plots are shown in panels c) and d), but with 90% posterior predictive distributions instead of confidence intervals for the data. Posterior distributions for depletion (e) and unfished spawning biomass, B_0 (f) are also shown with the median and the 90% HPD interval. Actual samples from the posterior distribution are indicated with small black marks immediately below the nonparametric density estimate of the posterior distribution.

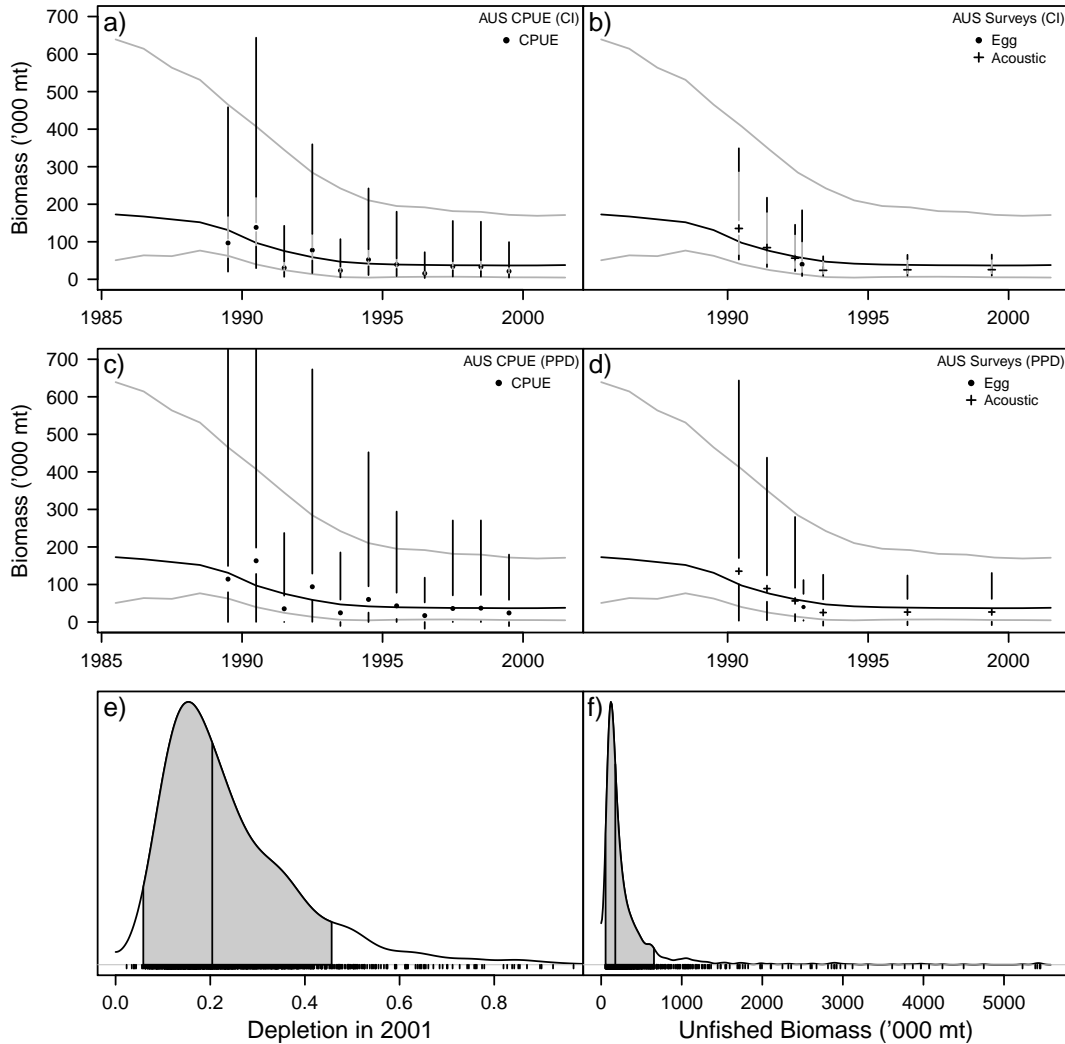


Figure B.4: Median of the posterior distribution for the spawning biomass trajectory of the Eastern Zone of Australia (AUS) stock with a 90% HPD interval in grey (panels a and b). Fitted CPUE (panel a) and survey indices (panel b) are also plotted with 90% confidence intervals calculated from the CV's provided with the data (grey lines) and CV's with the median of the estimated extra variability included (darker extended lines). The same plots are shown in panels c) and d), but with 90% posterior predictive distributions instead of confidence intervals for the data. Posterior distributions for depletion (e) and unfished spawning biomass, B_0 (f) are also shown with the median and the 90% HPD interval. Actual samples from the posterior distribution are indicated with small black marks immediately below the nonparametric density estimate of the posterior distribution.

Appendix C

OPERATING AND ESTIMATION MODELS

Operating models*Single area model*

The operating model simulated the “true” population and incorporated processes such as recruitment, growth, and maturation. The initial population, in numbers-at-age (N) at the start of the year, was determined from the user defined unfished, equilibrium recruitment (R_0).

$$N_{1,a} = \begin{cases} R_0 e^{\left(\varepsilon_a - \frac{\sigma_R^2}{2}\right)} & a = 1 \\ R_0 e^{-M(a-1)} & a = 2, \dots, (A-1) \\ \frac{R_0 e^{-M(A-1)}}{1 - e^{-M}} & a = A \end{cases} \quad (\text{C.1})$$

where a indexes age, A is the maximum age modeled, M is natural mortality, ε_a is a normal deviate for recruitment at age, and σ_R represents recruitment variability.

Weight-at-age was calculated from the weight-length relationship and the length-at-age relationship.

$$\bar{L}_a = L_\infty \left(1 - e^{-K(a-t_0)}\right) \quad (\text{C.2})$$

$$\bar{w}_a = (a_{wt}) (\bar{L})_a^{b_{wt}} \quad (\text{C.3})$$

Maturity-at-age (m_a) was knife-edged at age 29.

Unfished, equilibrium spawning biomass at the start of the year was found using weight-at-age, maturity-at-age, natural mortality, and unfished, equilibrium recruitment (R_0).

$$B_0 = R_0 \left[\sum_{a=1}^{A-1} e^{-M(a-1)} \bar{w}_a m_a + \frac{e^{-M(A-1)} \bar{w}_A m_A}{1 - e^{-M}} \right] \quad (\text{C.4})$$

Numbers-at-age for each year modeled ($y = 2, \dots, T$) are calculated by applying natural mortality and age-specific exploitation to the previous year's number-at-age.

$$N_{y,a} = \begin{cases} R_0 e^{\left(\varepsilon_t - \frac{\sigma_R^2}{2}\right)} & a = 1 \\ N_{y-1,a-1} e^{-M} (1 - E s_{a-1}) & a = 2, \dots, (A-1) \\ \left[N_{y-1,a} (1 - E_{y-1} s_a) + N_{y-1,a-1} (1 - E_{y-1} s_{a-1}) \right] e^{-M} & a = A \end{cases} \quad (\text{C.5})$$

Spawning biomass was calculated using start of the year numbers-at-age, maturity-at-age, and weight-at-age.

$$B_y = \sum_{a=1}^A N_{y,a} m_a \bar{w}_a \quad (\text{C.6})$$

Age specific exploitation is the product of the exploitation rate (E_y) and selectivity at age, where selectivity was knife-edged at age 29 and the exploitation rate was calculated from the mid-year vulnerable biomass (V_y).

$$E_t = \frac{C_t}{V_t} \quad (\text{C.7})$$

$$V_t = \sum_{a=1}^A N_{t,a} e^{-0.5M} s_a \bar{w}_a \quad (\text{C.8})$$

Two area models (Chapter 3)

The two-area operating models used the same underlying population dynamics as the single-area operating model within each area and moved mature fish between an area where fishing occurred (available area or area 1) and an area where fishing did not occur (unavailable area or area 2). Movement was a Type II response, dependent on either the harvest rate or the mature biomass in the available area.

$$\Omega_{1 \rightarrow 2, y} = \frac{\rho_1 H_y}{1 + \rho_1 H_y} \quad (\text{C.9})$$

$$\Omega_{2 \rightarrow 1, y} = \frac{\rho_2 (1 - H_y)}{1 + \rho_2 (1 - H_y)} \quad (\text{C.10})$$

where Ω represents the migration rate from area 1 to 2 or from 2 to 1, H is either the exploitation rate or the proportion of unfished equilibrium biomass in area 1, and ρ_1 and

ρ_2 are parameters of this simplified Holling's Disc equation. Movement was the last event to occur within a year, after fishing mortality and natural mortality were applied, as in Equation C.5.

$$N_{y,a,available} = N_{y,a,available} + \Omega_{2 \rightarrow 1} N_{y,a,unavailable} - \Omega_{1 \rightarrow 2} N_{y,a,available} \quad (C.11)$$

$$N_{y,a,unavailable} = N_{y,a,unavailable} + \Omega_{1 \rightarrow 2} N_{y,a,available} - \Omega_{2 \rightarrow 1} N_{y,a,unavailable} \quad (C.12)$$

Before the burn-in started for each simulation, the population began with all fish in the available area and was simulated with no recruitment deviations and without fishing until it reached equilibrium (defined as stable biomass in each area). The simulation process of burn-in, fishing, and then management followed.

Simulating data

Survey data (Z_y) and CPUE (U_y) data were simulated using lognormal distributions. It was assumed that survey data were proportional to biomass with a catchability coefficient (q) of 0.25. CPUE data were nonlinearly related to biomass with the power parameter β and a proportionality constant $\alpha = (1 \times 10^{-5})^\beta$.

$$Z_y \sim \text{LN}(\mu = qV_y, CV = SURVcv) \quad (C.13)$$

$$U_y = \text{LN}(\mu = \alpha V_y^\beta, CV = CPUEcv) \quad (C.14)$$

Estimation models

Three different estimation models are described below, all of which were investigated in Chapter 2. The state-space model was used in Chapter 1 and the age-structured model (Awatea) was used in the Chapter 3.

Deterministic delay-difference model

The deterministic delay-difference model (Deriso 1980; Schnute 1985) is

$$B_y = \begin{cases} B_0 & y = 1 \\ s_{y-1}B_{y-1} + \rho s_{y-1}B_{y-1} - \rho s_{y-1}s_{y-2}B_{y-2} - s_{y-1}\rho w_{k-1}R_0 + w_k R_0 & y = 2, \dots, T \end{cases} \quad (C.15)$$

where k is the age of recruitment, B_0 is an estimated parameter, and the virgin recruitment, R_0 , is a function of B_0 .

$$R_0 = B_0 \frac{1 - s_0 - \rho s_0 + \rho s_0^2}{w_k - s_0 \rho w_{k-1}} \quad (\text{C.16})$$

The survival rate at time t is

$$s_y = \begin{cases} e^{-M} & y = 0 \\ e^{-M} \left(1 - \frac{C_y}{B_y}\right) & y = 1, \dots, T \end{cases} \quad (\text{C.17})$$

where M is natural mortality and C_y is catch in year y . The variable ρ represents the slope of the linear relationship between weight-at-age and the weight-at-the-previous-age,

$$w_a = \zeta + \rho w_{a-1} \quad (\text{C.18})$$

Orange roughy assessments use allometric weight-at-length and von Bertalanffy length-at-age, which does not lead to Equation C.18. However, because maturity occurs later in life for orange roughy, a linear approximation is reasonable. Therefore, ρ was approximated by calculating weight-at-age of recruited fish from the length-at-age and weight-at-length relationships, then estimating the slope using Equation C.18.

Age-structured model (Awatea)

The age-structured model, called Awatea, is a modified version of Coleraine (Hilborn *et al.* 2003) which was adapted to satisfy some of the assumptions used in orange roughy assessments. The population dynamics were modeled the same as in the operating model (equations C.1–C.8), except that recruitment was deterministic.

State-space delay-difference model

The state (biomass) was modeled using a delay-difference model to predict the biomass at the start of year y , as in equations C.15–C.18, but with process error ε_y . This model was used in Chapters 1 and 2.

$$B_y = \begin{cases} B_0 e^{\varepsilon_1 - \sigma_\varepsilon^2/2} & y = 1 \\ (s_{y-1} B_{y-1} + \rho s_{y-1} B_{y-1} - \rho s_{y-1} s_{y-2} B_{y-2} - s_{y-1} \rho w_{k-1} R_0 + w_k R_0) e^{\varepsilon_y - \sigma_\varepsilon^2/2} & y = 2, \dots, T \end{cases} \quad (\text{C.19})$$

The process error ε_y was assumed to be normally distributed,

$$\varepsilon_y \sim N(0, \sigma_\varepsilon^2) \quad (\text{C.20})$$

We assumed that recruitment, on average, was constant (R_0) and fixed fishery selectivity, survey selectivity, and the maturity ogive equal and knife-edged at age k . Weight-at-length, length-at-age, natural mortality, and age of 50% recruitment were fixed parameters taken from realistic values for orange roughy stocks in New Zealand (Ministry of Fisheries, 2010). This left the states (biomass time series and B_0) as well as the process error (σ_ε^2) unknown in the state equations.

Likelihoods

CPUE and survey biomass were related to the predicted biomass through catchability parameters and bias corrected because from the mean of the lognormal distribution.

$$\begin{aligned} \ln(\hat{U}_i) &= \ln(\alpha^*) + \beta \left[\ln(B_i^{mid}) - \overline{\ln(B_{all\ i}^{mid})} \right] + \nu_i - \sigma_{\nu_i}^2/2 & 1 < i \leq T \\ \ln(\hat{Z}_j) &= \ln(q) + \ln(B_j^{mid}) + \tau_j - \sigma_{\tau_j}^2/2 & 1 < j \leq T \end{aligned} \quad (\text{C.21})$$

where B^{mid} is the mid-year biomass, calculated as the beginning of the year biomass with half of the natural mortality removed, and $\overline{\ln(B_{all\ i}^{mid})}$ is the mean of the natural logged mid-year biomasses that have a corresponding CPUE value. The notation U_i represents the CPUE for year i and Z_j represents the survey biomass in year j .

The errors for the natural log of each CPUE index, ν_i , and the natural log of each survey series, τ_j , were assumed normal and variances were equal to the variances used to generate the data (equations C.13 and C.14).

$$\nu_i \sim N(0, \sigma_{\nu_i}^2) \quad (\text{C.22})$$

$$\tau_j \sim N(0, \sigma_{\tau_j}^2) \quad (\text{C.23})$$

Table C.1: Parameters in the operating and estimation models.

Parameter	Description
B_0	Unfished equilibrium biomass
R_0	Unfished equilibrium recruitment
B_t	Biomass in year t
B_t^{mid}	Mid-year biomass in year t
ε_t	Process error in year t
σ_ε^2	Process error variance
M	Natural mortality
k	Age-at-recruitment to the fishery and age-at-maturity
s_t	Survival in year t
w_a	Weight-at-age
ρ	Slope in relationship of weight-at-age to weight-at-previous-age
ζ	Intercept in relationship of weight-at-age to weight-at-previous-age
$\Omega_{1 \rightarrow 2}$	Movement rate from the available area to the unavailable area
$\Omega_{2 \rightarrow 1}$	Movement rate from the unavailable area to the available area
ρ_1	Parameter for Type II functional response of movement from area 1 to area 2
ρ_2	Parameter for Type II functional response of movement from area 1 to area 2
<i>Survey parameters</i>	
Z_j	Survey index for year j
q	Survey catchability
τ_j	Error in year j for the survey series
$\sigma_{\tau_j}^2$	Total variability of the survey in year j
<i>CPUE parameters</i>	
$U_{u,i}$	CPUE for year i
α	Multiplier in relationship between CPUE and abundance for the CPUE series
β	Nonlinearity parameter in relationship between CPUE and abundance
ν_i	Error in year i for CPUE series
$\sigma_{\nu_i}^2$	Total variability of the CPUE series in year i